

ASM Science

JOURNAL

In Pursuit of Excellence in Science

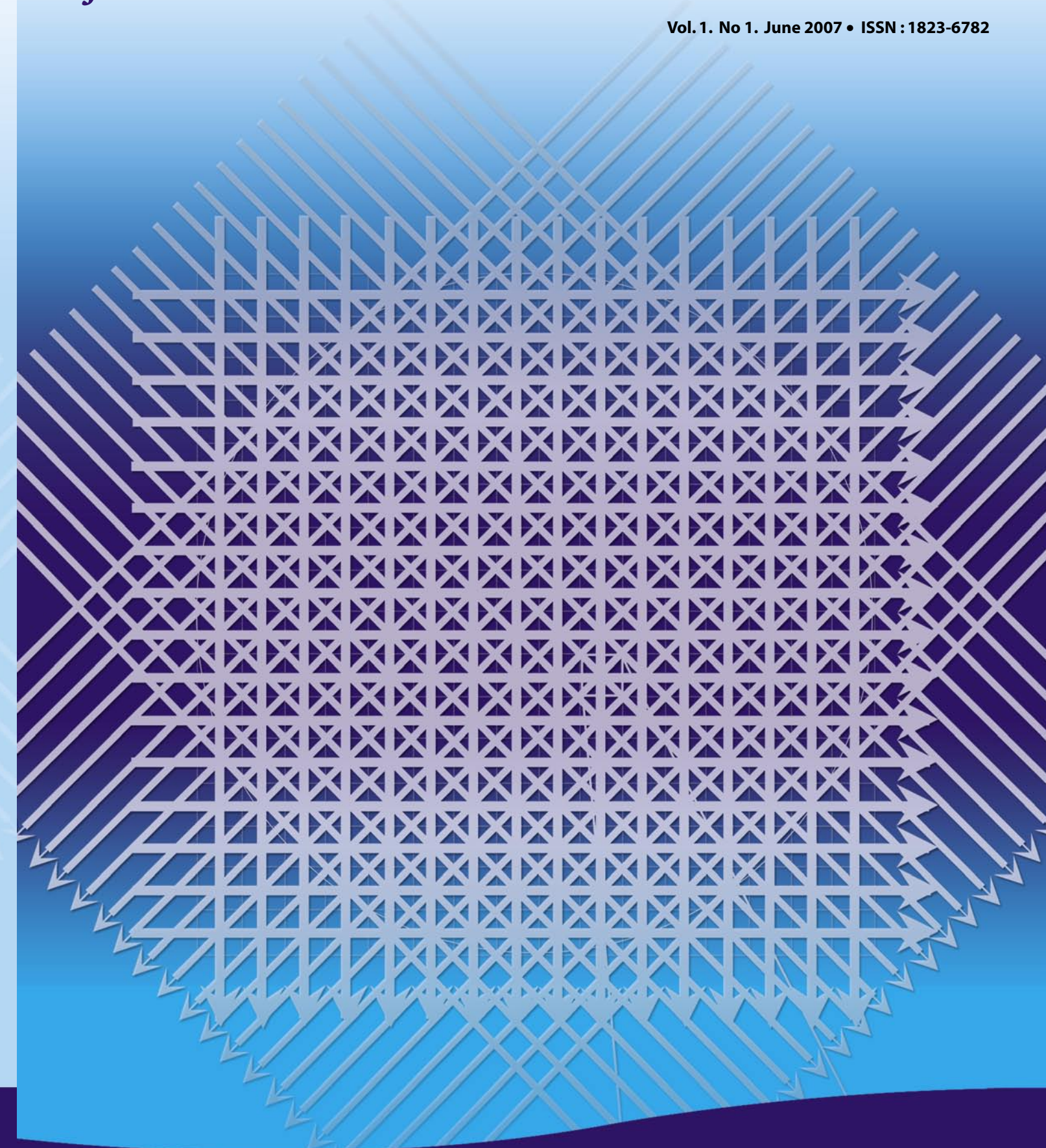
Vol. 1, No 1, June 2007 • ISSN : 1823-6782

Contents

ASM J. Sc.
vol. 1, no. 1, 2007

New reaction kinetic model derived from MD simulation data on nonlinearity of rate coefficients and their relation to activity coefficients.....00	
<i>Dr Christopher G. Jesudason</i>	
Optical Tomography: Real Time Image Reconstruction for Various Flow Regimes in Gravity Flow Conveyor.....00	
<i>Prof Dr Ruzairi Abdul Rahim, Pang Jon Fea, Chan Kok San, Leong Lai Chean and Mohd. Hafiz Fazalul Rahiman</i>	
Prevention of Ethanol-induced Gastric Mucosal Injury by <i>Ocimum basilicum</i> Seeds Extract in Rats.....00	
<i>Dr Mahmood Ameen Abdulla, Sidik K, and Fouad H M.</i>	
Carrier-to-Interference Power Ratio Enhancement in OFDM System.....00	
<i>Dr Sharifah Kamilah Syed Yusof, Norsheila Faisal and Muladi</i>	
Purification of Metallurgical Grade Silicon by Acid Leaching.....00	
<i>Dr Wahid Aghaei Lashgari, Hossein Yoozbashizadeh</i>	
Fourth Ordered Centered TVD Scheme for Hyperbolic Conservation Laws.....00	
<i>Dr Yousef Hashem Zahran</i>	

ISSN 1823-6782



ASM Science

JOURNAL

INTERNATIONAL ADVISORY BOARD

Ahmed Zewail (Nobel Laureate)
Richard R. Ernst (Nobel Laureate)
John Sheppard Mckenzie
M.S. Swaminathan

EDITORIAL BOARD

Editor-in-Chief/Chairman: Mazlan Othman

Abdul Latiff Mohamed
Chia Swee Ping
Ibrahim Komoo
Lam Sai Kit
Lee Chnoong Kheng
Looi Lai Meng
Mashkuri Yaacob
Md. Ikram Mohd Said
Mohd Ali Hashim
Francis Ng
Radin Omar Radin Sohadi

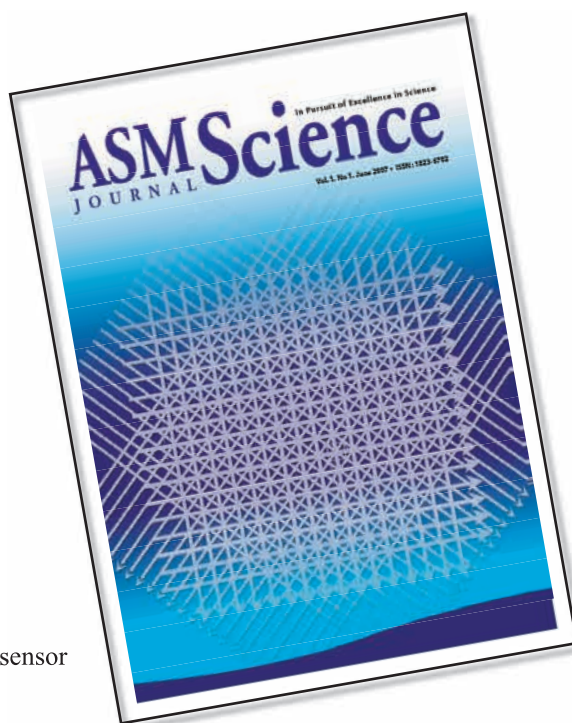
Editorial

The *ASM Science Journal* (*ASM Sc. J.*) is intended to be one of the primary vehicles of the Academy of Sciences Malaysia to stimulate and nurture excellence in science and technology for the development of the nation and for the benefit of mankind. Its purpose is also to widely disseminate significant research developments and deliberate on R&D strategies and policies. It will further provide a major opportunity for showcasing the effectiveness of scientific and technical efforts and increasing the efficiency of management of research and development which is linked with the ability to communicate information about current research efforts and the results of past work. This journal will pay attention to the importance of scientific and technical endeavour and contribute to the better understanding of problems of science and technology through its regular publication and wide circulation, thus promoting cooperation and exchange of views among the science community worldwide. All these objectives are fully in line with the aims and objectives of the Academy.

In this maiden issue, there are contributions from many fields covering both fundamental and applied research: medicine, engineering, chemistry, electronics, mechanics and physics. Our future plan is to gear one issue a year towards a particular theme. The papers in that issue will address current and impending issues, and the demands and needs of the scientific community and society pertaining to the selected theme.

It is hoped that this varied, vital and vigorous exchange of scientific information that the Journal provides will assist in better understanding the various forces and factors that affect the progress of humanity and safeguard its survival. The Academy of Sciences Malaysia, therefore, in earnestly discharging its responsibility, proudly associates itself with this Journal in striving to promote an international exchange of scientific information.

Mazlan Othman
Editor-in-Chief/Chairman, Editorial Board *ASM Sc. J.*



Cover:
Optical tomography sensor
projection geometry
(Article: p. 27)

Prevention of Ethanol-induced Gastric Mucosal Injury by *Ocimum basilicum* Seed Extract in Rats

A. A. Mahmood^{1*}, K. Sidik¹ and H. M. Fouad²

Ocimum basilicum seed extracts were found to possess significant anti-ulcer activity against ethanol-induced ulceration in experimental animal models. Three groups of adult male rats were used, with each group consisting of six rats. Oral administration of absolute ethanol to rats pre-treated with 10% Tween 20[®] (Group 1) produced extensive haemorrhagic lesions of the gastric mucosa. Rats orally pre-treated with *O. basilicum* extract suspended in 10% Tween 20[®] (Group 2) or cimetidine in 10% Tween 20[®] (Group 3), 30 min before oral administration of absolute alcohol had significantly reduced ($p < 0.05$) the formation of such lesions compared to Group 1 rats. Histologically, rats pre-treated with *O. basilicum* extract (Group 2) or cimetidine (Group 3) showed significantly ($p < 0.05$) a marked inhibition or reduction of gastric damage, submucosal oedema and leucocytes infiltration compared to animals pre-treated with 10% Tween 20[®] (Group 1).

Key words: *O. basilicum*; seed extract; cimetidine; gastric ulcer; histology; ethanol-induce; rats

Since ancient times, plants and herbs have been used to treat gastro-intestinal disorders, including gastric ulcers, in traditional medicine (Dharmani *et al.* 2004; Goel *et al.* 2005). Cabbage, previously employed as an oral anti-ulcer agent in folk medicine, led to the development of gefarnate (Adami *et al.* 1964) which acts as an anti-ulcer agent by enhancing gastric mucosal strength (Barbara *et al.* 1974). Raw banana has also been found to inhibit peptic ulceration by stimulating the growth of gastric mucosa (Best *et al.* 1984). Konturek *et al.* (1986) have reported the effectiveness of solon, a plant flavonoid, against ulcers in experimental animals. Pandian *et al.* (2002) showed that fenugreek seeds possess gastric anti-ulcer potential, and El-Abhar *et al.* (2003) reported that *Nigella sativa* oil thymoquinone possess gastro-protective properties against gastric lesions.

Ocimum basilicum (basil) essential oil has been used for many years to flavour foods; as an ingredient of dental and oral healthcare products and also in fragrances (Guenther 1952). *O. basilicum* has also been used in the treatment of a number of ailments like bronchitis, rheumatism and pyrexia (Nadkarni 1976). The fixed oil of *O. basilicum* was found to possess significant anti-inflammatory and anti-ulcer activity (Goel *et al.* 2005), along with anti-microbial (Suppakul *et al.* 2003; Singh *et al.* 2005), analgesic and spasmodic (Singh *et al.* 1996) properties without any noticeable toxicity or hypoglycemic effects (Agrawal *et al.* 1996), and is an effective anti-diarrhoeal (Ilori *et al.* 1996), antioxidant (Dasgupta *et al.* 2004), anti-depressant (Maity *et al.* 2000); and anti-helminthic (Asha *et al.* 2001) and enhances wound healing (Osugwu *et al.* 2004).

The present study was undertaken to examine the cytoprotective effects of *O. basilicum* seed extracts against ethanol-induced mucosal injury in rats.

MATERIALS AND METHODS

Tween 20[®]

It is manufactured by Merck Schuchardt OHG, 85662 Hohenbrunn, Germany. A dilution of (10% v/v) Tween 20[®] was used as a vehicle for dosing in all the rats (5 ml kg⁻¹).

Cimetidine

The reference anti-ulcer drug, cimetidine, was obtained from University Malaya Medical Centre. Each tablet contained 200 mg of cimetidine; the tablets were ground to powder and suspended in the vehicle (Tween 20[®], 10% v/v) and administered to the rats in a concentration of 50 mg kg⁻¹ orally as described by Tan *et al.* (2000).

Cimetidine (Tagamet[®]) is a drug historically used to reduce stomach acid production. It is a member of the H₂ blocker (histamine blocker) family of drugs that prevents the release of acid into the stomach. Histamine H₂ receptor antagonists have potent and sustained acid inhibitory action, and are now widely used as drugs of first choice in the treatment of both gastric and duodenal ulcers. It has been hypothesized that cimetidine promotes gastrin release through the elevation of intragastric pH due to anti-secretory action. Potent acid inhibitors may promote

¹ Department of Molecular Medicine, Faculty of Medicine, University of Malaya, 50603 Kuala Lumpur, Malaysia

² Department of Oral pathology, Oral Medicine and Periodontology, Faculty of Dentistry, University of Malaya, 50603 Kuala Lumpur, Malaysia

* Corresponding author (e-mail: mahmood955@yahoo.com)

gastric ulcer healing by the trophic action of gastrin rather than by an anti-secretory action (Ito *et al.* 1994). Cimetidine also inhibits histamine-induced immune suppression (Hast *et al.* 1989), an effect that has been tested in the treatment of various malignancies (Dillman *et al.* 2003), and may also be relevant to tumor development (Jakobisiak *et al.* 2003). Cimetidine is a competitive inhibitor of the histamine receptors on the cells of the stomach that secrete acid. It binds to these receptors, called H₂ receptors, and does not allow histamine to bind. Histamine is responsible for signaling these cells to secrete acid. If cimetidine is present, the cells do not get the signal to produce acid, thus the pH in the stomach is reduced.

Plant Materials

Dried *O. basilicum* seeds were purchased from the local market and identified by comparison with specimens available at the herbarium of the Forest Research Institute, Kepong, Malaysia. Voucher specimens of the *O. basilicum* are deposited at the Department of Pharmacy, University of Malaya, Malaysia. The seeds were washed with distilled water and oven dried at 50°C for 5–7 days, and then ground using a grinder.

Preparation of Extracts

The ground seeds were extracted by maceration in ethanol (100 g/1500 ml) in a conical flask for 5 days at 37°C. The solvent was then filtered using a filter funnel and distilled under reduced pressure in an EYELA rotary evaporator until excess solvent had evaporated. The extract was then suspended in vehicle (Tween 20[®], 10% v/v) and administered to rats in doses of 500 mg kg⁻¹ body weight (5 ml kg⁻¹) as described by Lima *et al.* (2006).

Experimental Animals

Eighteen adult male *Sprague-Dawley* rats were obtained from the animal house, Faculty of Medicine, University Malaya, Malaysia (Ethics No. PM 26/10/2005 MAA R). Rats weighing 180–200 g each were deprived of food for 24 h, but they were allowed free access to drinking water until 2 h before the experiment. During the fasting period, the animals were placed individually in cages with wide-mesh wire bottoms to prevent coprophagy. On the day of the experiment, the rats were randomly divided into three groups of six rats each.

Animal Treatment

Control animals (Group 1) received 5 ml kg⁻¹ of 10% Tween 20[®] orally by metal orogastric intubations (per os); whereas treated animals, Group 2 rats received oral doses of 500 mg kg⁻¹ of alcoholic *O. basilicum* extract (5 ml kg⁻¹) suspended in 10% Tween 20[®]; and

Group 3 animals received oral doses of 50 mg kg⁻¹ cimetidine in (5 ml kg⁻¹) suspended in 10% Tween 20[®]. Thirty minutes after this pre-treatment, the animals were gavaged with absolute ethanol (5 ml kg⁻¹). They were killed 30 min later by overdoses of diethyl ether and their stomachs were excised. Each stomach was then opened along the greater curvature, washed with distilled water and fixed in 10% buffered formalin for 15 min (Morimoto *et al.* 1991).

Gross Gastric Lesions Evaluation

Ulcers were found in the gastric mucosa, appearing as elongated bands parallel to the long axis of the stomach. The gastric mucosa was examined for damage under a dissecting microscope ($\times 1.8$) with a square-grid eyepiece (10 \times 10 mm² = ulcer area) to assess the ulcer areas (haemorrhagic lesions). The area of each ulcer lesion was measured by counting the number of small squares, 2 mm \times 2 mm, covering the length and width of each ulcer band. The sum of the area of all lesions for each stomach was applied in the calculation of the ulcer area (UA) wherein the sum of small squares $\times 4 \times 1.8 = UA$ mm² (Kauffman & Grossman 1978). The inhibition percentage (I%) was calculated by the following formula (Njar *et al.* 1995):

$$(I\%) = [(UA_{\text{control}} - UA_{\text{treated}}) \div UA_{\text{control}}] \times 100\% \quad (1)$$

Histological Examination

The gastric mucosa was transversely trimmed through the glandular mucosa in an area containing maximal haemorrhagic lesions. These specimens were fixed in 10% buffered formalin, processed into 5 μ sections and stained with haematoxylin and eosin (Hollander *et al.* 1985).

Statistical Analysis

All values are reported as mean + S.E.M. and the statistical significance of differences among groups was assessed using one-way ANOVA. A value of $p < 0.05$ was considered significant.

RESULTS

Gastric Mucosal Injury

Rats pre-treated with 10% Tween 20[®] before the absolute ethanol gavage showed extensive macroscopic lesions (Table 1 and Figure 1). There was 100% incidence of lesion formation in this group. Such damage was characterized by the presence of extensive elongated deep haemorrhagic necrotic lesions confined to the gastric corpus. The lesions were generally running parallel to the long axis of the stomach. In

Table 1. Anti-ulcerogenic effects of *O. basilicum* and cimetidine on ethanol-induced gastric mucosal ulcer in rats.*

Group	Treatment	Oral dosage (by orogastric tube)	Ulcer area (mm ²) mean ± S.E.M	Inhibition (%)
1	10% Tween 20 [®] (Control)	5 ml kg ⁻¹	1324.00 + 125.18 ^a	–
2	<i>O. basilicum</i> (500 mg kg ⁻¹)	5 ml kg ⁻¹	282.33 + 29.30 ^b	78.68
3	Cimetidine (50 mg kg ⁻¹)	5 ml kg ⁻¹	394.59 + 56.46 ^{bc}	70.20

* All values are expressed as mean and ± standard error mean. Means with different superscripts are significantly different (p<0.05).

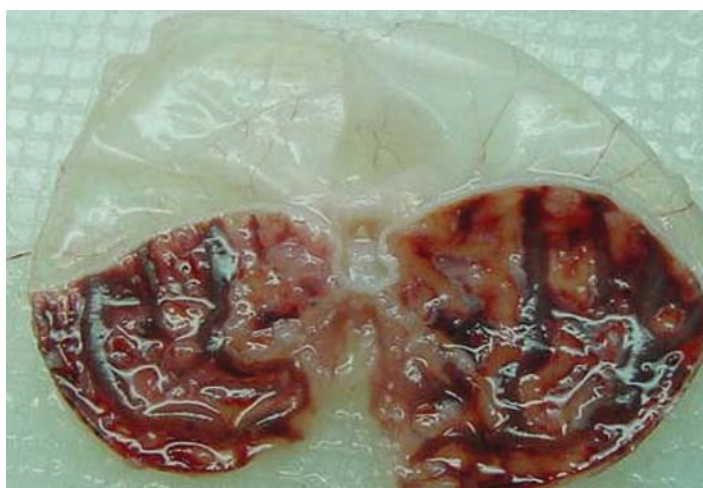


Figure 1. Control, gastric mucosal damage, 10% Tween 20[®] given orally 30 min before absolute ethanol. Severe lesions of the corpus are caused by absolute ethanol.

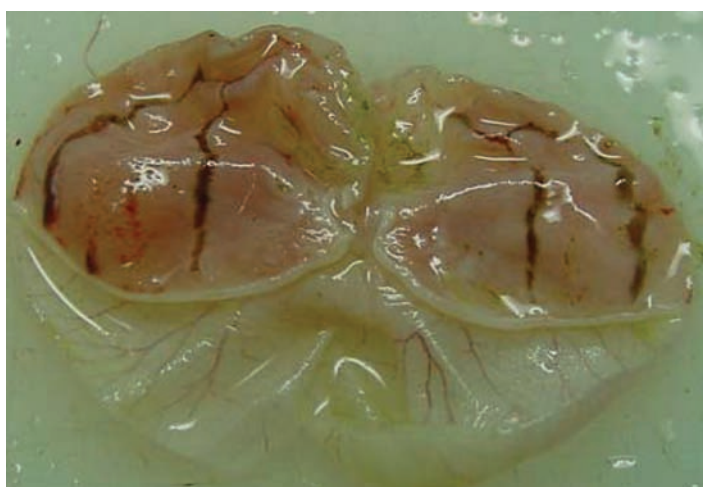


Figure 2. Gastric cytoprotection of *O. basilicum* oil extract administered 30 min before absolute ethanol reduced the formation of gastric lesions.

contrast, pre-treatment with alcoholic *O. basilicum* extract or with cimetidine significantly inhibited ($p < 0.05$) the formation of ethanol-induced gastric lesions to a great extent (Table 1 and Figure 2). The severity of ulcers is reflected in the ulcer area, which was significantly lower ($p < 0.05$) in the pre-treated *O. basilicum* or cimetidine groups compared to the 10% Tween 20[®] control of ulcer rats.

Microscopical Examination

Rats pre-treated with 10% Tween 20[®] (control) 30 min before administration of absolute ethanol showed

significantly ($p < 0.05$) severe acute gastric ulcerations (Figure 3). The lesions consisted of extensive haemorrhagic necrotic patches involving the full mucosal layer, hyperemia, prominent deep submucosal edema as well as leucocyte infiltration and severe congestion of vessels, disruption and desquamation of the surface epithelium. The submucosa was markedly thickened by edema. Rats pre-treated with *O. basilicum* extract or cimetidine showed marked reduction in gastric damage, submucosal edema and submucosal leucocyte infiltration compared to the control group (Figure 4).

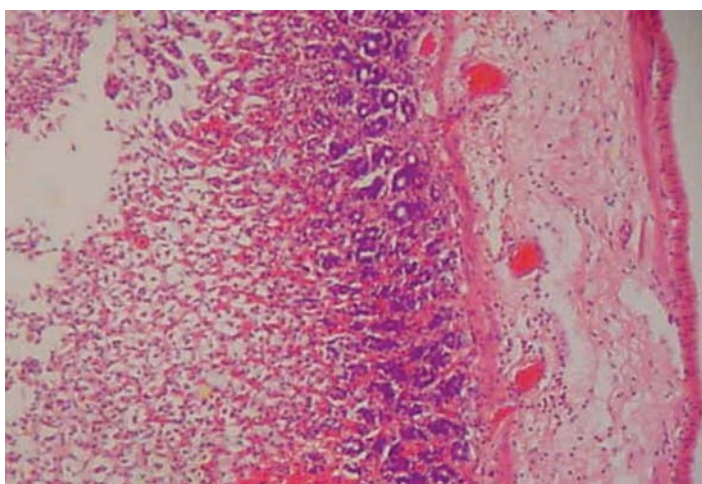


Figure 3. Histological study of the absolute alcohol-induced gastric mucosal damage in control animals (pretreated with 10% Tween 20[®]). Severe disruption of the surface epithelium and necrotic lesions penetrate deeply into mucosa and extensive edema of submucosa and leucocyte infiltration are present (H&E stain).

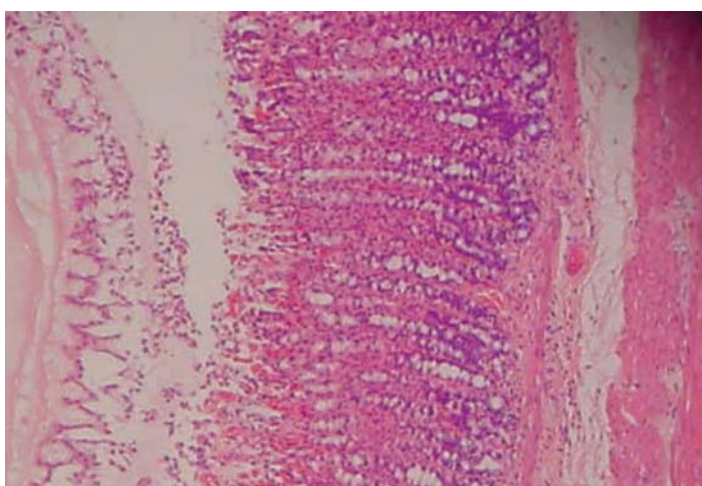


Figure 4. Histological study of the absolute alcohol-induced gastric mucosal damage in animals pretreated with extract (500 mg kg^{-1}). Mild disruptions of surface epithelium of gastric mucosa. Reduction of submucosal edema and leucocytes infiltration (H&E stain).

DISCUSSION

The ethanol gavage method of inducing gastric lesions is a rapid and convenient way of screening plant extracts for anti-ulcer potency. Cytoprotection is assessed in terms of the absence or reduction in macroscopically and microscopically visible lesions. This study showed that oral administration of alcoholic *O. basilicum* extract or cimetidine significantly reduced ($p < 0.05$) the formation of gastric lesions induced by absolute ethanol given 30 min later. The UA was markedly decreased in rats pretreated with *O. basilicum* extract. The cytoprotective effect was confirmed by histological examination that showed protection of mucosa and reduction of mucosal hyperemia, congestion, submucosal edema and haemorrhage. Inflammatory cell infiltration and deep mucosal necrosis were absent.

Disturbances in gastric secretion, damage to gastric mucosa, alterations in permeability, gastric mucus depletion and free-radical production are reported to be the pathogenic effect of ethanol (Salim 1990). *O. basilicum* extract offered significant protection against this absolute ethanol-induced ulceration. Ethanol-induced gastric lesion formation may be due to stasis in gastric blood flow, hence contributing to the development of the haemorrhage and necrotic aspects of tissue injury (Guth *et al.* 1984). It has also been reported that leukotriene antagonist and 5-lipoxygenase inhibitors are capable of inhibiting alcohol induced gastric ulceration in rats (Parnham & Brune 1987), so the protection afforded by the *O. basilicum* extract against alcohol could also be due to inhibition of the 5-lipoxygenase pathway or leukotriene antagonistic activity (Singh 1999a). *O. basilicum* blocks both cyclooxygenase and lipoxygenase pathways of arachidonic acid metabolism and could therefore be used as an anti-inflammatory agent (Singh 1999b). The lipoxygenase inhibiting, histamine antagonistic and antisecretory effects of the oil could probably contribute towards anti-ulcer activity. *O. basilicum* oil could be considered to be a drug of natural origin which possesses both anti-inflammatory and anti-ulcer activity (Tan *et al.* 2002; Goel 2005).

Cimetidine was used here as a reference anti-ulcer drug. Cimetidine significantly decreases the UA. It has been suggested (Tatsuta *et al.* 1986) that cimetidine may only be effective in healing gastric ulcers associated with a high level of gastric acid secretion and is ineffective against those associated with hypochlorhydria. Similarly, cimetidine protects against mucosal ulceration in experimental models (Guth *et al.* 1979). Mucosal protection was shown only by doses of cimetidine that significantly reduced acid secretion (Utley *et al.* 1985). In conclusion, it appears that *O. basilicum* possessed antiulcerogenic

activity; however, further investigations are required to isolate the active components of this extract to elucidate the exact mechanism of anti-ulcerogenic activity.

ACKNOWLEDGMENT

This study was financially supported by the University of Malaya through a grant: 06-02-03-1026 (Oracle 8361026).

Date of submission: November 2006

Date of acceptance: May 2007

REFERENCES

- Adami, E, Marzzil-Uberti, E & Turba, C 1964, 'Pharmacological research on gefarnate, a new synthetic isoprenoid with an antinuclear action', *Archives Internationales de Pharmacodynamie et de Therapie*, vol. 147, pp. 113-145.
- Agrawal, P, Rai, V & Singh, RB 1996, 'Randomized placebo-controlled, single blind trial of holy basil leaves in patients with non-insulin-dependent diabetes mellitus', *International Journal of Clinical Pharmacology*, vol. 34, no. 9, pp. 406-409.
- Asha, MK, Prashanth, D, Murali, B, Padmaja, R & Amit, A 2001, 'Anthelmintic activity of oil of *O. sanctum* and eugenol', *Fitoterapia*, vol. 72, no. 6, pp. 669-670.
- Barbara, L, Corinaldesi, R, Giorgi-Conciato, M, Luchetta, L & Busca, G 1974, 'Mechanism of action of gefarnate in the light of the latest data on digestive physio-pathology', *Current Medical Research and Opinion*, vol. 2, no. 7, pp. 399-410.
- Best, R, Lewis, DA & Nasser, N 1984, 'The anti-ulcerogenic activity of unripe plantain banana (*Musa spp.*)', *British Journal of Pharmacology*, vol. 82, no. 1, pp. 107-116.
- Dasgupta, T, Rao, AR & Yadava, PK 2004, 'Chemomodulatory efficacy of basil leaf (*Ocimum basilicum*) on drug metabolizing and antioxidant enzymes, and on carcinogen-induced skin and forestomach papillomagenesis', *Phytomedicine*, vol. 11, nos. 2-3, pp. 139-151
- Dharmani, P, Kuchibhotla, VK, Maurya, R, Srivastava, S, Sharma, S & Palit, G 2004, 'Evaluation of anti-ulcerogenic and ulcer-healing properties of *Ocimum sanctum* Linn', *Journal of Ethnopharmacology*, vol. 93, nos. 2-3, pp. 197-206.
- Dillman, RO, Soori, G & DePriest, C 2003, 'Treatment of human solid malignancies with autologous activated lymphocytes and cimetidine: a phase II trial of the Cancer Biotherapy Research Group', *Cancer Biother Radiopharm*, vol. 18, pp. 727-733.
- El-Abhar, HS, Abdullah, DM & Saleh, S 2003, 'Gastro-protective activity of *Nigella sativa* oil its constituent, thymoquinone, against gastric mucosal injury induced by ischaemia reperfusion

- in rats', *Journal of Ethnopharmacology*, vol. 84, nos. 2–3, pp. 251–258.
- Goel, RK, Sairam, K, Dorababu, M, Prabha, T & Rao, CV 2005, 'Effect of standardized extract of *Ocimum sanctum* Linn on gastric mucosal offensive and defensive factors', *Indian Journal of Experimental Biology*, vol. 43, no. 8, pp. 715–21.
- Guenther, E 1952, *The essential oils*, D. Van Nostrad Co., Inc., New York.
- Guth, PH, Aures, D & Paulsen, G 1979, 'Topical aspirin plus HCl gastric lesions in the rat, cytoprotective effect of prostaglandin, cimetidine, and probanthine', *Gastroenterology*, vol. 76, no. 1, pp. 88–93.
- Guth, PH, Paulsen, G & Nagata, H 1984, 'Histologic and microcirculatory changes in alcohol-induced gastric lesions in the rat effect of prostaglandin cytoprotection', *Gastroenterology*, vol. 87, no. 5, pp. 1083–1090.
- Hast, R, Bernell P & Hansson, M 1989, 'Cimetidine as an immune response modifier', *Med. Oncol. Tumor Pharmacother*, vol. 6, pp. 111–113.
- Hollander, D, Tarnawski, A, Krause, WJ & Gergely, H 1985, 'Protective effect of Sucralfate against alcohol-induced mucosal injury in the rat', *Gastroenterology*, vol. 88, no. 1, pp. 106–174.
- Ilori, M, Sheteolu, AO, Omonigbehin, EA & Adeneve, AA 1996, 'Antidiarrhoeal activities of *O. gratissimum*', *Journal of Diarrhoeal Diseases Research*, vol. 14, no. 4, pp. 283–285.
- Ito, M, Segami, T, Inaguma, K & Suzuki, Y 1994, 'Cimetidine and omeprazole accelerate gastric ulcer healing by an increase in gastrin secretion', *European Journal of Pharmacology*, vol. 263, no. 3, pp. 253–259.
- Jakobisiak, M, Lasek W & Golab, J 2003, 'Natural mechanisms protecting against cancer', *Immunol. Letter*, vol. 90, pp. 103–122.
- Kauffman, GL & Grossman, MI 1978, 'Prostaglandin and cimetidine inhibit the formation of ulcers produced by parenteral salicylates', *Gastroenterology*, vol. 75, no. 6, pp. 1099–1102.
- Konturek, SJ, Radecki, T, Brzozowski, T, Drozdowicz, D, Piastucki, I, Muramatsu, M, Tanaka M & Aihara, H 1986, 'Antiulcer and gastroprotective effects of solon, a synthetic flavonoid derivative of sophoradin', *European Journal of Pharmacology*, vol. 125, no. 2, pp. 185–192.
- Lima, ZP, Severi, JA, Pellizzon, CH, Brito, AR, Solis, PN, Caceres, A, Giron, LM, Vilegas, W & Hiruma-Lima, CA 2006, 'Can the aqueous decoction of mango flowers be used as an antiulcer agent?', *Journal of Ethnopharmacology*, vol. 106, pp. 29–37.
- Maity, TK, Mandal, SC, Saha, BP & Pal, M 2000, 'Effect of *O. sanctum* roots extract on swimming performance in mice', *Phytotherapy Research*, vol. 14, no. 2, pp. 120–121.
- Morimoto, Y, Shimohara, K & Oshima, S 1991, 'Effects of the new anti-ulcer agent KB-5492 on experimental gastric mucosal lesions and gastric mucosal defensive factors, as compared to those of teprenone and cimetidine', *Japanese Journal of Pharmacology*, vol. 57, pp. 495–505.
- Nadkarni, KM 1976, *Indian material medica*, Popular Prakashan, Bombay, India.
- Njar, VC, Adesanwo, JK & Raji, Y 1995, 'Methyl angolensate: the antiulcer agent of the stem bark of *Etandrophragma angolense*', *Planta Medica*, vol. 61, no. 1, pp. 91–92.
- Osuagwu, FC, Oladejo, OW, Imosemi, IO, Adewoyin, BA, Aiku, A, Ekpo, OE, Oluwadara, OO, Ozegbe, PC & Akang, EE 2004, 'Wound healing activities of methanolic extracts *Ocimum gratissimum* leaf in Wistar rats — a preliminary study', *African Journal of Medicine and Medical Science*, vol. 33, no. 1, pp. 23–26.
- Pandian, RS, Anuradha, CV & Viswanathan, P 2002, 'Gastroprotective effect of fenugreek seeds (*Trigonella foenum graecum*) on experimental gastric ulcer in rats', *Journal of Ethnopharmacology*, vol. 81, no. 3, pp. 393–397.
- Parnham, MJ & Brune, K 1987, 'Agents actions', vol. 21, pp. 232.
- Salim, AS 1990, 'Removing oxygen-derived free radicals stimulates healing of ethanol induced erosive gastritis in the rat', *Digestion*, vol. 47, no. 1, pp. 24–28.
- Singh, S 1999a, 'Evaluation of gastric anti-ulcer activity of fixed oil of *O. basilicum* Linn and its possible mechanism of action', *Indian Journal of Experimental Biology*, vol. 37, pp. 253–257.
- Singh, S 1999b, 'Mechanism of action of anti-inflammatory effect of fixed oil of *O. basilicum* Linn', *Indian Journal of Experimental Biology*, vol. 37, pp. 248–252.
- Singh, S, Majumdar, DK & Yadav, MR 1996, 'Chemical and pharmacological studies on fixed oil of *O. sanctum*', *Indian Journal of Experimental Biology*, vol. 34, no.12, pp. 1212–1215.
- Singh, S & Majumdar, DK 2005, 'Antibacterial activity of *Ocimum sanctum* L. fixed oil', *Indian Journal of Experimental Biology*, vol. 43, no. 9, pp. 835–837.
- Suppakul, P, Miltz, J, Sonneveld, K & Bigger, SW 2003, 'Antimicrobial properties of basil and its possible application in food packaging', *Journal of Agricultural & Food Chemistry*, vol. 51, no. 11, pp. 197–207.
- Tan, PV, Dimo, T & Dongo, E 2000, 'Effects of methanol, cyclohexane and methylene chloride extracts of *Bidens pipsa* on various gastric ulcer models in rats', *Journal of Ethnopharmacology*, vol. 73, pp. 415–421.
- Tan, PV, Nyasse, B, Dimo, T & Mezui, C 2002, 'Gastric cytoprotective anti-ulcer effects of the leaf methanol extract of *Ocimum suave* (Lamiaceae) in rats', *Journal of Ethnopharmacology*, vol. 82, nos. 2-3, pp. 69–74.
- Tatsuta, M, Iishi, H & Okuda, S 1986, 'Effects of cimetidine on the healing and recurrence of duodenal ulcers and gastric ulcers', *Gut*, vol. 27, no. 10, pp. 1213–1218.
- Uteley, RJ, Salim, AS & Carter, DC 1985, 'Effects of cimetidine and omeprazole on aspirin- and taurocholate-induced gastric mucosal damage in the rat', *Gut*, vol. 26, no. 8, pp. 770–775.

New Reaction Kinetic Model Derived from Molecular Dynamics Simulation Data on Non-linearity of Rate Coefficients and Their Relation to Activity Coefficients

C. G. Jesudason¹

Molecular dynamics reaction simulation showed that the rate constant is not constant over the concentration profile of reactants and products over a fixed temperature regime, and this variation is expressed in terms of the defined reactivity coefficients. The ratio of these coefficients for the forward and backward reactions were found to equal that of the activity coefficient ratio for the product and reactant species. A theory was developed to explain kinetics in general based on these observations. Several other theorems had first to be developed, most striking of all was the inference that the excess Helmholtz free energy was the thermodynamical function which had a direct relation to these activity factors than the Gibbs free energy. The theory is applied to a class of ionic reactions which could not be rationalized using the standard Bjørn-Bjerrum theory of ionic reactions.

Key words: elementary reaction; rate constant; activity and reactivity coefficients; elementary and ionic; reactions; pre-equilibrium; kinetic model; simulation; molecular dynamics

A model of a chemical reaction is presented and the forward and reverse rates were monitored. By examining the rates as functions of concentration whilst fixing the value of the constant at any fixed temperature in accordance with general definition, relationships were discovered relating the activity coefficient ratio with the so-called reactivity coefficients; as ratios are involved, there was no immediate reason to suppose that they had to be equal. Indeed, it was shown that there was equality in terms of a non-constant multiplicative factor or function. This factor was determined by considerations concerning the thermodynamics of the species; both the Helmholtz and Gibbs free energies were considered in attempting to elucidate the factors. By referring to the excess Helmholtz free energies determined from previous work for the Lennard-Jones (LJ) fluid (Nicolas *et al.* 1979), one could infer which was the correct form for this multiplicative function. This choice also implies that the two-stage kinetic model is the more consistent one compared with the single-stage model for reaction systems, which was utilized in the Bjørn-Bjerrum theory. One might ask object orientated questions such as (i) Why are we doing this research? and (ii) What are the issues that will be addressed? In this case, the answer to (i) was the discovery, quite unexpectedly, of the connection between the activity and ‘reactivity coefficients’ not detailed in standard kinetics textbooks, and certainly here a different interpretation is given. As with any unexpected result of such a striking kind, it is natural to create a theory to account for the observation,

and if possible, to verify this theory with experimental or other evidence. This quest lead to answering (ii) above: the issues addressed include the relating of the reactivity and activity coefficients, the need to clarify that the Helmholtz rather than the Gibbs free energy is related exponentially to the coefficients, and also to predictions in kinetic theory. The current literature and definition, whilst mentioning activity coefficients and thermodynamics, have not formulated the problem in a way that utilizes the reactivity coefficients and the 2-stage theory presented here (Wojciechowski & Rice 2003; Mortimer & Taylor 2002; Pilling & Seakins 2005).

In order to rule out non-elementary processes which would interfere with the equations, it was found convenient to utilize a model where the region of transition from dimer to atom and vice-versa was separated. Previous work has detailed a hysteresis model of a simple dimer reaction (Jesudason 2005) where the coordinates for molecular formation r_f and breakdown r_b are not at the same vicinity, as shown in Figure 1. If both these points coincide, then one could in principle define a volume region about the point $r_f = r_b$ that would serve as the transition state pre-equilibrium *TS*, suggesting a composite reaction such as:



which is therefore not strictly elementary since Equation 1 is a summation of elementary steps to yield a net reaction.

¹ Chemistry Department, Faculty of Science, University of Malaya, 50603 Kuala Lumpur, Malaysia
(e-mail:jesu@um.edu.my)

The Eyring model is an example of such a scheme (Eyring *et al.* 1980), where in reversible potentials, a simply-connected surface S separates reactant and product regions, with the TS region being defined over a volume region $S \cdot \delta r$ where either products or reactants can be formed. The current model, on the other hand, does not allow a molecule to move back to the atomic state about r_f , and likewise at r_b , there is no way in which the disintegration to atomic states could form molecules about that coordinate. This is due to the hysteresis mechanism, which implies a clear separation in one direction (either to products or reactants respectively), so that in this type of reaction, there is less ambiguity with respect to the presence of composite processes.

Modern reaction theories have eliminated the transition state (Kosloff 1996). In this model, the definition of atom and molecule allows for complete monitoring based on the algorithm given by Equations 3–6. The other references already mentioned give details of the method.

The simulation model is a dimeric particle reaction:



at the LJ supercritical regime ($T^* = 8.0$, $0.03 < \rho < 1.1$) in a range of equilibrium fluid states. Details of the mechanism have already been described and will not be repeated here (Jesudason 2006a,b,c). In the current study, the potentials given in Figure 1 are used. In this model, two free atoms ‘react’ at r_f where a switch mechanism converts the potential to the harmonic intermolecular

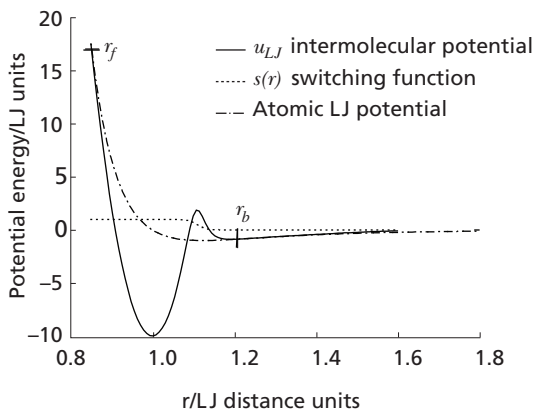


Figure 1. Potentials used for this work.

potential. The molecule ‘breaks’ at r_b where the potential reverts to the LJ type. An atom at a distance r to another particle possesses a mutual potential energy u_{LJ} where:

$$u_{LJ} = 4\epsilon \left[\left(\frac{\sigma}{r} \right)^{12} - \left(\frac{\sigma}{r} \right)^6 \right] \quad \text{for } r \leq r_s \quad (3)$$

$$u_{LJ} = a_{ij} (r - r_c)^2 + b_{ij} (r - r_c)^3 \quad \text{for } r_s \leq r \leq r_c$$

$$u_{LJ} = 0 \quad \text{for } r > r_c$$

and where $r_s = (26/7)^{1/6} \sigma$ (Hafskjold & Ikeshoji, 1995). At r_f , the potential is switched to the molecular potential given by:

$$u(r) = u_{vib}(r)s(r) + u_{LJ} [1 - s(r)] \quad (4)$$

where $u_{vib}(r)$ is the vibrational potential given by Equation 6 below and the switching function $s(r)$ has the form given by Equation 5.

$$s(r) = \frac{1}{1 + \left(\frac{r}{r_{sw}} \right)^n} \quad (5)$$

where,

$$\begin{cases} s(r) \rightarrow 1 & \text{if } r > r_{sw} \\ s(r) \rightarrow 0 & \text{for } r < r_{sw} \end{cases}$$

The switching function becomes effective when the distance between the atoms approaches the value r_{sw} (see Figure 1). The intramolecular vibrational potential $u_{vib}(r)$ for a molecule is given by:

$$u_{vib}(r) = u_o + \frac{1}{2}k(r - r_o)^2 \quad (6)$$

LJ reduced units are used throughout this work unless stated otherwise. The details of the parameters have been given elsewhere (Jesudason 2006c)

METHOD AND RESULTS

Details of the runs have been described elsewhere (Jesudason 2006c). Typical runs of 10 million (10M) time steps were performed at each general system particle density ρ (where ρ refers to the particle which is either free or part of a molecule), the first 200,000 steps were discarded so that proper equilibration could be achieved for our data samples. The sampling methods have been previously described (Hafskjold & Ikeshoji 1995) where sampling of all data variables were done each 20th time step and where the data were averaged and written into a dump file of 100 dumps for the 10M million time steps. The averaged values in each dump were further averaged to yield the final averages and standard errors. Dynamical quantities however had to be sampled at each time step $\delta t^* = 0.00005$. In view of the abnormally high temperatures—not hitherto encountered in almost all simulation studies—this time step value was found to be not too small. The system was thermostated at the ends of the molecular dynamics (MD) cell only, but very similar unpublished results with less variable fluctuation was obtained by thermostating each layer with strict conservation of momentum during the thermostating

process (Ikeshoji & Hafskjold 1994) which involved solving coupled equations for each thermostated layer. The reason was to mimic the actual experimental situation where the reservoirs occurred at the boundary location of the system. It is surmised that reservoir boundary conditions might play a pivotal role in determining the product outcomes of reactions sensitive to energy fluctuations. The term *sde* in the figure captions refer to the standard error.

Numerical Computations

The equilibrium constant K_{eq} can be determined by extrapolative methods (Jesudason 2006c) to zero density of the concentration ratio, K_c defined as:

$$K_c = \frac{x_{A_2}}{x_A^2} \quad (7)$$

The resulting constant was:

$$K_{eq} = \lim_{\rho \rightarrow 0} K_c = 0.061 \pm 0.02 \text{ LJ units} \quad (8)$$

for $T^*=8$ (all units scaled to LJ units. The activity coefficient ratio $\Phi_e = \frac{\gamma_{A_2}}{\gamma_A^2}$ is calculated for the other densities using:

$$K_{eq} = K_c \frac{\gamma_{A_2}}{\gamma_A^2} = K_c \Phi_e \quad (9)$$

The ratio of activity coefficients Φ_e is shown in Figure 2, where Φ_k refers to the same ratio determined by another kinetic method which is defined in Equation 13 but not described in detail here but elsewhere (Jesudason 2006c).

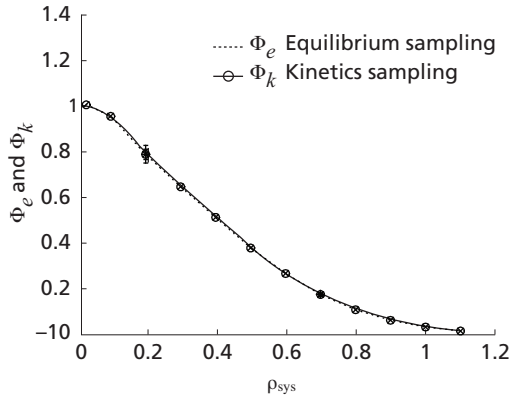


Figure 2. Variation of Φ_e and Φ_k with ρ , which is the system number density at LJ temperature $T^*=8.0$ where there is empirically complete coincidence within experimental uncertainty.

Relationship between Coefficients and Their Ratios

From the rates determined previously, we can define the following γ 's. The forward and backward rate constant (respectively k_1 and k_{-1} varies with the system density as:

$$\begin{aligned} Q &= k_1^0 \gamma_A'^2 = k_1 \\ R &= k_{-1}^0 \gamma_{A_2}' = k_{-1} \end{aligned} \quad (10)$$

where γ_A' and γ_{A_2}' are defined as 'reactivity' coefficients, and where the forward rate per unit volume of dimer formation is given by $Q[A]^2$ and the reverse rate as $R[A_2]$, where these rates can be monitored by the computer simulation. Obviously, $\gamma_A' = \frac{Q}{k_1^0}$ and $\gamma_{A_2}' = \frac{R}{k_{-1}^0}$ are computable since all the other terms are. These coefficients are graphed in Figure 3. The results for the low density limit extrapolation were as follows:

$$\lim_{\rho \rightarrow 0} Q = k_1^0 = 0.870 \pm 0.06 \text{ LJ units} \quad (11)$$

$$\lim_{\rho \rightarrow 0} R = k_{-1}^0 = 14.32 \pm 0.1 \text{ LJ units} \quad (12)$$

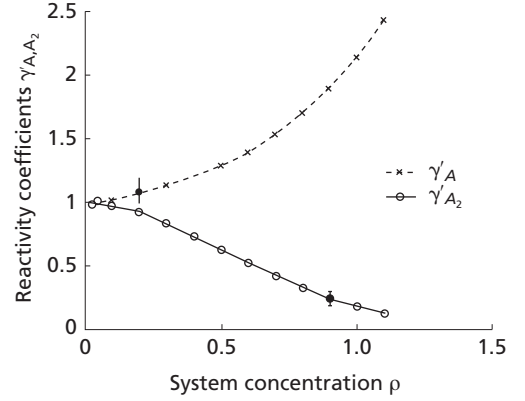


Figure 3. Variation of reactivity coefficients γ_A' and γ_{A_2}' with ρ , the system number density at temperature $T^*=8.0$.

and taking ratios lead to the following:

Observation 1.

$$\Phi_k = \frac{\gamma_{A_2}'}{\gamma_A'^2} \quad (13)$$

is coincident with Φ_e within computational accuracy for all physically feasible ρ .

This is an remarkable and unexpected result which is based on Figure 2, where over the entire system concentration profile ρ , there is a coincidence of Φ_e and Φ_k within the error bars provided in the figure. It is to be noted that the computations were carried out for the points indicated in the graphs over typically steps of 0.1 in ρ . Each ρ coordinate represents an entire simulation. Further properties issue forth such as:

Lemma 1. The general solution to Observation 1 is:

$$\begin{aligned} \gamma_A^2 c(\rho) &= \gamma_A'^2 \\ \gamma_{A_2} c(\rho) &= \gamma_{A_2}' \end{aligned} \quad (14)$$

where γ_A and γ_{A_2} are the activity coefficients.

Proof. The reactivity coefficients for any species X is known i.e. $\gamma'_X = \gamma'_X(\rho)$ and γ_A, γ_{A_2} exists by hypothesis (Observation 1). Then $\exists d_i$ such that $\gamma'_A d_i = \gamma'^2_A d_i$ and similarly $\gamma_{A_2} d'_i = \gamma'^2_{A_2} d_i$. Observation 1 implies $\left(\frac{d'_i}{d_i} = 1\right)$ for all ρ or $d'_i = d_i$ for every ρ_i . Define the function $c: \rho_i \rightarrow d_i$ or $c = c(\rho)$.

It is suggestive that the γ' and γ coefficients for the respective species might be equated to be the same, implying a constant $c(\rho)$. It can be shown (Jesudason 2006b) that the Gibbs-Duhem condition demands $c(\rho) = \text{constant}$ if we use the γ' coefficients as actual activity coefficients. The inference that this is not the correct assumption comes from extra information of simulation data of the LJ fluid activity coefficients relative to the boundary conditions imposed. If $c(\rho)$ is a more complex function than unity, then $\gamma'_A = \gamma_A c(\rho)^{1/2}$, $\gamma'_{A_2} = \gamma_{A_2} c(\rho)$. The problem reduces to a method of deriving $c(\rho)$ to obtain the desired activity coefficients, because the γ' coefficients are experimentally obtainable.

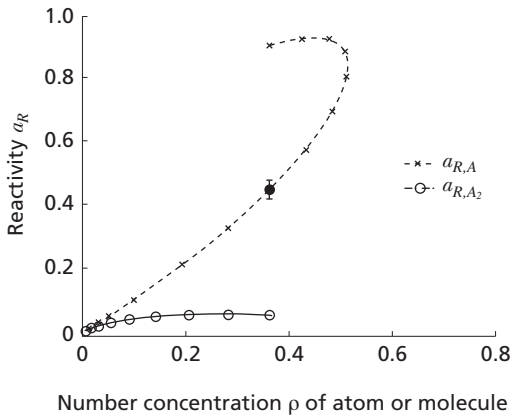


Figure 4. Variation of reactivity coefficients a_A and a_{A_2} with ρ_A and ρ_{A_2} , the actual number density of the species concerned at LJ temperature $T^*=8.0$ with $sde = 10, 40$ respectively, for the uncertainty in a_A and a_{A_2} .

The plot of the γ' reactivity coefficient is given in Figure 3 as a function of average system density. Both coefficients extrapolate to unity at zero density. While the reactivity coefficient of A is larger than unity, that of A_2 is smaller than unity, and one might expect such behaviour to arise from the differing potentials and net surface area to volume ratio that exists for these two species. The reactivity of species p , a_p is defined by $a_p = \gamma'_p \rho_p$ where ρ_p is the concentration (e.g. number density) of species p . A plot of the variation of these quantities appears in Figure 4, where the densities refer to the actual number density of the concerned species and not to the general system density ρ .

The $c(\rho)$ Scaling Function

One can expect the activity coefficient of the A atom to be approximately that of the LJ fluid at the same density and temperature at low dimer concentrations. A rationale must be provided on how to estimate this quantity from available data. Some data exists (Nicolas *et al.* 1979; Johnson *et al.* 1993) for the LJ fluid up to $T^*=6.0$. The parameters for the various estimates for the monomer activity was scanned from the $x(i)$ values in Table 4. of Nicolas *et al.* (1979) and fitted into the equations found in Johnson *et al.* (1993). The residual or excess Helmholtz free energy in reduced units, which is the difference between the ideal gas value and the actual value is given by Johnson *et al.* (1993, Equation 5)

$$A_r^* = \sum_{i=1}^8 \frac{a_i \rho^{*i}}{i} + \sum_{i=1}^6 b_i G_i \quad (15)$$

with the pressure having the expression:

$$P^* = \rho^* T^* + \sum_{i=1}^8 a_i \rho^{*(i+1)} + \sum_{i=1}^6 b_i \rho^{*(2i+1)} \quad (16)$$

with $F = \exp(-\gamma \rho^{*2})$, γ being a non-linear adjustable parameter. The excess free energy G_r^* is given by:

$$G_r^* = A_r^* + \frac{P^*}{\rho^*} - T^* \quad (17)$$

The reduced unit variables are denoted by * superscripts, and the a_i and b_i coefficients are given as complex polynomials in $x(i)$ and T^* in the tables in Johnson *et al.* 1993. It was found that at $T^*=6$, a good value for γ (to the nearest digit) was 2.7 which yielded the fitting pressure of 12.7931, close to the experimental value of 12.43(2) in the phase diagram. The simulations here were off-scale at $T^*=8.0$, but nevertheless the value of γ given above was adopted for estimating the excess free energies at the simulation temperature as well as the atomic γ_A coefficients according to the theoretical model below.

To estimate the activity coefficient of the LJ fluid, one must refer to the excess work done on the particle $\delta w_{e,x,i}$; where conventionally, the activity coefficient γ_i refers to this work. Robbins (1972, Chap.1, p. 4–8) where $kT \ln \gamma_i = \delta w_{e,x,i}$; shows that the term $kT \ln c_i$ refers to the external work done on the system to the state concerned, and this work is also equivalent to introducing unit amount of substance i from the standard state condition of unit activity coefficient. The work done for a perfect fluid on the system is:

$$\delta w = -NkT \ln \frac{V_2}{V_1} = -NkT \ln \frac{c_2}{c_1} \quad (18)$$

between states 2 and 1. Under the typical convention $c_1 \rightarrow 0$, $\gamma_1 \rightarrow 1$, the standard state c_1 leads to a singularity in this limit. Write $\delta c_i M_i = 1$ for any small value of c_1 of

amount δc_1 when $\gamma_i \rightarrow 1$. So, $M_i \rightarrow \infty$ but for any small δc_i , it is a large finite number. The form of the chemical potential, if rescaled to conform to these limits must be of the form:

$$\mu'_i = \mu_i^0(T) + kT \ln \frac{c_i \gamma_i}{(1 \text{Unit})} \quad (19)$$

Heat-work Interchange and Helmholtz Energy

An approximate value for the multicomponent activity coefficient may be derived from the Helmholtz free energy for single systems by considering the work-heat transformations. The single component Helmholtz free energy A is given in standard form as $A = U - TS$, where its differential $dA = dw - SdT$ implies that at constant T , the work done on the system dw is the so-called external work (such as the $P - V$ work connected with compression) where for fluids, $dA = PdV = dw$. From this, a theorem follows which may be stated thus:

Theorem 1. *The heat absorbed by a system during an isothermal transition is equivalent to that which is absorbed by an ideal system and the heat absorbed when an intermolecular potential is introduced within the system.*

From this theorem, we may derive a corollary.

Corollary 1. *The activity coefficient for a single component system γ_i relative to the standard state is given by*

$$\gamma_i = \exp\left(\frac{\delta A_{ext}}{kT}\right).$$

Details of proofs may be derived from Jesudason (2006b). The term activity coefficient and reactivity coefficient used in the figures and the text are synonymous because to first order they are equated in this particular model, due to the very large r_b value that implies that the dissociated molecule would have a spatial distance approximately that of free atoms, and likewise the molecule when formed has a spatial dimension which is typical of that of an average molecular configuration.

In the dimeric reaction $2A \rightleftharpoons A_2$ for lower A_2 concentrations (lower ρ values), the limit $\gamma_{A, \text{pure}}$ (pure phase) $\rightarrow \gamma_{A, \text{reaction}}$, the activity coefficient for the reactive system A is exactly that as for the single component fluid because the force fields acting on A are essentially the same as for the pure component, except there would be clumps of A atoms held together by intermolecular harmonic potential whenever A_2 is present, but these internal forces do not affect the external forces acting on the A atom. This identification and limit is used to choose the general form of γ vs. ρ curve for atom and dimer, since the two different assumptions that are used leads in one case to semi-quantitative agreement of γ_A for

the reaction and $\gamma_{A, \text{pure}}$ (pure phase), and it is therefore inferred that the system conforms better to one of the two assumptions made to derive estimates of the activity coefficients. We can infer that the results from Figure 5 is the more consistent one, by referring to the monomer situation, for which some data exists. By estimating the monomer activity from the data and inferring that the form and trend provided for the monomer at lower concentrations should be approximately that for our pure atomic species as deduced from readily available functions. This figure uses the inverse Φ convention, as detailed in Equations 34 and 35.

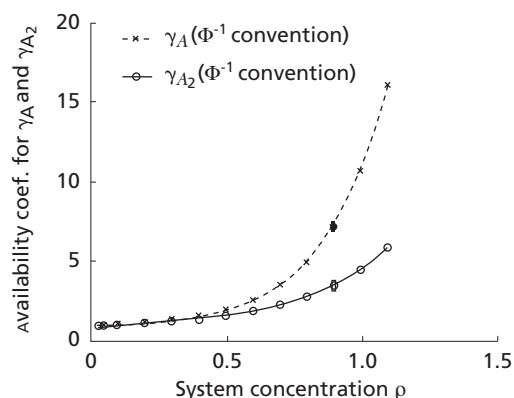


Figure 5. Activity coefficients using the inverse Φ convention due to boundary conditions.

The γ estimates are derived from Corollary 1. It is clear from Figure 6 that the activity estimates show values all greater than unity. The system ρ for this figure and all others refer to ρ_{system} , all in reduced units where $\rho_{\text{system}} = \rho_A + 2\rho_{A_2}$, where ρ_A is the number density for the monomer (Atom) and ρ_{A_2} refers to the dimer species number density in this homogeneous system at equilibrium. Figure 6 is computed for the situation $\rho_{\text{Atom}} = \rho_{\text{system}}$. Since what is being depicted is the external potential work done in bringing the atom to the system, then the forces acting on the atom can arise from either the dimer or the atoms within the system, and since the potentials are of the same LJ form for each nucleus, then we would expect this density to be the most appropriate one. If we just consider what the activity might be for the actual density of the monomer, ignoring its interaction with the dimer, then Figure 7 gives the results from the simulation results and the fitting functions for G_{res} and A_{res} where the system concentration $\rho \equiv \rho_A$. From the previous theorem, only A_{res} is relevant for the determination of the activity coefficient, but G_{res} is also plotted as a reference for comparison. Finally, if we supposed that whatever energy that is available to the monomer is lost whenever a dimer is formed from the activation energy, then the available energy per atom is given by Figure 8. What is

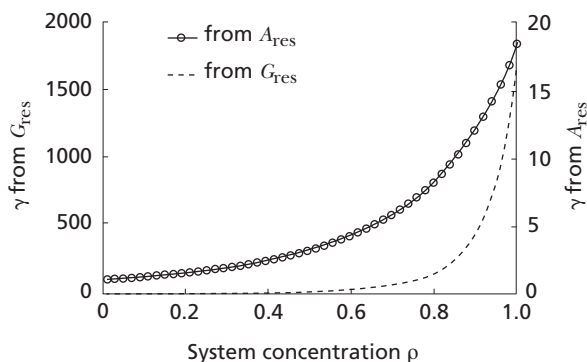


Figure 6. Computed monomer-only activity from residue Helmholtz (A) and Gibbs (G) functions.

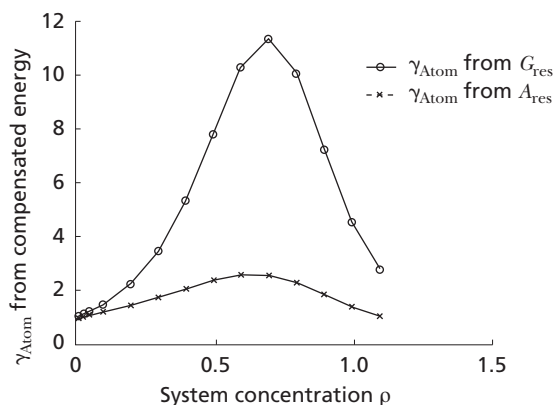


Figure 8. Estimated activities from the residual energy left after dimer formation using density distribution data from the simulations.

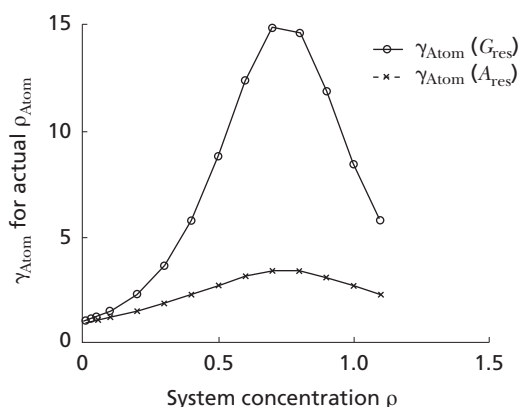


Figure 7. Computed monomer-only activity from residue Helmholtz (A) and Gibbs (G) functions.

meant in this case is that let the residual free energy per particle be F_r , where $F_r = G_{res}$ or $F_r = A_{res}$. The vacuum activation energy is 17.652. So the net energy left per particle is surmised to be $F_{res} = \frac{F_r N_A - 17.652 N_{A_2}}{N_A} = F_r - 17.652 \rho_{A_2} / \rho$ and $\gamma_{F_{res}} = \exp(F_{res} / kT)^*$ which is a measure of the available energy after dimer formation. This expression is plotted in the figure mentioned above where N_A is the number of atoms for that general system concentration in the MD cell. These figures are plotted to determine which would be the best approximation to the first order theory of elementary reactions developed here.

Kinetic Mechanisms Consonant with the Above

The proposed models for particle interactions yielding chemical reactions for the forward (F) and backward (B) steps are given in Figures 9–10 below. These models enable one to calculate the activity coefficients where one model

contradicts experimental observation whereas the other does not, in addition to corroborating the deductions of the activity from thermodynamical functions. The inverse Φ convention yields the activity coefficients given in Figure 5. On the other hand, the non-inverse Φ convention yields results for the activity coefficient given in Figure 11 according to the defining Equations 43 and 44. The present work provides an outline of how rates can determine these coefficients in principle for elementary reactions. The next section provides the broad methodology.

Proposed models from numerical data

The elementary rate constants have the form (Hänggi *et al.* 1990):

$$k_i = A(T, \Omega) \exp \frac{-E}{kT} \quad (20)$$

where E is termed the activation energy and Ω are variables intrinsic to the reaction, such as impact and structure parameters. The object here is to relate the γ' reactivity coefficients to the γ availability (activity) coefficient based on the first order single or two stage energy perturbation mechanism (Figures 9–10), respectively. Refinements include perturbing the pathway itself, and introducing a continuous potential field along the entire length of the reaction pathway where calculations to any degree of accuracy might be attempted. For both these mechanisms, A_2^* and A_2 are the states of the reactants just prior to product formation. The first order perturbation lifts the degeneracy of the $*$ levels relative to the vacuum state; in the vacuum state, no singularities are observed in the potentials. Singularities due to the perturbation arise because the product and reactant states are distinct and distinguishable, and need not have the same activity in general; the form factor $A(T, \Omega)$ is not altered to first order since they specify the type of reaction; only E is altered

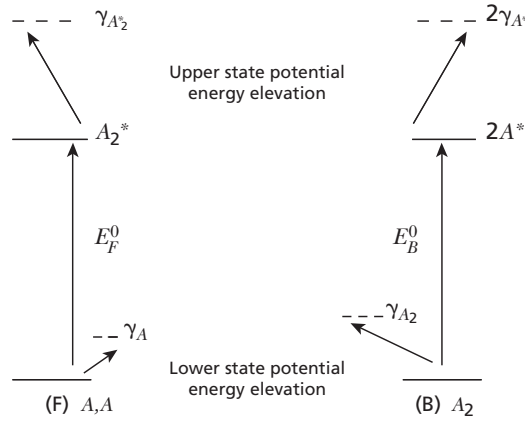


Figure 9. Single stage model with external potential interaction leading to chemical reaction, and which is similar to the elementary Bjørn-Bjerrum theory of ionic reactions where (B) denotes the backward direction and (F) the forward direction of the Dimer reaction in Equation 2. Note that the terms written above refer to the perturbation energy due to these terms as explicitly defined in Equation 21.

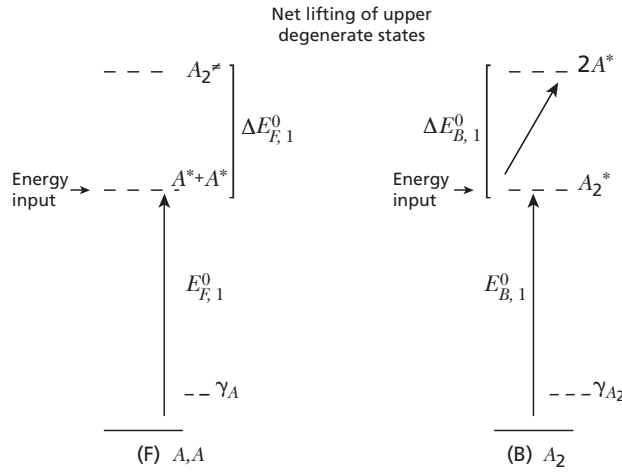


Figure 10. Double stage model with external potential interaction leading to chemical reaction, which goes beyond the single stage model and analogs where (B) denotes the backward direction and (F) the forward direction of the Dimer reaction in Equation 2. Note that the γ terms written above refer to the perturbation in energy due to these terms as explicitly defined in Equation 21.

due to the external potential that modifies the ground state energies of the particles relative to the vacuum level. The availability coefficient γ_X is expressed as:

$$\frac{\epsilon_X}{kT} = \ln \gamma_X \quad (21)$$

for any species X , and the excitation energy is written δB for species B . For what follows, ϵ always refers to an energy term associated with the activity or availability coefficient. In the single stage model, the upper X^* species is perturbed by an absolute energy amount given by γ_{X^*} in Equation 21; for the double stage model, the upper level is

perturbed by the relative energy $\Delta E_{\{FB\},2}^0$, due to the singularity induced by the change of state from product to reactant or vice-versa. The lower state for both models are perturbed (lessened) by the same factor γ_X since this is the ground state availability. It will be shown that the 2-stage relative model is the more accurate and logical, based on a comparison with estimates of the activity coefficient for the monomer or atom A . The backward activation energy ϵ_{act}^b for $A_2 \rightarrow A_{2,\text{out}}^* \rightarrow \text{Product}$ for either the 1 or 2 stage model can be written (superscript o refers to the vacuum state):

$$-\epsilon_{\text{act}}^b = -\epsilon_b^0 + \epsilon_{A_2} - \delta A_{2,\text{out}} \quad (22)$$

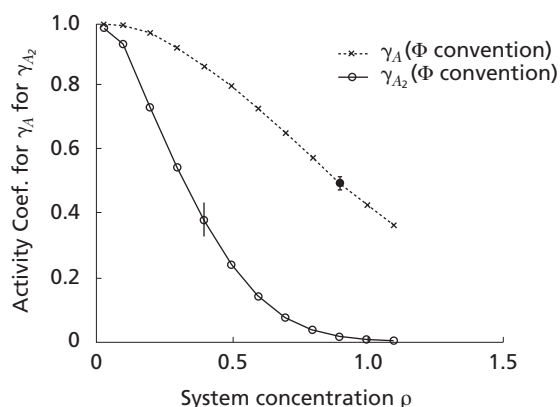


Figure 11. Φ convention determination of activity coefficients.

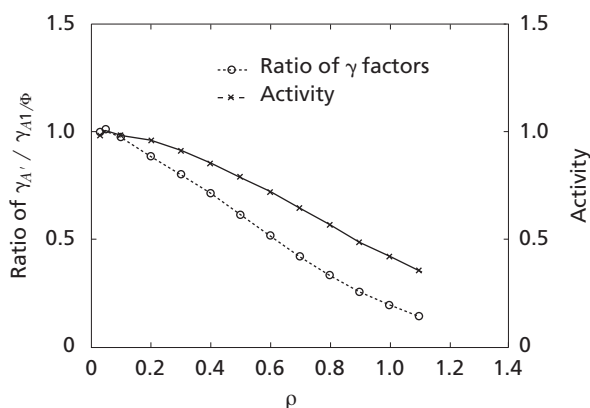


Figure 12. Availability coefficient ratios to illustrate the expected constancy of the availability coefficients of the excited species.

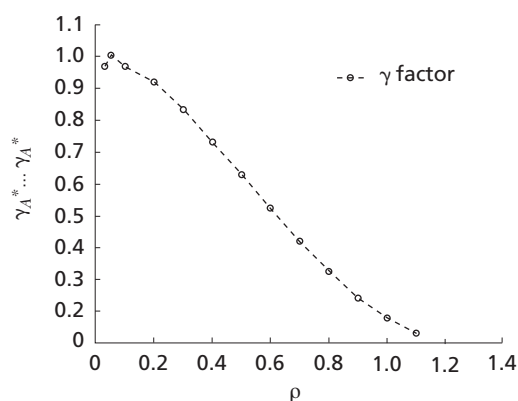


Figure 13. Excited state activity for dimer before bonding for forward rate showing relatively lower change compared to the bulk activity coefficients (which would be the square of the values given in Figure 5).

where we also write $\delta A_{2,\text{out}} = \delta A_b \cdot \delta A_b$. These terms refer to the upper state perturbation of the $A_{2,\text{out}}^*$ species. The forward model yields:

$$-\epsilon_{\text{act}}^f = -\epsilon_f^0 + \epsilon_A + \epsilon_A - \delta A_{2,\text{in}} \quad (23)$$

where $\delta A_{2,\text{in}}$ refers again to the upper energy state energy perturbations. Using Equation 21 to convert to availability, where $\delta X = kT \ln \gamma_X$, Equations 22 and 23 yield:

$$\gamma_A' \gamma_A' = \frac{\gamma_A \gamma_A}{\gamma_{A_2,\text{in}}} \quad (24)$$

On the other hand, the exact experimental condition in Observation 1 can be written $\Phi = \Phi'$ where the prime refers to the same expression in γ_X' where:

$$\gamma_{A_2}' = \frac{\gamma_{A_2}}{\gamma_{A_b} \gamma_{A_b}} = \frac{\gamma_{A_2}}{\gamma_{A_2,\text{out}}} \quad (25)$$

Hence, Equations 24 and 25 leads to the exact result:

$$\frac{\gamma_{A_2,\text{in}}}{\gamma_{A_2,\text{out}}} = \frac{\gamma_{A_2,\text{in}}}{\gamma_{A_b} \gamma_{A_b}} = 1 \quad (26)$$

or $\delta A_b \cdot \delta A_b = \delta A_{2,\text{in}}$. In view of the fact that the product/reactant potential interface is completely different from the reactant/product potential interface for this hysteresis dimer, the result of Equation 26 is indeed remarkable and may be stated as a kinetic principle:

Principle 1. *The perturbed energy required to promote reactants to products at the reactant/product potential interface is of the same magnitude as for the reverse transition of products to reactants at the product/reactant potential interface, even if these interfaces are discontinuous, i.e. are spatially and energetically distinct, for elementary reactions in equilibrium.*

Figure 1 shows that for this study the interfaces are distinct; ‘reversible’ pathways have coincident interfaces.

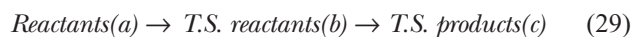
Two stage backward reaction model.

B. Process. In view of Equation 26 we can write the exact form:

$$\gamma_A = \frac{\gamma_A}{\sqrt{\gamma_{A_2,\text{out}}}} \quad (27)$$

$$\gamma_{A_2}' = \frac{\gamma_{A_2}}{\gamma_{A_2,\text{out}}} \quad (28)$$

If a complete characterization of the γ_{A_2} species were known, then $\gamma_{A_2,\text{out}}$ could be calculated from the theory presented in Section 2. Some estimates or approximations may be made to determine the γ 's. The reaction pathway for this 2 stage backward step model may be written:



When considered in isolation, (normal vacuum state analysis), there is continuity of the potentials between

states (b) and (c). On the other hand, if the environment is considered where species are either reactants or products, singularities in the energetics would develop about the same arbitrary volume of the TS of the reaction co-ordinate; for instance at (b), two atoms in proximity $A...A$ are separated by distance $\delta r_{A,A}$ and the mean activity of this state is strongly influenced by the potential $V(\delta r_{A,A})$ dependent on the $\delta r_{A,A}$ distance, in addition to the surrounding non-participatory environmental molecules $V'(r_{\text{others}})$. On the other hand, at the same vicinity (c) where the switch modifies the potentials, then the activity of the instantaneously formed molecule would be determined by $V'(r_{\text{others}})$, where $V(\delta r_{A,A})$ now represents the potential of internal coordinates not connected to the activity. An apparent discontinuity arises according to this first order treatment, which has no apparent analog in the traditional or other QM theories computed at vacuum densities. For the two stage reaction, two types of approximations for activity coefficients may be made for the forward (F) $2A \rightarrow A_2$ and backward (B) $A_2 \rightarrow 2A$ kinetic pathways and the results may be checked with the apparent activity coefficient values derived from the LJ single phase fluid.

Case B: The first order perturbation energy ($\gamma_{A_2, \text{out}}$) is:

$$E(\gamma_{A_2, \text{out}}) = 2\epsilon_{A_b} - \epsilon^*_{A_2} \quad (30)$$

where A_b denotes the product atom just dissociated from the dimer at coordinate of species A_2^* . The following approximation will be derived:

$$\delta A_{2, \text{out}} = \frac{\gamma_{A_b} \gamma_{A_b}}{\gamma_{A_2}} \quad (31)$$

where $\gamma_{A_b} \approx \gamma_A$. Clearly, $\delta A_{2, \text{out}}$ serves as a 'retardant' to the rate for positive ϵ 's in the numerator of Equation 31. Figure 10 can be correlated with Equation 29 as follows: $E_{B,1}^0$ is the activation energy to the level A_2^* which consists of two degenerate states relative to the vacuum denoted $TS(b)$ with molecule A_2 , and $TS(c)$ which refers to the two atoms $2A$ after dissociation; in real time the molecule disintegrates along the trajectory $(a) A_2 \rightarrow (b) \rightarrow (c)$ according to Equation 29. Unlike the atom, the dimer state may be characterized according to the inter particle $A-A$ distance r_{A-A} , (as well as the magnitude of the external potential). The mean external forces acting on this dimer would lead to a potential which would be to a first approximation relatively invariant, even if the internal potential and internuclear distance varies; thus we assign $\epsilon[A_2(a)] \approx \epsilon[A_2(TS,b)]$ The potential energy is utilized to overcome the activation barrier; the boundary ∂C imposes a fixed density on the system which elevates the mean potential of the reactants relative to the vacuum ground state. During the transition to the state $TS(b)$, external forces with a mean potential $\epsilon[A_2(TS)]$ would operate on the dimer; $r_b = 1.20$ for this reaction, where for a b.c.c. approximation for a LJ fluid at $\rho = 0.70$, the approximate nearest neighbouring distance is 1.22, implying that the

environment of $A(TS)$ is very close to that of the bulk or generic A atom, i.e. a typical atom with activity coefficient γ_A , so that the transition state A_2 availability coefficient for the atom $\gamma_{A,TS}$ can be equated with the bulk, $\gamma_{A,TS} \approx \gamma_A$ and the relative energy to be overcome from this TS state is $\Delta E_{B,2}^0$ where $\Delta E_{B,2}^0 \approx [2\epsilon_{A_2}(T.S.) - \epsilon_{A_2}(T.S.)]$ leading to:

$$\exp - \frac{\Delta E_{B,2}^0}{kT} \approx \left(\frac{\gamma_{A_2}}{\gamma_A \gamma_A} \right) \quad (32)$$

As $\exp - \Delta E_{B,1} = \exp - \Delta E_{B,1}^0 \gamma_{A_2}$, we have the forms for the backward rate given as:

$$\begin{aligned} k_B &\approx k_B^0 \gamma_{A_2} \frac{\gamma_{A_2}}{\gamma_{A,TS} \gamma_A} \\ &\approx k_B^0 \gamma_{A_2} \\ &\approx k_B^0 \gamma_{A_2} \Phi = k_B^0 \frac{\gamma_{A_2}}{(1/\Phi)} \end{aligned} \quad (33)$$

But Equations 32 and 33 implies:

$$\gamma'_{A_2} = \frac{\gamma_{A_2}}{\gamma_{A_2, \text{in}}} \Rightarrow \gamma_{A_2, \text{in}} = \gamma_{A_2, \text{out}} \approx \frac{1}{\Phi}$$

leading to the useful approximation:

$$\gamma_{A_2} \approx \frac{\gamma'_{A_2}}{\Phi} \quad (34)$$

From Equation 28, $\gamma_{A_2} = \gamma'_{A_2} \gamma_{A_2, \text{out}}$ so that Equation 31 follows with $\gamma_{A_b} \approx \gamma_A$. Since $\gamma_{A_2, \text{in}} = \gamma_{A_2, \text{out}}$ and $\gamma'_A \gamma'_A = \frac{\gamma_A \gamma_A}{\gamma_{A_2, \text{in}}}$, we get:

$$\gamma_A \approx \frac{\gamma'_A}{\sqrt{\Phi}} \quad (35)$$

Since the r.h.s. of Equations 34 and 35 are available, we plot γ_A and γ_{A_2} in Figure 5. γ_A was expected to be close or at least follow the trends of those derived from the Free Energy estimates given in Figures 6 to 8, especially Figure 6. The other two figures were plotted to show that the coefficient estimates are all greater than unity (>1). As expected from the theory provided, the activity coefficients from the A_{res} function show semi-quantitative agreement with the simulation results. The other A_{res} functions which eliminate the dimer contribution showed markedly lower values; we would expect a slight lowering of value due to dimer interference, leading to the conclusion that simulation results with the above two models are plausible, and that A_{res} is the more appropriate function to use for estimation. Since the adjacent atom in the dimer cannot contribute to the potential energy of the dimer contributing to its activity, one would expect its coefficient to be lower. The (B) reaction above has its counterpart in the forward (F) reaction, but because the transition state atomic activity coefficient is severely affected by its own force acting on the other target atom, it would not be reasonable to assume that the activity coefficient at that TS state due to the particle potentials can be equated with the bulk activity, especially when the internuclear distance at $r_f = 0.85$ corresponding to an energy of over 17.0 LJ

units! However it would be instructive to follow through the consequences of this approach so that comparisons with the activity coefficients derived from the literature may be made.

F. Process Using the same arguments as for the B Process, Figure 10 (F Process) gives the net elevation of the vacuum levels about $\Delta E_{F,2}^0$ such that:

$$\exp - \frac{\Delta E_{F,2}^0}{kT} \approx \left(\frac{\gamma_{A_2}^*}{\gamma_A^* \gamma_A^*} \right) \quad (36)$$

The ground state relative to the vacuum is elevated by ϵ_A per particle, so that:

$$E_{F,1} = E_{F,2}^0 - 2\epsilon_A \quad (37)$$

where as usual the ϵ 's to the potential energy associated with the availability coefficients. The total activation energy $\Delta E_{F, \text{tot}}$ is then given by:

$$\Delta E_{F, \text{tot}} = E_{F,1} + \Delta E_{F,2}^0 \quad (38)$$

By the definition of the reactivity coefficients,

$$\gamma_A' \gamma_A' = \exp \left(\frac{2\epsilon_A - \Delta E_{F,2}^0}{kT} \right) \quad (39)$$

and Equation 39 leads to:

$$\gamma_A' \gamma_A' = \gamma_A \gamma_A / \left(\frac{\gamma_{A_2}^*}{\gamma_A^* \gamma_A^*} \right) \quad (40)$$

where the asterisked states are at the *TS*. Despite the arguments above, if we were to make the approximation $\gamma_A^* \approx \gamma_A$ (where in general, only a detailed perturbation theory would yield an appropriate value of γ_A^*) then $\gamma_{A_2}^* \approx \gamma_{A_2}$ and $\gamma^* \approx \gamma_A$ yields:

$$\frac{\gamma_{A_2}^*}{\gamma_A^* \gamma_A^*} \approx \Phi \quad (41)$$

Then Equation 40 implies:

$$\gamma_A' \gamma_A' = \frac{\gamma_A \gamma_A}{\Phi} \quad (42)$$

yielding:

$$\gamma_A \approx \gamma_A' \sqrt{\Phi} \quad (43)$$

$$\gamma_{A_2} \approx \Phi \gamma_{A_2}' \quad (44)$$

since here $\Phi = \Phi^*$. The above so-called Φ convention plots for the activity coefficients are given in Figure 11 where $\gamma_A \cdot \gamma_{A_2} < 1$. This contradicts the results of the free energy estimates given in Figures 6 to 8, especially Figure 6; this was to be expected from the assumptions made for state A^* . Since $\delta A_{2, \text{out}}$ can be determined from the more reliable (B) process, we might be able to derive an estimate for $\gamma_A^* \gamma_A^*$ for the ($A \dots A$) *TS* state of two atoms about to dimerize where the (B) process assignment is used for the determination. We would expect $\gamma_A^* \gamma_A^*$ to change *relatively* much more slowly compared to the

γ_A and γ_{A_2} variations over the system ρ if the activity coefficient is strongly influenced by the isolated large repulsive potential of the two atoms at the *TS* region. Evidence in this direction would serve as a prototype for describing ionic reactions along the classical ideas of Brönsted and Bjerrum.

Single-stage Model

There is no reference state at the *TS* to compute energy differences. For instance, for the backward reaction:

$$\gamma_{A_2}' = \frac{\gamma_{A_2}}{\gamma_A^*} \gamma_A^* \approx \Phi \quad (45)$$

if $\gamma_A^* \approx \gamma_A$ as before for (B) (2 stage process). Then from $\Phi = \Phi'$ we get $\gamma_A' \approx 1$ which is contrary to the simulation results. Similarly, for the (F) reaction, we have $\gamma_A' \gamma_A' = \frac{\gamma_A \gamma_A}{\gamma_{A_2}^*}$ and with the assignment $\gamma_{A_2}^* \approx \gamma_{A_2}$, we get $\gamma_A' = \frac{1}{\sqrt{\Phi}}$ and from Equation 28 there results $\gamma_{A_2}' \approx \frac{\gamma_{A_2}}{\gamma_{A_2}} = 1$ which is also not observed. Hence the absolute single-stage process are not expected although they seem to conform to the Brönsted-Bjerrum (B-B) form (where the z 's are the associated charges):



with $k = k^0 \Delta$, where $\Delta = \frac{\gamma_{A^{za}} \gamma_{B^{zb}}}{\gamma_{AB}^{\dagger(z_a+z_b)}}$ with \dagger referring to the

upper level in the energy diagrams of Figures 9 and 10 or transition state of conventional theory. These observations suggest that the B-B form could well be described as an approximation of another mechanism which does not have pre-equilibria transition states; an example being the two stage process below which subsumes the B-B equations.

Application to Ionic Reactions

The potentials used here are general two body potentials leading to the theoretical structure. Regions of discrimination also exists, as in the switch between a collective dimer and the individual atoms. An exactly analogous situation is to be found in the case of ionic reactions which are Coulombic potentials which are 2 body and long ranging, as with at least the molecular potential here. The other important point is that for ionic systems, there is a switch mechanism in the Bjerrum theory concerning the potential due to the charge transfer onto one theoretical nuclear centre (in this case the entire molecule). In such systems, there is no change in overall mechanism of interaction, and what pertains for this potential is application to other similar 2-body systems such as outlined in the current kinetic theory; only the magnitude and form of the defined potentials would change, but not the structure of the equations, nor the coupling of the terms as given here, for example through the $c(\rho)$ coupling function. The classical kinetic theory of

salt effects applied to recent investigations by Sanchez *et al.* (Dominguez *et al.* 1998; Garcia-Fernandez *et al.* 2005) gives the B-B equation for the rate constant k as:

$$k = k_0 \frac{\gamma_A \gamma_B \dots}{\gamma_{\ddagger}} \quad (46)$$

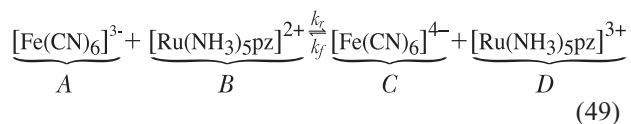
where k_0 is the reference rate constant for the solvent, $\gamma_A, \gamma_B \dots$ are the reactant activity coefficients of reactants A, B, \dots and γ_{\ddagger} is that of the transition state where if the charge of the reactants are z_a, z_b, \dots then the charge of the TS denoted by \ddagger is $z_{\ddagger} = z_a + z_b + \dots$. The activity coefficient γ_J (Debye-Huckel limiting law approximation) for any species J conforms to:

$$\log \gamma_J = -AZ^2 J^{1/2} = -QZ^2 \quad (47)$$

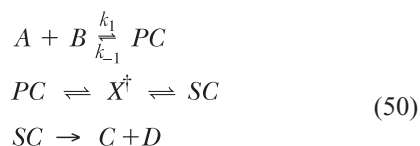
where $Q=AI^{1/2}$ is a positive number, leading from Equation 46 to the rate form:

$$\log k_2 = \log k_2^0 + 2AZ_A Z_B I^{1/2} \quad (48)$$

where a negative salt effect is expected for anion/cation bimolecular reactions, such as the recently studied reaction (with pz = pyrazine)



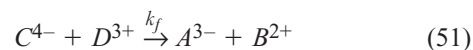
where the forward reaction with rate constant k_f shows a contradictory positive salt effect; other violations have been reported (Garcia-Fernandez *et al.* 2005, see Reference 4 of this citation). The interpretation of these anomalies has been made using the theory of Marcus and Hush (Garcia-Fernandez *et al.* 2005). These workers introduced composite reactions, leading to a pseudo-elementary process such as:



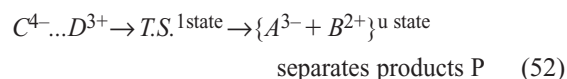
for the overall reaction $A+B \rightarrow C+D$. Violations of the B-B formula Equation 46 have been attributed to differences in activity coefficient properties of the precursor complex PC and activated state X^{\ddagger} ; SC is a postulated 'successor complex', where the Marcus-Hush ideas are also incorporated (Garcia-Fernandez *et al.* 2005, p. 15089). It would be of interest therefore to frame theories and proposals for elementary reactions that might also explain some of the above results; this is attempted below.

Proposal of mechanism to explain positive deviation for forward reaction of Equation 49.

Rewriting Equation 49 with reactants C and D , products A and B with the charges, we have an elementary reaction:



The postulated reaction sequence route of an ideal model is:



In Equation 52, $C \dots D$ represents a *pre-associated* complex which retains the spectroscopic details (e.g. in UV-IR range used for measuring concentrations) but which are close enough to ideally form an effective single charge of magnitude -1 . The $T.S.$ is the lower (l) degenerate state relative to the vacuum, and P the upper level u . In the presence of the solution dielectric, the first order perturbation according to the two stage model give a total pre-exponential total γ_{tot} as

$$\gamma_{\text{tot}} = \gamma_{C \dots D} \left/ \left(\frac{\gamma_A \gamma_B^{(u \text{ state})}}{\gamma_{T.S. (l \text{ state})}} \right) \right. \quad (53)$$

for the overall rate $k_2 = k_2^0 \gamma_{\text{tot}}$. Taking Equation 47 logarithms to base 10, results in:

$$\log \gamma_{\text{tot}} = \log \gamma_{C \dots D} + \log \gamma_{T.S.} - \log \gamma_A - \log \gamma_B \quad (54)$$

$$\begin{aligned} &= -1Q -1Q + 9Q + 4Q \\ &\approx +11Q \end{aligned} \quad (55)$$

and so:

$$\log k_2 = \log k_2^0 + 11Q \quad (56)$$

which leads a positive deviation in contradiction to the standard B-B equation for cation/anion reactants. The above model had no intermediate forms; all charges were discrete etc. As a further refinement, one can write down intermediate forms of association with charge parameter $-\lambda$ and the l state with charge $-\tau$ leading to

$$\log k_2 = \log k_2^0 + Q(13 - \lambda - \tau^2) \quad (57)$$

Further elaborations of intermediate forms of association along the lines of the above where the positive deviation is not a discrete multiple of Q above have been given (Jesudason 2006b). As stated previously, more recent theories have eliminated the transition state in kinetic descriptions (Kosloff 1996); of the many alternatives that are currently being mooted, the present model seeks to describe the overall rate process as being moderated by two factors at the interface of product and reactant which leads to a stochastic discontinuity in the energy so that there is an energy contribution to the reactant state, and another which is derived from the product state along the reaction coordinate. There is ample scope here to generalize this model to partial charges, and to other perturbations apart from the elementary ones due to the product/reactant transition.

CONCLUSION

Given that non-linearity is exhibited in the rate constants for elementary reactions, and the equivalence of the ratio of the reactivity and activity coefficients which is taken as axiomatic, a first order kinetic theory was constructed to explain the simulation results. Under stipulated conditions, such as obtained for the two stage models and the nature of the reaction, explicit first order expressions might be derived connecting the reactivity and activity coefficients. The theory of ionic reactions as developed by Brönsted and Bjerrum might be subsumed by the simple first order models provided here using a strictly elementary reactive process; in particular these models could also explain apparent violations of the standard Brönsted and Bjerrum theory involving composite reactions. The framework given here could be extended to other more complex particle reactions which are moderated by strong external fields, such as what might be obtained in the plasma state.

ACKNOWLEDGMENTS

The author is grateful to the Ministry of Science, Technology and Innovation for funding the study under Intensification of Research in Priority Areas (IRPA) grant [09-02-03-1031 (2003–2006)].

Date of submission: November 2006

Date of acceptance: May 2007

REFERENCES

- Dominguez, A, Jimenez, R, Lopez-Cornejo, P, Perez, P & Sanchez, F 1998, 'On the calculation of the transition state activity coefficient and solvent effects on chemical reactions', *Collect. Czech. Chem. Commun.*, vol. 63, pp. 1969–1976.
- Eyring, H, Lin, SH & Lin, SM 1980, *Basic Chemical Kinetics*, Wiley-Interscience, New York.
- Garcia-Fernandez, E, Prado-Gotor, R & Sanchez, F 2005, 'Abnormal salt and solvent effects on anion/cation electron-transfer reactions: An interpretation based on marcus-hush treatment', *J. Phys. Chem. B*, vol. 109, pp. 15087–15092.
- Hafskjold, B & Ikeshoji, T 1995, 'Partial specific quantities computed by non-equilibrium molecular dynamics', *Fluid Phase Equilibria*, vol.104, pp.173–184.
- Hänggi, P, Talkner, P & Borkovec, M 1990, 'Reaction-rate theory: fifty years after kramers', *Reviews of Modern Physics*, vol. 81, no. 2, pp. 251–341.
- Ikeshoji, T & Hafskjold, B 1994, 'Non-equilibrium molecular dynamics calculation of heat conduction in liquid and through liquid gas interface', *Mol. Phys.*, vol. 81, no. 2, pp. 251–261.
- Jesudason, CG 2006a, 'Model hysteresis dimer molecule.ii. Deductions from probability profile due to system coordinates', *J. Math. Chem. (JOMC)*. In Press.
- Jesudason, CG 2007, 'The form of the rate constant for elementary reactions at equilibrium from md: Framework and proposals for thermokinetics', *LAN Archive (http://xxx.lanl.gov)*, physics/0608073', *J. Math. Chem. JOMC*. In press.
- Jesudason, CG 2005, 'The Clausius inequality: Implications for non-equilibrium thermodynamic steady states with NEMD corroboration', *Nonlinear Analysis*, vol. 63, no. 5–7, pp e541–e553.
- Jesudason, CG 2006c, 'Model hysteresis dimer molecule. I. equilibrium properties', *J. Math. Chem. (JOMC)*, In Press.
- Johnson, JK, Zollweg, JA & Gubbins, KE 1993, 'The Lennard-Jones equation of state revisited', *Molec. Phys.*, vol. 78, no. 3, pp. 591–618.
- Kosloff, R 1996, 'Quantum molecular dynamics on grids', in *Dynamics of molecules and chemical reactions*, eds RE Wyatt & JZH Zhang, Marcel Dekker Inc., New York, chap. 5.
- Mortimer, M & Taylor, P 2002, *The Molecular world*, Open University Press, Milton Keynes, England.
- Nicolas, JJ, Gubbins, KE, Streett, WB & Tildesley, DJ 1979, 'Equation of state for the Lennard-Jones fluid', *Mol. Phys.*, vol. 37, no. 5, pp. 1429–1454.
- Pilling, MJ & Seakins, PW 2005, *Reaction kinetics*, Oxford University Press, England.
- Robbins, J 1972, 'Ions in solution 2 — an introduction to electrochemistry', *Oxford Chemistry Series*, (eds PW Atkins, SE Holker & AK Holliday, Oxford University Press, England.
- Wojciechowski, BW & Rice, NM 2003, *Experimental methods in kinetic studies*, revised edn, Elsevier, Amsterdam.

Simulation Study of Carrier-to-Interference Power Ratio Enhancement in Orthogonal Frequency Division Multiplexing System

S. Y. Sharifah^{1*}, F. Norsheila¹ and Muladi¹

Orthogonal Frequency Division Multiplexing (OFDM) is a successful technique in wireless communication systems. Frequency offset in the OFDM system leads to loss of orthogonality among subcarriers which results in the occurrence of intercarrier interference (ICI). To improve the efficiency of bandwidth performance in the ICI self-cancellation scheme, frequency domain partial response signaling (PRS) was investigated. In this study, the integer polynomial partial response coefficients were exploited to enhance carrier-to-interference power ratio (CIR) in the OFDM system. CIR was enhanced up to 4.1 dB to 5 dB when the lengths of PRS polynomial, K was 2 and 5, respectively.

Key words: Carrier-to-interference power ratio; intercarrier interference; frequency offset; orthogonal frequency division multiplexing; partial response signaling; integer polynomial coefficients

In an Orthogonal Frequency Division Multiplexing (OFDM) system, the entire bandwidth is divided into many orthogonal subcarriers, where information symbols are transmitted in parallel with long symbol duration in order to deal with frequency-selective fading of wireless environments. The overlapping spectrum of the subcarriers in an OFDM system requires an accurate frequency recovering system. However, in a time variant mobile radio environment, the relative movement between transmitter and receiver results in frequency offset due to Doppler frequency shifts, hence the carriers cannot be perfectly synchronised. This imperfection destroys orthogonality among subcarriers and causes intercarrier interference (ICI) to occur in addition to rotation and attenuation.

Several methods have been proposed to reduce the effect of the ICI. One of the methods is frequency-domain equalisation (Ahn & Lee 1993). Time-domain windowing is another way to reduce the effect of frequency offset (Li & Stette 1995). A self-ICI-cancellation approach has also been proposed which transmits each symbol over a pair of adjacent or non-adjacent subcarriers with a certain phase shift (Zhao & Haggman 2001, Sathanathan *et al.* 2000, Fu *et al.* 2002). This method can suppress the ICI significantly but with a reduction in bandwidth efficiency. In single-carrier systems, partial response signaling has been studied to reduce the sensitivity to time offset, without sacrificing bandwidth (Kabal & Pasupathy 1975). In the frequency domain, partial response with correlative coding has been used to mitigate the ICI caused by carrier frequency offset (Zhao & Haggman 1998). Partial response signaling (PRS) was

also considered to suppress the ICI caused by phase noise without decreasing bandwidth efficiency (Kim & Kim 2005). The optimum weights for PRS that minimised ICI power have been derived (Zhuang & Li 2003). The deployment of integer PRS can lead to less cost and complexity of the hardware implementation (Brown & Vranesic 2005). In this paper, we have studied the partial response signaling of the OFDM (PRS-OFDM) system with integer polynomial coefficients.

OFDM System with Frequency Offset Occurrence

In an OFDM system with N subcarriers, if a unit signal is modulated onto the k^{th} subcarrier and zero on the rest of subcarriers, the signals received from all of the subcarriers are defined as the subcarrier frequency offset (SFO) response for the k^{th} subcarrier (Zhao & Haggman 2001). Considering only a single path from the transmitter to the receiver, the signal on the k^{th} subcarrier influences the other subcarriers which are recognised as intercarrier interference (ICI) for $l \neq k$ which is represented by Zhao and Haggman (2001) as:

$$G(l-k) = \frac{\sin[\pi(\varepsilon+l-k)]}{N \sin\left[\frac{\pi}{N}(\varepsilon+l-k)\right]} \cdot \exp\left\{j\frac{\pi}{N}(N-1)[\varepsilon+(l-k)]\right\} \quad (1)$$

Equation 1 denotes the ICI effect of the l^{th} subcarrier on the k^{th} subcarrier with the occurrence of the normalised carrier frequency offset at the receiver denoted as ε . Some indoor environments can be modelled with this design, because of the negligible channel time delays. If ε is zero

¹ Faculty of Electrical Engineering, Universiti Teknologi Malaysia, 81310 UTM Skudai, Johor, Malaysia

* Corresponding author (e-mail: kamilah@fke.utm.my)

in Equation 1, it means that no frequency offset exists, hence resulting in no ICI amongst the subcarriers of the OFDM signal.

Consider OFDM system with N subcarriers and M OFDM frames, the demodulated OFDM symbols could be formulated as:

$$Y = GX + W \quad (2)$$

where X is the $N \times M$ input data. Each frame consists of N input symbols, and W is the white noise. Ideally, when the transmission channel is fixed, G is an $N \times N$ identity matrix. However, with the presence of frequency offset, the matrix has non-trivial off-diagonal elements. In this paper, we have assumed that all subcarriers under the influence of the same carrier frequency are offset with ε . Therefore, the demodulated symbol at the k^{th} subcarrier can be written as:

$$Y(k) = X(k)G(0) + \sum_{\substack{l=0 \\ l \neq k}}^{N-1} X(l)G(l-k) \quad (3)$$

The first part in Equation 3 consists of desired signals, while the second part is the unwanted ICI components.

Partial Response Signaling (PRS) OFDM System

In this study, we have considered the PRS-OFDM system. The baseband model of PRS-OFDM is shown in Figure 1. At the transmitter, the modulated symbol, $X(k)$ was encoded by the PRS encoder. If $X(k)$ were the symbols

to be transmitted and $c(i)$ the coefficients for partial response polynomial, the transmitted signal at the k^{th} subcarrier can be expressed as:

$$S(k) = \sum_{i=0}^{K-1} c(i)X(k-i) \quad (4)$$

where K is the number of coefficients or length of the PRS polynomial. In this study, BPSK symbols were evaluated, where $X(k)$ consisted of $\{1, -1\}$. Without loss of generality, $E|X(k)|^2 = 1$ and $E[X(k)X^*(j)] = 0$ for $k \neq j$ is assumed.

Using N subcarriers, the transmitted OFDM signal in time domain:

$$y(t) = \sum_{k=0}^{N-1} S(k) e^{j2\pi f_k t}, \quad 0 \leq t < T_s \quad (5)$$

where $f_k = f_0 + k\Delta f$ is the frequency of the k^{th} subcarrier, f_0 is the fundamental subcarrier frequency, $\Delta f = 1/T_s$ is the OFDM subcarrier spacing, and T_s is the symbol duration. The coded signals can be recovered by a maximum-likelihood (ML) sequence detector at the receiver.

At the receiver, by performing FFT on the received signal, the demodulated signal can be written as...

$$Y(k) = \sum_{m=0}^{N-1} \tilde{y}(t) e^{-j2\pi f_m t}, \quad 0 \leq t < T_s \quad (6)$$

For the purpose of analysis, the additive white Gaussian noise (AWGN) is not taken into account in the following derivations. Therefore, by considering Equations 3 and 4, Equation 6 can be written as:

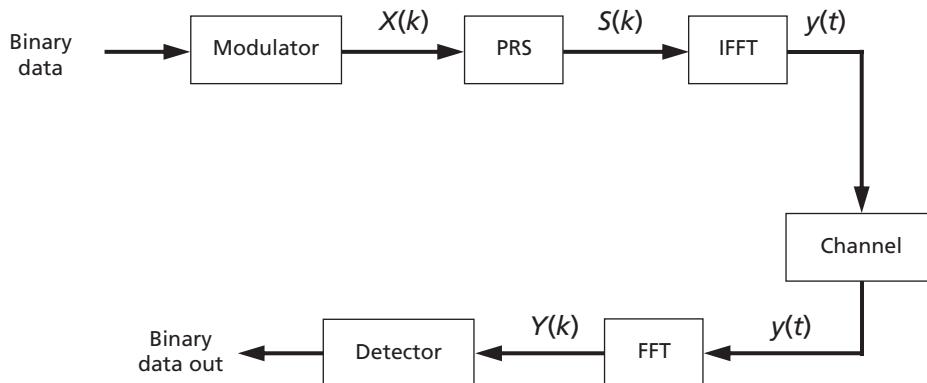


Figure 1. Baseband model of the PRS-OFDM system.

$$\begin{aligned}
 Y(k) &= \sum_{m=0}^{N-1} S(l)G(l-k) \\
 &= S(k)G(0) + \sum_{\substack{l=0 \\ l \neq k}}^{N-1} S(l)G(l-k) \\
 &= C(k) + I(k)
 \end{aligned} \tag{7}$$

for $k = 0, \dots, N-1$. The ICI power of PRS-OFDM system can be expressed as:

$$P_{ICI} = E(|I(k)|^2) = E \left[\left| \sum_{\substack{l=0 \\ l \neq k}}^{N-1} S(l)G(l-k) \right|^2 \right] \tag{8}$$

By applying Equation 4 to 8, the ICI power of K length PRS-OFDM system where $k = 0$ also can be written as:

$$P_{ICI} = E \left[\left| \sum_{l=1}^{N-1} \sum_{i=0}^{K-1} c(i) X(l-i) G(l) \right|^2 \right] \tag{9}$$

Assuming $K = 2$ the ICI power shown in Equation 9 can be derived as:

$$P_{ICI}^2 = E \left\{ \left[\sum_{l=1}^{N-1} [c(0)X(l) + c(1)X(l-1)] G(l) \right]^2 \right\} \tag{10}$$

The equation above can be elaborated as:

$$P_{ICI}^2 = E \left\{ \sum_{l=1}^{N-1} \sum_{p=1}^{N-1} [c(0)X(l) + c(1)X(l-1)] [c(0)X(p) + c(1)X(p-1)] G(l)G^*(p) \right\} \tag{11}$$

where p and l are indexes for subcarriers and each has a value from 1 to $N-1$. The above equation can be expanded as:

$$P_{ICI}^2 = E \left\{ \sum_{l=1}^{N-1} \sum_{p=1}^{N-1} \left[\begin{array}{l} c(0)c(0)X(l)X(p) + c(1)c(0)X(l-1)X(p) \\ + c(1)c(0)X(l)X(p-1) + c(1)c(1)X(l-1)X(p-1) \end{array} \right] G(l)G^*(p) \right\} \tag{12}$$

In this work, we have assumed that $E[X^2(k)] = 1$ and $E[X(k)X(j)] = 0$ for $k \neq j$. Therefore, by taking considerations of all the possible cases of the position of p when $k = 0$, we can have the different possibilities. If $p = l$ and by considering the respective position of p , Equation 12 can be written as:

$$\begin{aligned}
 P_{ICI}^2 &= E \left\{ \sum_{l=1}^{N-1} [c(0)^2 X(l)^2 + 2c(0)c(1)X(l-1) + c(1)^2 X(l-1)^2] |G(l)|^2 \right\} \\
 &= E \left\{ \sum_{l=1}^{N-1} [c(0)^2 X(l)^2 + c(1)^2 X(l-1)^2] |G(l)|^2 \right\}
 \end{aligned} \tag{13}$$

Next we consider the case when $p = l \pm 1$. By contemplating the position of p at $l+1$, Equation 12 becomes:

$$E \left\{ \sum_{l=2}^{N-1} \left[\begin{array}{l} c(0)c(0)X(l)X(l+1) + c(1)c(0)X(l-1)X(l+1) \\ + c(1)c(0)X(l)X(l) + c(1)c(1)X(l-1)X(l) \end{array} \right] G(l)G^*(l+1) \right\}$$

which can be simplified as:

$$\left\{ \sum_{l=1}^{N-1} c(0)c(1)E[X(l)X(l)] G(l)G^*(l+1) \right\}$$

by using one reference point with respect to l , the equation above can be written as:

$$\left\{ \sum_{l=1}^{N-1} c(0)c(1)E[X(l) X(l)]G(l-1)G^*(l) \right\} \quad (14)$$

whereas when the position of p is at $l-1$, Equation 12 becomes:

$$\begin{aligned} E \left\{ \sum_{l=2}^{N-1} \left[\begin{array}{l} c(0)c(0)X(l)X(l-1) + c(1)c(0)X(l-1)X(l-1) \\ + c(1)c(0)X(l)X(l-2) + c(1)c(1)X(l-1)X(l-2) \end{array} \right] G(l)G^*(l-1) \right\} \\ = \left\{ \sum_{l=1}^{N-1} c(0)c(1)E[X(l-1)X(l-1)]G(l)G^*(l-1) \right\} \end{aligned} \quad (15)$$

For $K = 2$, P_{ICI}^2 becomes 0 at any other placement or position of p . Hence P_{ICI}^2 becomes:

$$\left\{ \sum_{i=0}^{K-1} \sum_{l=1}^{N-1} c(i)^2 G^2(l) + \sum_{l=1}^{N-1} c(1)c(0) [G(l)G^*(l-1) + G(l-1)G^*(l)] \right\} E(X^2) \quad (16)$$

Now, consider the case when $K = 3$, the same procedure is repeated as done on $K = 2$. The ICI power in Equation 9 can be written as:

$$P_{ICI}^3 = E \left\{ \sum_{l=1}^{N-1} \sum_{p=1}^{N-1} \left[\begin{array}{l} c(0)X(l) + c(1)X(l-1) + c(2)X(l-2) \\ [c(0)X(p) + c(1)X(p-1) + c(2)X(p-2)] \end{array} \right] G(l)G^*(p) \right\} \quad (17)$$

Besides the c_i^2 coefficients at $l = p$, the existence of other coefficients also depends on the position of subcarrier p , as shown below:

If p is at $l-1$, the coefficients are $c(1)c(0)X(l-1)X(p)$, $c(2)c(1)X(l-2)X(p-1)$,

If p is at $l+1$, the coefficients are $c(1)c(0)X(l)X(p-1)$, $c(2)c(1)X(l-1)X(p-2)$,

If p is at $l-2$, the coefficients are $c(0)c(2)X(l-2)X(p)$,

If p is at $l+2$, the coefficients are $c(2)c(0)X(l)X(p-2)$,

If p is at $l-3$, the coefficients are $c(3)c(0)X(l-3)X(p)$,

And lastly, if p is at $l+3$, the coefficients are $c(3)c(0)X(l)X(p-3)$.

Therefore, for $K = 3$, P_{ICI}^3 in Equation 17 becomes:

$$\left\{ \sum_{l=1}^{N-1} \left\{ c(i)^2 G^2(l) + \left[\begin{array}{l} c(1)c(0)[G(l)G^*(l-1) + G(l-1)G(l)] \\ + c(2)c(1)[G(l)G^*(l-1) + G(l-1)G(l)] \\ + c(2)c(0)[G(l)G^*(l-2) + G(l-2)G(l)] \end{array} \right] \right\} E(X^2) \right\} \quad (18)$$

Next by considering $K = 4$, the ICI power, P_{ICI}^4 can be derived as:

$$E \left\{ \sum_{l=1}^{N-1} \sum_{p=1}^{N-1} \left[\begin{array}{l} c(0)X(l) + c(1)X(l-1) \\ + c(2)X(l-2) + c(3)X(l-3) \end{array} \right] \left[\begin{array}{l} c(0)X(p) + c(1)X(p-1) \\ + c(2)X(p-2) + c(3)X(p-3) \end{array} \right] G(l)G^*(p) \right\} \quad (19)$$

Again, besides $c(i)^2$ coefficients at l equals to p , the existence of other coefficients depended on the position of subcarrier p ,

such as, if p is at $l-1$, the coefficients are $c(1)c(0)X(l-1)X(p)$, $c(2)c(1)X(l-2)X(p-1)$, $c(3)c(2)X(l-3)X(p-2)$.

Meanwhile at $l+1$, the coefficients are, $c(1)c(0)X(l)X(p-l)$, $c(2)c(1)X(l-1)X(p-2)$, $c(3)c(2)X(l-2)X(p-3)$

If p is at $l-2$, the coefficients are $c(2)c(0)X(l-2)X(p)$, $c(3)c(1)X(l-3)X(p-1)$,

If p is at $l+2$, the coefficients are $c(2)c(0)X(l)X(p-2)$, $c(3)c(1)X(l-1)X(p-3)$. If p is at $l-3$, the coefficients are $c(3)c(0)X(l-3)X(p)$, and lastly, if $p = l+3$, the coefficient is $c(3)c(0)X(l)X(p-3)$.

Therefore, for $K = 4$, P_{ICI}^4 becomes:

$$\left\{ \sum_{l=1}^{N-1} \{c(i)^2 G^2(l)\} + \sum_{l=1}^{N-1} \left\{ \begin{array}{l} c(1)c(0)[G(l)G^*(l-1)+G(l-1)G(l)] + c(2)c(1)[G(l)G^*(l-1)+G(l-1)G(l)] \\ + c(3)c(2)[G(l)G^*(l-1)+G(l-1)G(l)] + c(2)c(0)[G(l)G^*(l-2)+G(l-2)G(l)] \\ + c(3)c(1)[G(l)G^*(l-2)+G(l-2)G(l)] + c(3)c(0)[G(l)G^*(l-3)+G(l-3)G(l)] \end{array} \right\} \right\} E(X^2) \quad (20)$$

By generalising Equation 9 for any value of K , ICI power due to PRS can be expressed as:

$$P_{ICI} = \sum_{i=0}^{K-1} \sum_{l=1}^{N-1} c(i)^2 |G(l)|^2 + \sum_{i=0}^{K-1} \sum_{l=1}^{K-1-k} c(i)c(i+k) \left[\sum_{l=k+1}^{N-1} G(l)G^*(l-k) + G(l-k)G^*(l) \right] \quad (21)$$

The desired PRS-OFDM signal power was:

$$P_C = \sum_{i=0}^{K-1} \sum_{l=1}^{N-1} [c(i)X(l-i)G(0)]^2$$

When $N \gg \pi\epsilon$ is assumed, the $\left(\frac{\sin \pi\epsilon}{N}\right)$ in Equation 1 can be approximated as $\frac{\pi\epsilon}{N}$. Therefore at $l - k = 0$, the equation above could be derived as:

$$P_C = \left(\frac{\sin \pi\epsilon}{\pi\epsilon}\right)^2 \sum_{i=0}^{K-1} c(i)^2 E[X^2] \quad (22)$$

Therefore, using Equations 21 and 22, the carrier-to-interference power ratio (CIR) of PRS-OFDM system can be formulated as the ratio of $\frac{P_C}{P_{ICI}}$ given in Equation 23:

$$CIR = \frac{\left(\frac{\sin \pi\epsilon}{\pi\epsilon}\right)^2 \sum_{i=0}^{K-1} c(i)^2}{\left\{ \sum_{i=0}^{K-1} \sum_{l=1}^{N-1} c(i)^2 G^2(l) + \left[\sum_{k=1}^{K-1} \sum_{i=0}^{K-1-k} c(i)c(i+k) \sum_{l=k+1}^{N-1} G(l)G^*(l-k) + G(l-k)G^*(l) \right] \right\}} \quad (23)$$

Usually CIR is expressed in dB units. Equation 23 will subsequently be used in order to find the simplified polynomial coefficients that maximise the CIR for the respective K value.

NUMERICAL RESULT

We were concerned in finding the PRS polynomial coefficients that would result in maximum CIR in the OFDM system. By using the CIR in Equation 10, appropriate coefficients could be found for each of the respective polynomial length, K . The CIR is a function of PRS polynomial coefficients and the normalised carrier frequency shift, ϵ .

Exhaustive search methodology was used to find the optimum integer coefficients of PRS-OFDM that maximises the CIR. Some restrictions were applied in order

to simplify the findings. Given below are restrictions that were applied in the coefficient identification procedures:

Restriction 1: c_0 was set to integer 1;

Restriction 2: The maximum value of c_i was set to the maximum coefficient value used in the polynomial of the form $(1-r)^{K-1}$ where K was an integer value and $K > 0$.

Lastly, with the presence of ϵ , the value of CIR for each combination of c_i was calculated. At each length K , the appropriate polynomial that yielded a maximum CIR was identified. Table 1 shows the PRS coefficient

combination, which gives the maximum CIR for the respective polynomial length, K when $N = 64$.

Table 1. The optimum PRS-OFDM polynomial integer coefficients for the respective K lengths.

Length, K	PRS integer coefficients
2	1, -1
3	1, -2, 1
4	1, -2, 2, -1
5	1, -3, 4, -4, 2

The CIR performance of ε from 0.1 to 0.5 are depicted in Figures 2a-2d. As ε increased, the CIR was reduced. Compared to normal OFDM, the CIR of the integer PRS-OFDM system was significantly better than the normal OFDM system. As shown from the figures, $K = 2$ had the lowest range of CIR gain followed by $K = 3$ and $K = 4$ with maximum CIR gain of 4.1 dB, 4.7 dB, and 5 dB, respectively. Although $K = 5$ had the highest CIR gain, its increment was very small compared to the gain when $K = 4$. Approximately 0.8% to 0.95% difference was obtained between the two lengths of K .

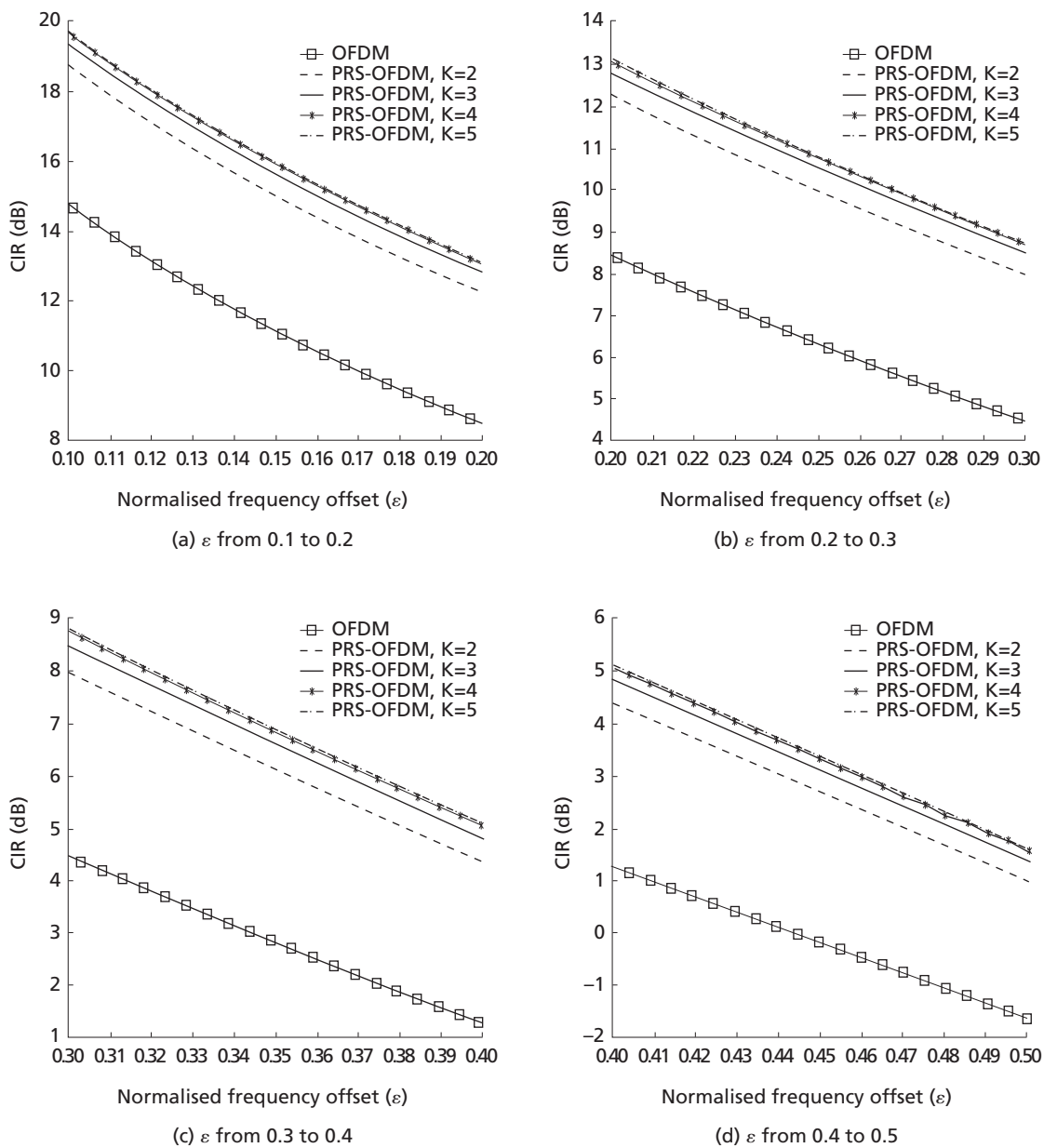


Figure 2. The CIR performance of integer coefficients for the PRS-OFDM system.

CONCLUSION

In this paper, the PRS-OFDM system was studied. Polynomial coefficients with integer values were used to reduce the complexity of the receiver. ICI was deliberately introduced in a controlled manner through the polynomial functions. The effectiveness of PRS-OFDM system with integer polynomial coefficients on enhancing CIR was investigated. Furthermore, the CIR of PRS-OFDM system was also derived. The integer coefficients of PRS for the respective polynomial length in single OFDM system with maximised CIR were determined through exhaustive search. Numerical and simulation results showed that the longer the polynomial length, K , the higher the CIR. PRS managed to enhance further the CIR of the OFDM system by about 3.8 dB to 4.75 dB when the lengths of polynomial, K was 2, 3, 4, and 5, respectively. This system could be applied in future broadband systems development such as the MIMO-OFDM system.

Date of submission: October 2006

Date of acceptance: June 2007

REFERENCES

- Ahn, J & Lee, HS 1993, 'Frequency domain equalisation of OFDM signal over frequency nonselective Rayleigh fading channels', *IEEE Electronic Letters*, vol. 29, pp. 1476–1477.
- Brown, S & Vranesic, Z (2005), *Fundamentals of digital logic with VHDL design. 2nd ed*, McGraw-Hill.
- Fu, Y, Kang, SG & Ko, CC 2002, 'A new scheme for PAPR reduction in OFDM systems with ICI self-cancellation', in *Proceedings IEEE Vehicular Technology Conference, 24–28 Sept. 2002*, vol. 3, pp. 1418–1421.
- Kabal, P & Pasupathy, S 1975, 'Partial-response signaling', *IEEE Transaction on Communications*, vol. 23, no. 9, pp. 921–934.
- Kim, K & Kim, H 2005, 'A suppression scheme of the ICI caused by phase noise based on partial response signaling in OFDM systems', *Proceedings IEEE International Conference on Information, Communications and Signal Processing, 6–9 December 2005*, pp. 253–257.
- Li, R & Stette, G 1995, 'Time-limited orthogonal multicarrier modulation schemes', *IEEE Transaction on Communications*, vol. 43, no. 234, pp. 1269–1272.
- Sathananthan, K, Rajatheva, R & Slimane, SB 2000, 'Cancellation technique to reduce intercarrier interference in OFDM', *IEEE Electronics Letters*. vol. 36, no. 25, pp. 2078–2079.
- Zhao, Y & Haggman, SG 2001, 'Intercarrier interference self-cancellation scheme for OFDM mobile communication systems', *Transaction on Communications*, vol. 49, no. 7, pp. 1185–1191.
- Zhao, Y & Haggman, SG 1998, 'Intercarrier interference compression in OFDM communication systems by using correlative coding', *IEEE Communication Letters*, vol. 2, pp. 214–216.
- Zhuang, H & Li, Y 2003, 'Optimum frequency-domain partial response encoding in OFDM system', *Transaction on Communications*, vol. 51, no. 7, pp. 1054–1068.

Optical Tomography: Real Time Image Reconstruction for Various Flow Regimes in Gravity Flow Conveyor

R. Abdul Rahim^{1*}, J. F. Pang¹, K. S. Chan¹, L. C. Leong¹ and M. H. Fazalul Rahiman²

In this study, real-time imaging was monitored for flowing solid particles when various baffles were created to block certain areas of the pipe. The generated flow regimes were full-flow, three-quarter-flow, half-flow and quarter-flow. A vertical pneumatic conveyor was designed to hold a 85 mm inner diameter pipeline. The four projection optical tomography systems used, applied the parallel beam projection approach and use infrared light sources so that the sensor was free of noise from the surrounding visible light source. The two orthogonal and two rectilinear projections were axial, but ideally they should have been in the same layer. The sensor readings could be related to the varying light intensity effects of the dropping particles and were used to provide cross-sectional distribution information for the conveyor. By using computer programming, the information was reconstructed to produce coloured images and concentration was obtained by reference to a colour code. The results obtained from this study showed how imaged flow followed the artificial flow regime. This study could benefit industrial production lines in maintaining the desired flow rates.

Key words: pneumatic conveyor; pipeline; optical tomography; computer programming; flow imaging; infrared light sensor; material packaging

Tomography is an imaging technique that produces high-resolution cross-sectional images of the internal structure of an object (Cruz 2003). In the processing industry, information describing material distribution and validating internal modes of the process are necessary for optimum design and operation of process equipment (Ruzairi 1996). Hence, the tomography approach using non-invasive sensors is a novel and safe way to visualize the inside of a mixing vessel. Some flow information can be obtained uniquely through process tomography, for example the local concentration, velocity of movement, flow rate, composition of flow and others. Optical tomography is an attractive method since it may prove to be less expensive, have a better dynamic response, and be more portable for routine use in process plants compared to other radiation-based tomographic techniques, such as positron emission, nuclear magnetic resonance, gamma photon emission and X-ray tomography (Chan & Ruzairi 2002). Process tomography provides several real-time methods (Cruz Meneses-Fabian *et al.* 2003) to obtain cross-section parameters in process plants related to material distribution. These methods involve taking numerous measurements from sensors placed around the vessel of the investigated process plant. The measured data are then fed into a computer program to obtain the internal behaviours of the conveyor.

Generally, vertical pneumatic conveying is defined as the transport of various granular solids and dry powders using air or other inert gas stream as a transportation medium in gravity flow. Nowadays, material handling by pneumatic conveying is increasingly becoming routine in industrial businesses. Pneumatic conveying offers many advantages over other methods of granular solids transport such as low routine maintenance and manpower costs, dust-free transportation and flexible routing. Some of the applications of pneumatic conveying systems can be found in industries dealing with food processing, plastic product manufacturing, textile, paper, power generation and solids waste treatments (Arko 1999).

Sensor Configuration

In optical tomography, there are many types of projection patterns used to detect flow material within pipelines. Basically, they can be divided into groups of parallel beam projections and fan beam projections. As mentioned earlier, this study uses the first approach. The parallel beam projection is obtained through the parallel arrangement of several transmitter sensors and the view angle of each receiver sensor is designed to be small. Four parallel beam projections result in patterns of two orthogonal projections, two rectilinear projections, combination of

¹ Process Tomography Research Group, Control and Instrumentation Engineering Department, Faculty of Electrical Engineering, Universiti Teknologi Malaysia, 81310 UTM Skudai, Johor, Malaysia

² Department of Mechatronics Engineering, North Engineering College University, Universiti Teknologi Malaysia, 81310 UTM Skudai, Johor, Malaysia

* Corresponding author (e-mail: ruzairi@fke.utm.my; ruzairiabdulrahim@yahoo.co.uk)

one orthogonal with two rectilinear projections and combination of two orthogonal with two rectilinear projections (Sallehuddin 2000). This latter arrangement can provide sufficient information to minimize ambiguous effects arising during cross-sectional image detection compared to the previous three projections.

In the two orthogonal projections, there were two arrays of projections. Both have their viewing planes parallel to the horizontal axis of the vertical flow pipe; the two arrays are at 90° to each other. In this project, each orthogonal array used 16 pairs of transmitter-receiver and this resulted in a true image resolution of 16 × 16 pixels. For the two rectilinear projections, the arrays of projections were inclined at plus and minus 45° to the horizontal axis respectively. The number of transmitter-receiver pairs used in one array was 23, because each emitter projection in this layer must cross over the center point of the

corresponding pixel and also the area within the pipeline, as shown in Figure 1. The hardware resolution in this project doubled the resolution obtained from the previous research conducted by Sallehuddin *et al.* (2000) that used 8 × 8 pairs of transmitter-receivers, in the layer of two orthogonal projections and 11 × 11 pairs of transmitter-receivers in the layer of two rectilinear projections.

A typical optical tomography system consists of a sensor, an electronic circuit, a data acquisition system, and a host computer as the data processing and display unit. The block diagram of the developed system is shown in Figure 2. A transmitter circuit sequentially switches on the emitter lights and projects them to receivers. The signal conditioning circuit then converts the signals received into voltage readings and amplifies them to a sufficient level. Finally, the output signals pass through a sample and hold circuit and the data

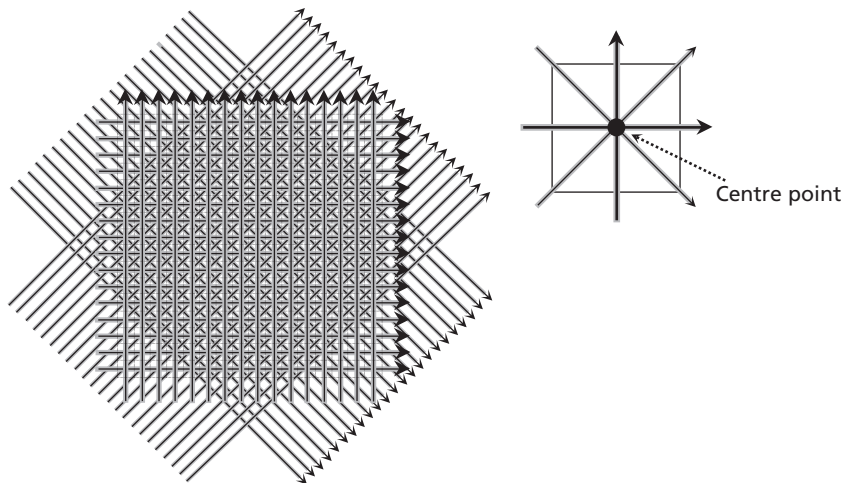


Figure 1. Optical tomography sensor projection geometry.

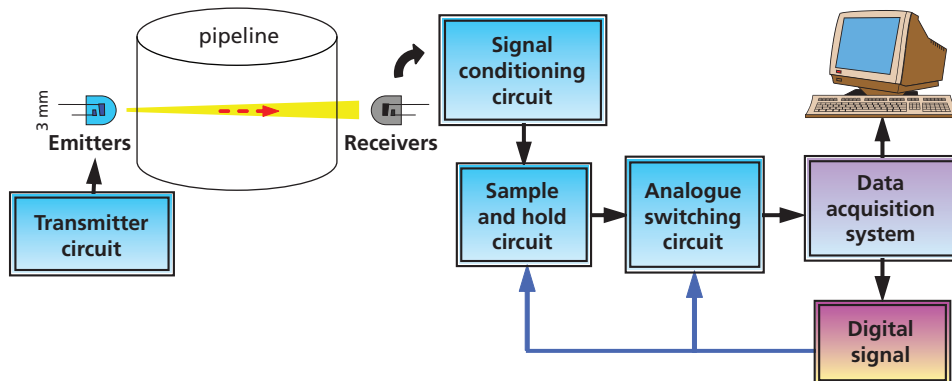


Figure 2. Block diagram of the developed system.

acquisition system based on the control signals from the digital signal controller. The data acquisition system digitises the signals and passes them into the computer for further processing.

A fixture was designed for holding all emitters and receivers so that four parallel projection arrays could be created easily. The two orthogonal projections and two rectilinear projections are ideally in the same layer. Practically, if all projections were in one layer, three main problems would occur. Firstly, light from the emitters travelled a longer distance to reach the receivers since the inner diameter of the pipe used in the system was already at 85 mm. This meant that the emitter itself should have a higher light intensity capability. Unfortunately, for the emitter that had a higher intensity, the physical size was greater than 3 mm in diameter and also the cost was higher. Secondly, the developed fixture would look bulky. Thirdly, since the radiant intensity of the emitter was proportional to the forward current used, the power consumed for the whole system would increase. Thus, the fixture was constructed using two layers as shown in

Figure 3. The upper layer was for two rectilinear projections and contained 92 holes in total, 23 holes per side. The lower layer was for two orthogonal projections and it contained 64 holes in total, 16 holes per side. The distance between these two layers was 7 mm to provide mechanical stability.

It is essential for the beam of light to diverge as little as possible to avoid overlapping of the received signals and loss of beam intensity (Ruzairi 1996). Three methods were used to collimate the light source. Firstly, infrared emitters and phototransistors that had small view angles were used. Secondly, an optical stop was placed in front of the infrared emitter. In this system, a ferrule was used as the stop. This method is effective in limiting the divergent angle (Chan 2001). The stop was 1 mm in diameter and it successfully limited the light from the 3 mm infrared emitter as shown in Figure 4. Thirdly, all emitters and receivers were arranged in an alternate manner as shown in Figure 4. This arrangement helps to cut down any divergent light reaching receivers adjacent to the designated receiver.

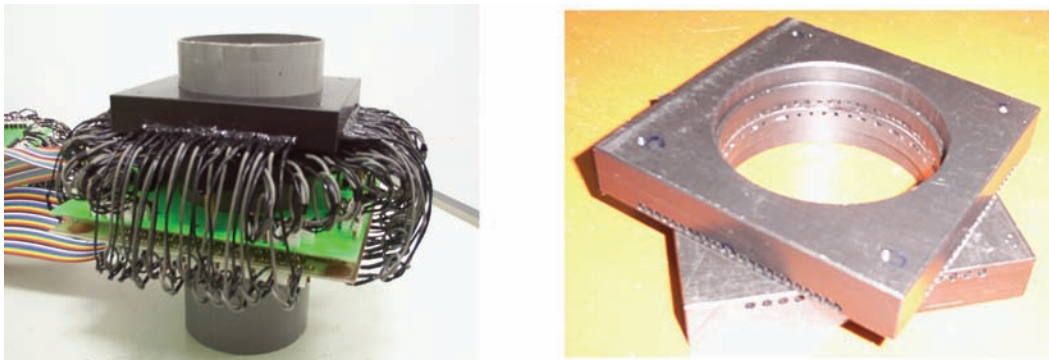


Figure 3. Fixture for holding emitters and receivers.

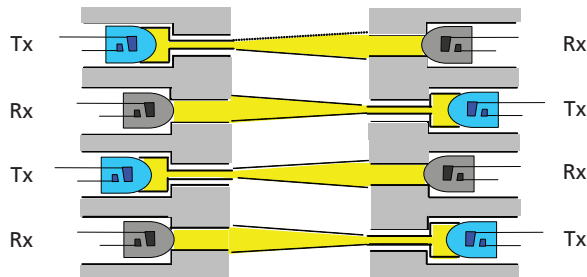


Figure 4. Optical stopper and alternate arrangement of emitters and receivers.

Concentration Profile

The concentration profile is the result obtained from the concentration measurements. The profile is generated when all corresponding sensor readings are applied into an algorithm, namely the image reconstruction algorithm. There are many different algorithms, e.g. Linear Back Projection (LBP), Filtered Back Projection, Convolution Back Projection, Hybrid Reconstruction Algorithm (HRA) and Algebraic Reconstruction Technique. For this project, the HRA was chosen since it can improve the accuracy of the image reconstruction obtained using LBP by neglecting the blurry image. According to Sallehuddin (2000), this algorithm assumes binary values from the sensor, either zero for no material or one for the presence of material. The sensor value is first measured, if the reading is zero, then any pixels traversed by that sensor's beam are set to zero and omitted from further calculations. Only the rest of the pixels will perform LBP to complete the process. In other words, this algorithm can be easily explained as a make up or packing of the LBP algorithm with several masking conditions. The mathematical expression of this algorithm is shown below:

$$V_{Hybrid}(x_{sa}, y_{sb}) = \begin{cases} V_{Sa} - V_{th} + V_{Sb} - V_{th}; & V_{Sa} \geq V_{th} \text{ AND } V_{Sb} \geq V_{th} \text{ AND} \\ & V_{Sc} \geq V_{Sp} \text{ AND } V_{Sd} \geq V_{Sp} \\ 0; & V_{Sa} < V_{th} \text{ OR } V_{Sb} < V_{th} \text{ OR} \\ & V_{Sc} < V_{Sp} \text{ OR } V_{Sd} < V_{Sp} \end{cases} \quad (1)$$

where $V_{hybrid}(x_{sa}, y_{sb})$ is the voltage of pixel (x_{sa}, y_{sb}) inside the concentration profile using the Hybrid image reconstruction algorithm; V_{Sa} or V_{Sb} is the voltage value referring to the sensor S_a or S_b in two orthogonal projections (also called the 16×16 layer). V_{Sc} or V_{Sd} is the voltage value referring to the sensor S_c or S_d in two rectilinear projections (also called the 23×23 layer); a is the sensor number between 0 to 15 in the first 16×16 layer projection, b is the sensor number between 16 to 31 in the orthogonal 16×16 layer projection, c is the sensor number between 0 to 22 in the first 23×23 layer projection, d is the sensor number between 23 to 45 in the orthogonal 23×23 layer. V_{th} is threshold voltage of the 16×16 layer and V_{sp} is threshold voltage of the 23×23 layer. When an obstacle, for example, passes through the sensing field, the concentration profile obtained by applying Equation 1 is illustrated in Figure 5.

Experimental Flow Rig Setup

The flow rig is designed to create the continuous gravity flow of plastic beads. The configuration of the flow rig is illustrated in Figure 6. It consisted of a hopper, a valve, two gaps, a space for the arrays of tomographic sensors, a tank and a blower. The blower conveys the plastic beads from the tank to the hopper; the valve is a switch to open or close the hopper to ensure that the plastic beads flowing inside the pipe could drop down or be obstructed. Two gaps near to the hopper were filled with the corresponding cut-off blades for controlling the

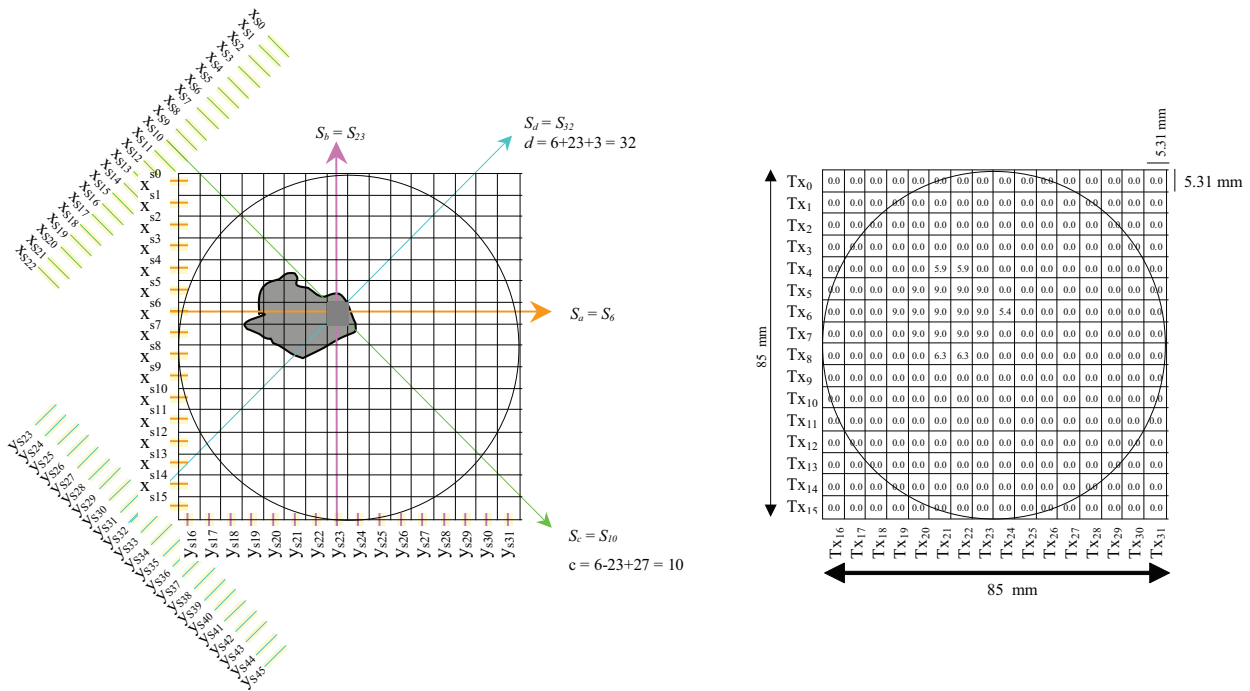


Figure 5. Concentration profile of detected obstacle.

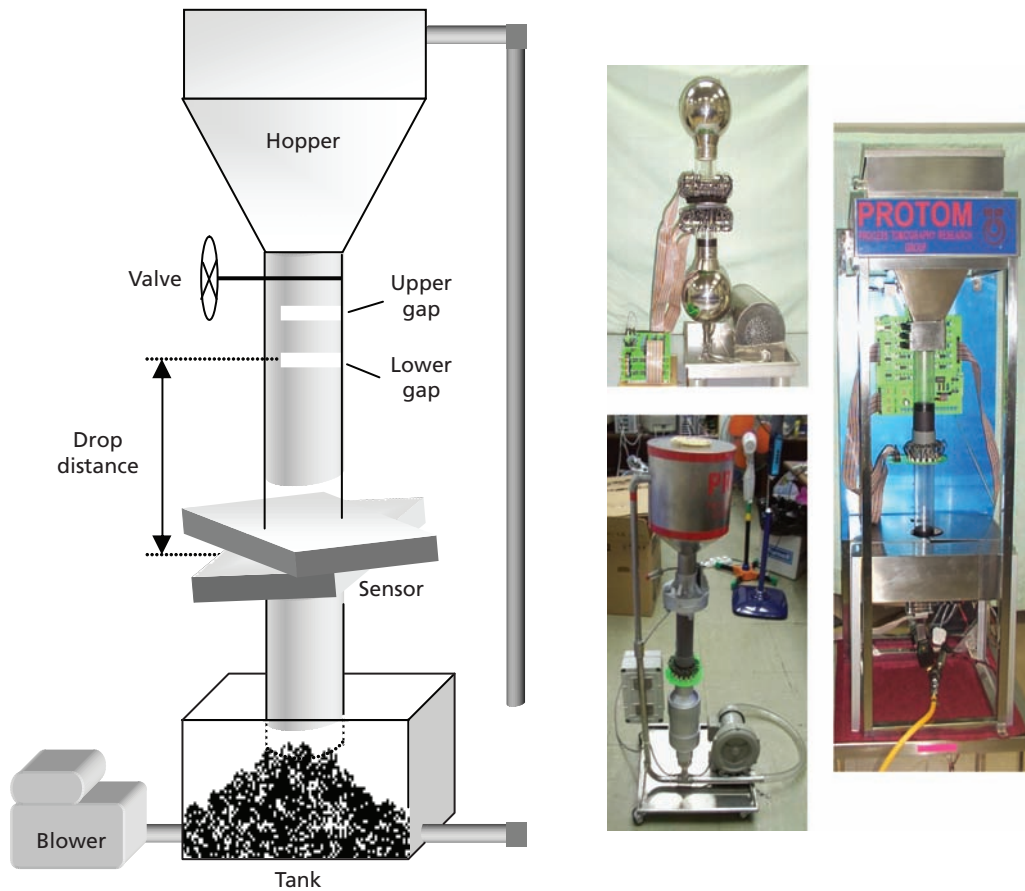


Figure 6. Vertical flow rig configuration.

mass flow rate and flow regime. The upper gap was located 3 cm below the valve and the lower gap at 8 cm from the upper gap. The pipeline of the flow rig had an inner diameter of 85 mm. The plastic beads used in the flow rig had a volume of approximately $2 \times 2 \times 3 \text{ mm}^3$. It was very light (less than 1 g) and also of a pure material that could be used in the manufacturing industry.

Designation of artificial flow regime. Four artificial flow regimes were investigated: full-flow, three-quarter flow, half-flow and quarter-flow (Ruzairi 1996). They were created by placing the corresponding cut-off blade or baffle into the lower gap of the flow rig. In the full-flow regime, no baffle was created to block the flow. The flow expectation is shown in Figure 7.

In the three-quarter-flow regime, the designed baffle cuts-off was at a quarter of the area of pipeline, thus three quarters were clear for plastic bead flow. The three-quarter flow expectation in the pneumatic conveyor is illustrated in Figure 8.

In the half-flow regime, the designed baffle cut off half the area of the pipeline leaving the half clear for the

plastic beads to flow. The half-flow expectation in the conveyor is shown in Figure 9.

In the quarter-flow regime, the designed baffle cut off three quarters of the area of the pipeline, thus only a quarter was clear for the flow of the plastic beads. The quarter-flow expectation is illustrated in Figure 10.

Mass flow rate controlling baffle. Three experimental mass flow rates were created by placing the corresponding cut-off blade in the upper gap of the flow rig. The configuration of the three baffles are shown in Figure 11. The cut-off regions of these baffles were circular with diameters of 4.5 cm, 4 cm and 3.5 cm respectively. They fix and maintain the corresponding mass flow rate.

RESULTS AND DISCUSSION

To construct real time cross-sectional images of different flow regimes, the corresponding flow rate control baffle and flow regime baffle were first placed into the appropriate gaps of the conveyor. When the measurement process was in running phase, a total of 78 sensor output readings were

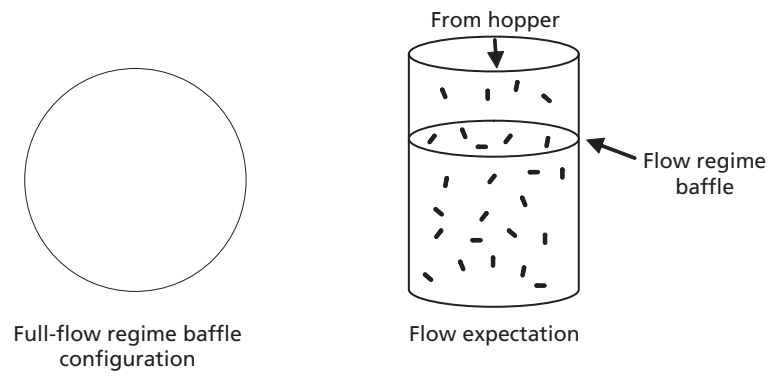


Figure 7. Full-flow regime creation.

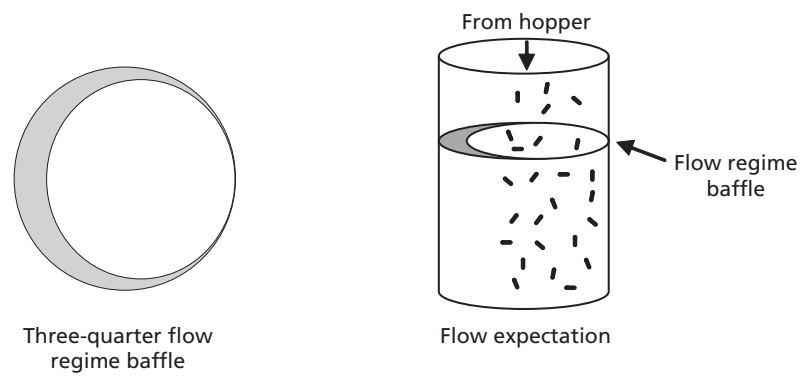


Figure 8. Three-quarter flow regime creation.

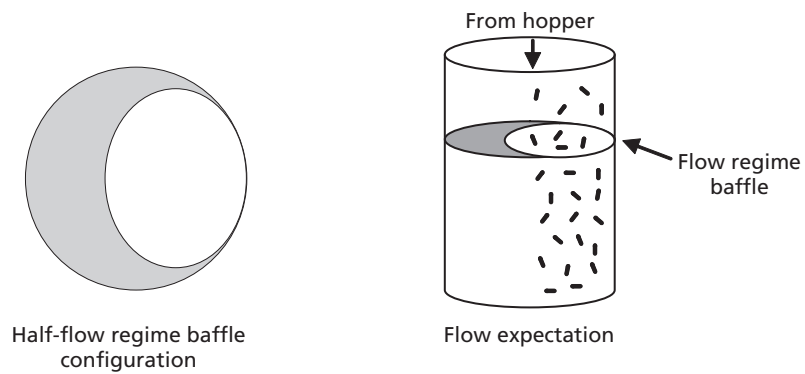


Figure 9. Half-flow regime creation.

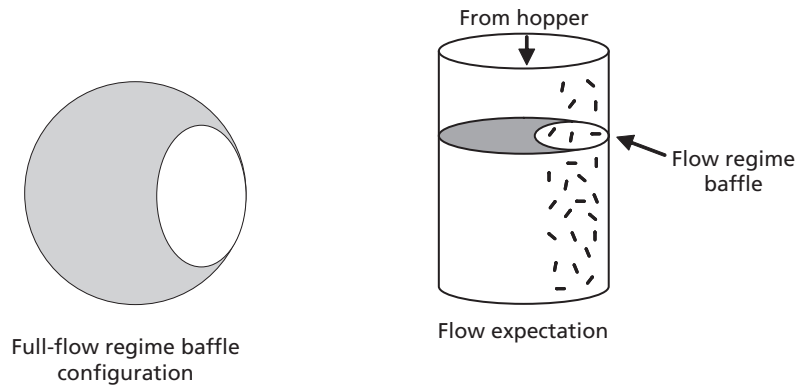


Figure 10. Quarter-flow regime creation.

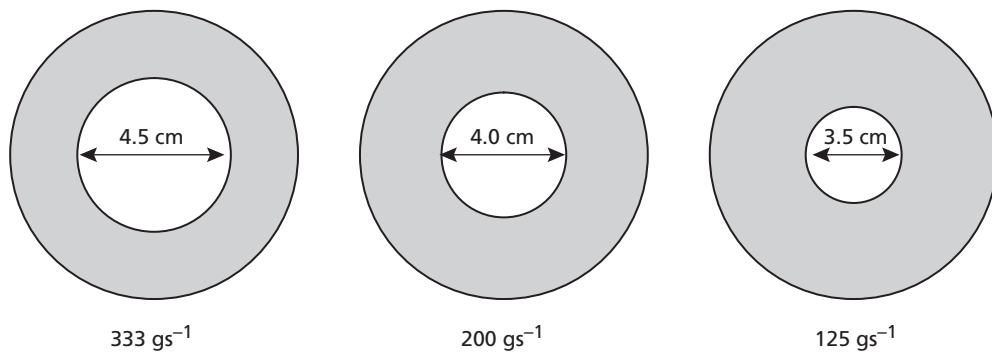


Figure 11. Baffle configurations for controlling mass flow rate.

captured by the data acquisition system for each frame of process. After applying the hybrid reconstruction algorithm or Equation 1, the concentration profile was generated with a resolution of 16×16 pixels. By referring to a colour code showing the % ratio of light absorbed by the sensor (100% means the obstacle was fully blocking the light transmitted), the concentration profile detected, was converted to the flow image with a resolution of 16×16 pixels. If filtering and image interpolation methods were used, the generated cross-sectional image could be upgraded into the high resolution image shown in Figure 12.

In the concentration measurement, the measured cross-sectional images were made at three different drop distances, these were from 16 cm, 36 cm and 56 cm, respectively (Figure 6). This was done by relocating the tomographic sensor array's position relative to the lower gap of the pneumatic conveyor. The results obtained are illustrated in Figure 13.

The results showed that the images for the drop distance of 16 cm had a higher concentration compared to the drop distances of 36 cm and 56 cm. When flow passed

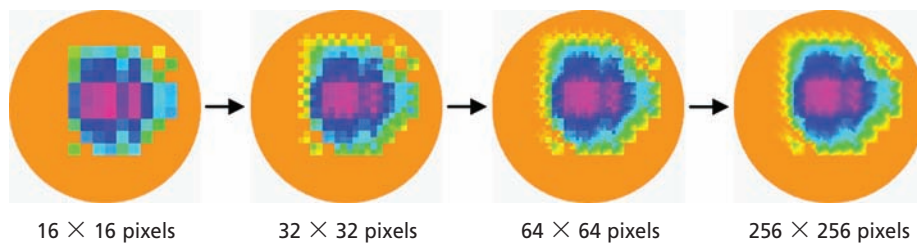
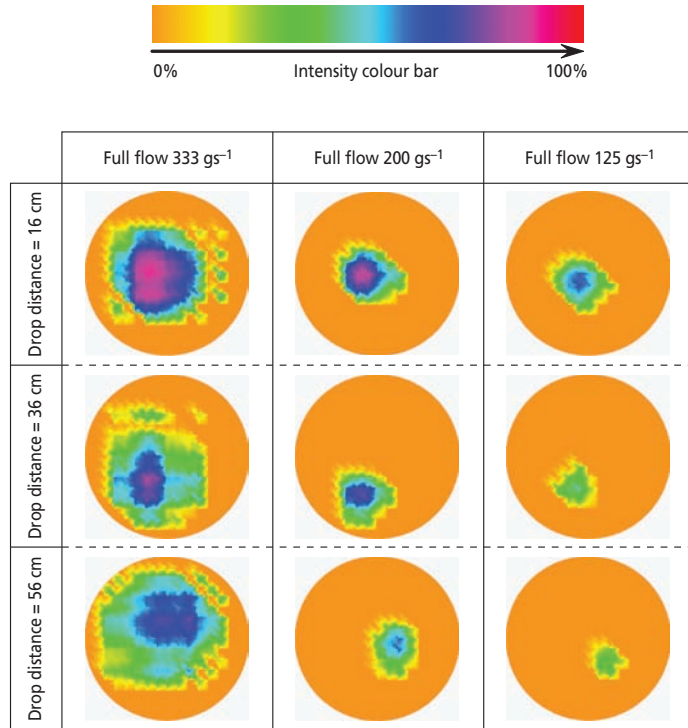


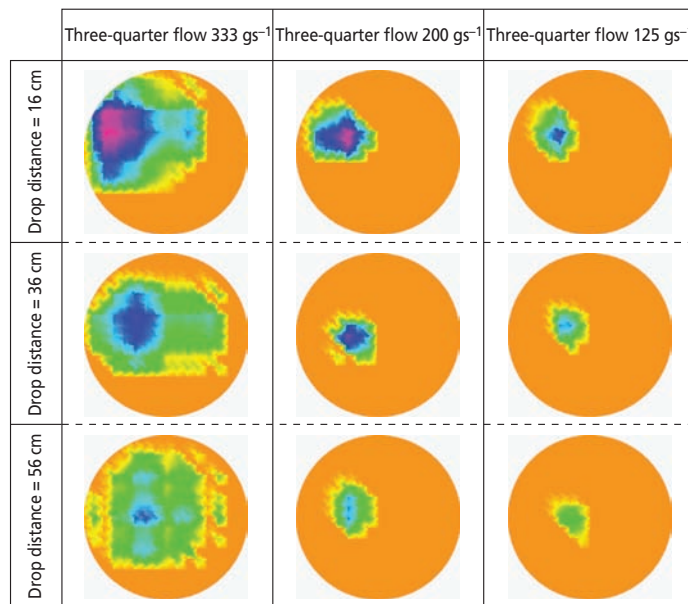
Figure 12. Upgrading original image resolution to higher resolution.

through a long distance in gravity flow, it is affected by the velocity, wall friction and collision among the particles. These factors make the flow of particles less predictable and they are scattered and more randomly distributed within the pipeline. This is demonstrated by

observing the half-flow and quarter-flow regimes at the flow rate of 333 gram/s, and comparing them with the cross-sectional images constructed at the drop distance of 56 cm where the flow is fairly uniformly distributed and unable to follow the required regime.

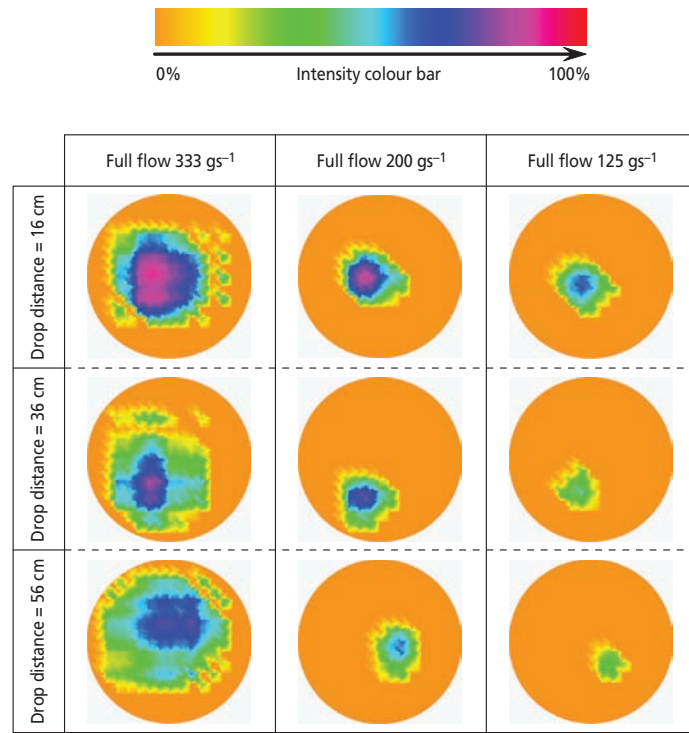


(a) Full-flow regime

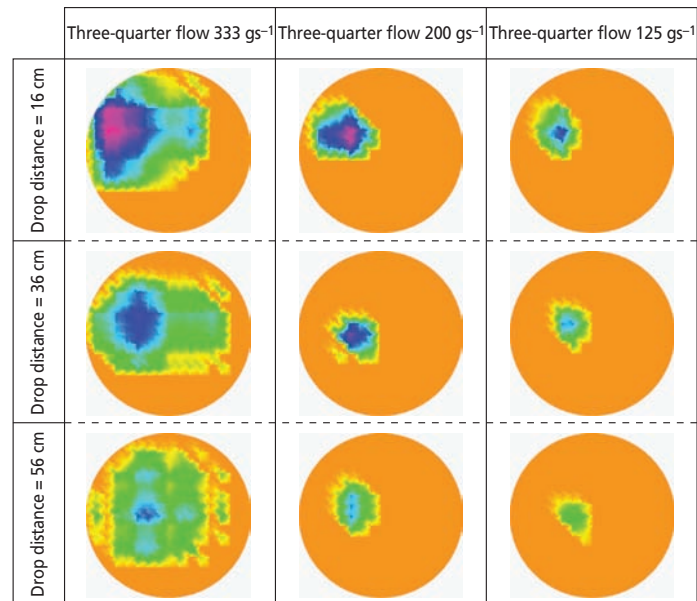


(b) Three-quarter flow regime

Figure 13. Cross-sectional images of various flow regimes.



(c) Half-flow regime



(d) Quarter-flow regime

Figure 13 cont. Cross-sectional images of various flow regimes.

CONCLUSION

Image reconstruction was conducted for four different flow regimes (full-flow, three-quarter flow, half-flow and quarter-flow) in three mass flow rates with drop distances of 16 cm, 36 cm and 56 cm. It could be concluded that

at the longest drop distance used, fewer of the plastic beads followed the required flow regimes. This was because collisions made the plastic beads deviate from the original flow. It also showed that the developed system was capable of showing the concentration profile of the flow.

An optical tomography system and the gravity pneumatic conveyor could have applications in industrial solid material handling and facilitate material control in a pre-mixing phase. The mass flow rate is a valuable parameter to be measured to control the flow. The proposed more recent method of using optical tomographic techniques to measure mass flow rate by integrating flow concentration, flow velocity and density of flow material together was investigated. This project provided the important points to be considered when undertaking flow velocity measurement and the velocity result obtained was of sufficient accuracy for computation of mass flow rate.

Date of submission: September 2006

Date of acceptance: May 2007

REFERENCES

- Arko A, Waterfall RC, Beck MS, Dyakowski T, Sutcliffe, P & Byars, M 1999, 'Development of electrical capacitance tomography for solids mass flow measurement and control of pneumatic conveying systems', *Proceedings 1st World Congress on Industrial Process Tomography*, 14–17 April, Buxton, Greater Manchester, pp. 140–146.
- Chan, KS 2001, 'Image reconstruction for optical tomography', B.Sc. dissertation, Universiti Teknologi Malaysia'.
- Chan, KS & Ruzairi Abdul Rahim 2002, 'Tomographic imaging of pneumatic conveyor using optical sensor', paper presented at the World Engineering Congress, Sarawak, Malaysia, IEEE.
- Cruz Meneses-Fabian, Gustavo Rodriguez-Zurita, Ramon Rodriguez-Vera & Jose F. Vazquez-Castillo 2003, 'Optical tomography with parallel projection differences and electronic speckle pattern interferometry', *Optics Communications*, vol. 228, pp. 201–210.
- Ibrahim S, Green, RG, Evans, K, Dutton, K & Abdul Rahim, R 2000, 'Optical tomography for process measurement and control', paper presented at the *Control 2000*, UKACC International Conference, University of Cambridge, 4–7 Sept.
- Ruzairi Abdul Rahim 1996, 'A tomography imaging system for pneumatic conveyors using optical fibres', PhD. thesis, Sheffield Hallam University, UK.
- Sallehuddin Ibrahim 2000, 'Measurement of gas bubbles in a vertical water column using optical tomography', PhD. thesis, Sheffield Hallam University', UK.
- Sallehuddin Ibrahim, Green, RG, Dutton, K & Ruzairi Abdul Rahim 2000, 'Modelling to optimize the design of optical tomography systems for process measurement', paper presented at *WARSAW 2000*, T-14.

Purification of Metallurgical Grade Silicon by Acid Leaching

V. A. Lashgari^{1*} and H. Yoozbashizadeh²

Silicon, as the most important electronic material, has a lot of applications in the electronic industry and this includes the use of silicon in solar cells. One of the solar grade silicon production processes is the use of acid leaching for the removal of metallic impurities from silicon. The main advantage of this process for silicon purification is that it is based on a low temperature process. The purification of metallurgical grade silicon by acid leaching was studied as a function of time, temperature and etching. Based upon experimental results and under optimum conditions, it was possible to remove 41%, 71% and 25% of iron, calcium and aluminum respectively, with the use of aqua regia.

Key words: Metallurgical grade silicon; refining; solar grade silicon; acid leaching

At present, due to the use of clean and inexhaustible energy sources such as solar energy and the high demand of silicon for solar cells, much effort has been made to produce low cost pure silicon (Morita & Miki 2003, p.1111). It is known that the chlorosilane process (conversion of silicon to chlorosilanes, chlorosilanes purification by distillation and other means and reduction of chlorosilane in chemical vapour deposition reactors) is a highly complicated and costly process. Thus in recent years, research activities have been carried out on alternative methods to purify silicon, especially for solar cells of a lower purity level rather than those for semiconductors (Lian *et al.* 1992, p. 269). One of the improved methods to enhance silicon quality is the hydrometallurgical refining process which is termed acid leaching (Dietl 1983, p. 145).

The large diversity of experimental conditions and results, frequently contradictory, clearly illustrate the fact that the different types of metallurgical grade silicon (MG-Si) from different origins have different leaching behaviour. Hunt *et al.* (1976, p. 200) reported the removal of more than 90% of the impurities in MG-Si by leaching with aqua regia for 12 h at 75°C. Dietl (1983, p. 145) reported that the best purification results were obtained using hydrochloric acid and hydrofluoric acid mixtures and finely ground MG-Si. Norman *et al.* (1985, p. 859) obtained 99.9% Si by leaching in three successive steps with aqua regia, hydrofluoric and hydrochloric acid.

In comparison to the structural composition, the size of particles or the leaching system seem unimportant to the final leaching yield. The choice of the correct phase structure makes it possible to work with coarser particles

and obtain greater purification using less aggressive leaching systems. From these observations, controlling the alloy composition during solidification is very important for the removal of metallic impurities from silicon (Margarido *et al.* 1993, p. 1).

To remove all the harmful impurities from silicon, a combination of several refining processes will be needed. This is because of the different behaviour and their characteristics of the various impurities present (Morita & Miki 2003, p. 1111).

IMPURITIES IN MG-SI AND REFINING PROCESS

Carbothermic reduction of quartzite at high temperature arc furnace yields silicon with a purity of 98% (MG-Si) which is used for metallurgical applications as a deoxidizer and alloying element (Habashi 1997). Molten silicon from the arc furnace is cast into ingots. Table 1 represents the segregation coefficients of impurity elements in silicon. During solidification, elements with low segregation coefficients and concentrations higher than maximum solid solubility are precipitated along grain boundaries. When MG-silicon is ground and subjected to acid leaching process, the impurities are exposed to acidic agents (Santos *et al.* 1990, p. 237).

In Figure, 1 solid solubilities of impurity elements with temperature in silicon are presented. In most cases the maximum solubility occurs at around 1300°C and are retrograde in behaviour both for lower temperatures and for temperatures nearer melting point (Dietl 1983, p. 145).

¹ School of Materials and Mineral Resources Engineering, Universiti Sains Malaysia, Engineering Campus, 14300 Nibong Tebal, Penang, Malaysia

² Department of Material Science and Engineering, Centre of Excellence in Advanced Materials, Sharif University of Technology, Tehran, Iran

* Corresponding author (e-mail: lashgari_v@hotmail.com.)

Table 1. Segregation coefficient of impurities in silicon.^a

Impurity	Segregation coefficient
B	$8.00 \cdot 10^{-1}$
P	$3.50 \cdot 10^{-1}$
C	$5.00 \cdot 10^{-2}$
Al	$2.80 \cdot 10^{-3}$
Fe	$6.40 \cdot 10^{-6}$
Ti	$2.00 \cdot 10^{-6}$
Cu	$8.00 \cdot 10^{-4}$

^a Morita & Miki 2003, p. 1111

Figure 2 demonstrates the attractiveness of hydrometallurgical purification. The lower the solid solubility, the lower is the value of the corresponding segregation coefficient (Dietl 1983, p.145).

EXPERIMENTAL PROCEDURE FOR REFINING PROCESS

The chemical analysis of silicon is shown in Table 2. The atomic absorption method (by HF-HNO₃ acid digestion, HCl leaching and AAS) was used to determine the amount

of metallic impurities. The results showed that, acid leaching was unable to remove impurities such as boron and phosphorus; however the main metallic impurities (Fe, Ca and Al) were effectively removed. After ballmilling, the silicon sample was sieved and a fraction with an average size under 100 μm was selected. Experiments were carried out in glass vessels with constant stirring and the temperature was controlled thermostatically.

Table 2. Chemical analysis of MG-silicon.

Element	Concentration (ppm)
Si	96%–98%
Fe	3150
Ca	70
Al	60
K	44
Mn	42
Mg	21

RESULTS

The influence of increasing the leaching time of aqua regia on the removal of impurities is illustrated for the three main impurities in Figure 3. Samples were leached with aqua regia at 50°C and with a liquid:solid ratio of 10:1.

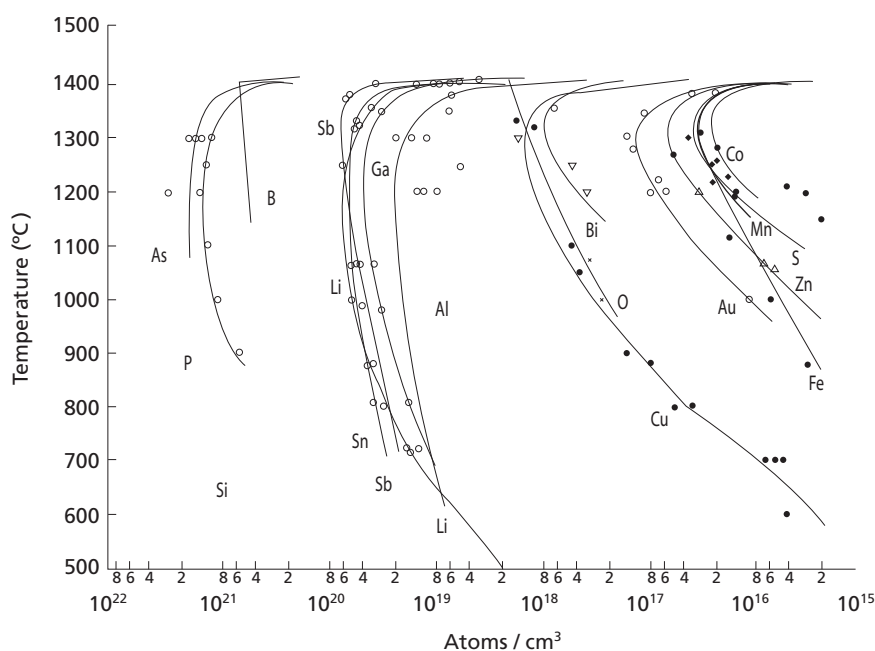


Figure 1. Solid solubility in silicon (Dietl 1983, p. 145).

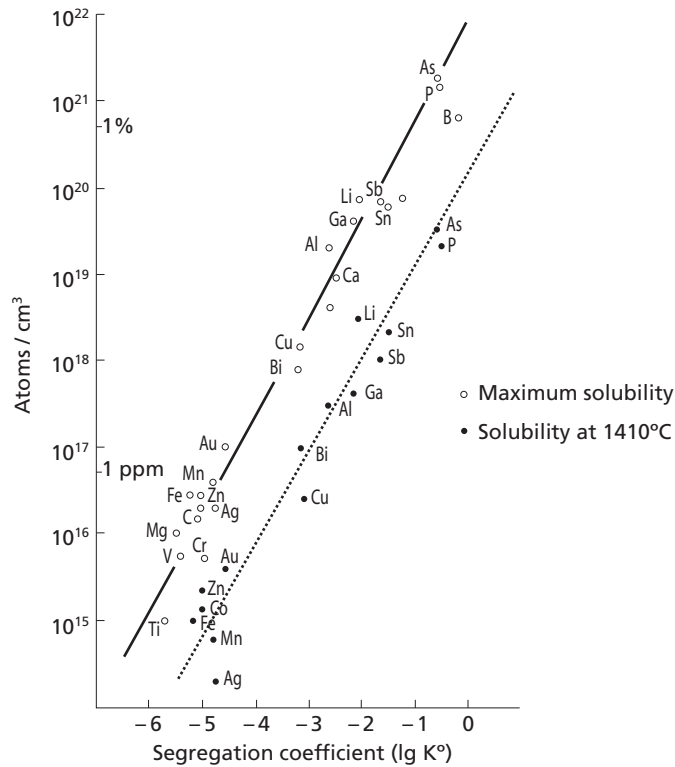


Figure 2. Correlation of solid solubility and segregation coefficient for different impurities in silicon (Dietl 1983, p.145).

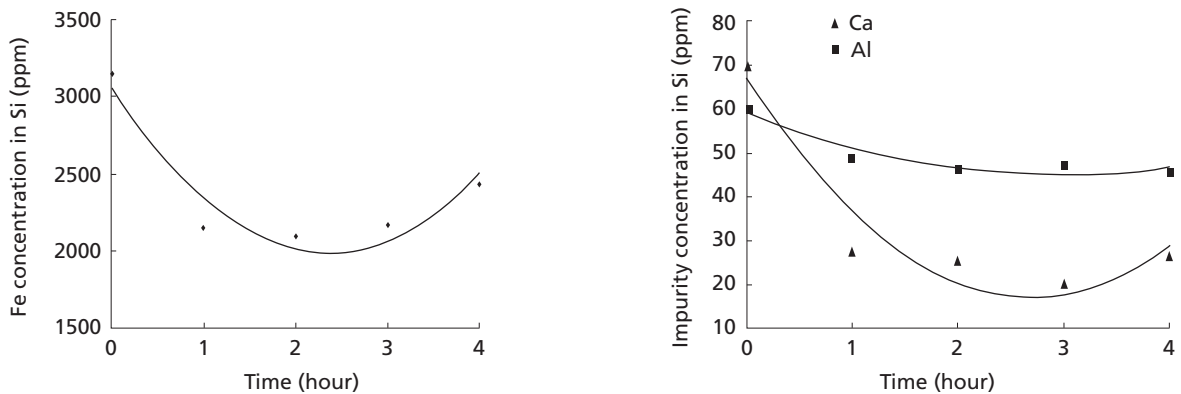


Figure 3. The effect of leaching time on the removal of impurity.

It could be seen that the leaching time of 2 h was suitable for iron and 3 h for calcium removal; but in the case of aluminum, time did not have a significant effect on the removal of Al. As aqua regia is a very strong oxidizing agent, Al particles were surrounded with an oxide layer and the leaching solution had no more effect on the removal of Al after about 1 h.

In Figure 4, the effect of leaching temperature on the removal of impurities is shown. Samples were leached with aqua regia for 3 h and with a liquid:solid ratio of 10:1.

A decrease in the purification of iron was observed at higher temperatures, while an increase was seen in the

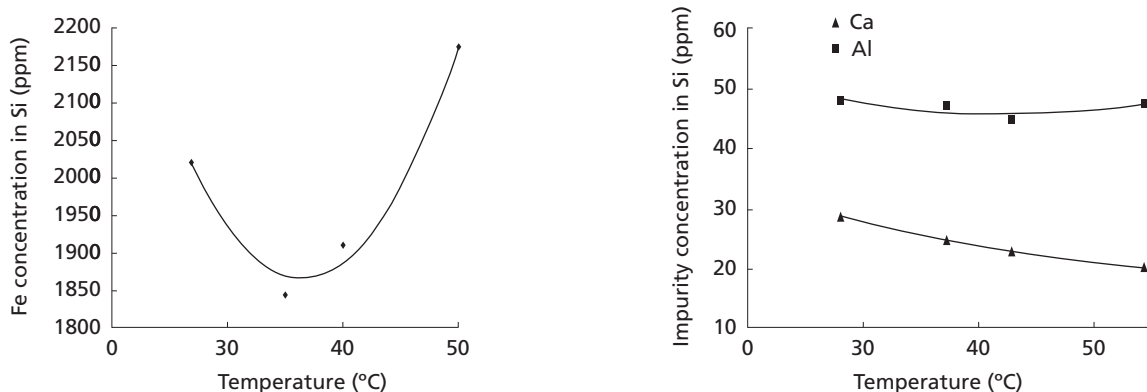


Figure 4. The effect of leaching temperature on the removal of impurity.

removal of calcium at higher temperatures; but in the case of Al, increase of temperature had no significant effect on the purification of silicon.

Etching Effects

To determine the effect of etching on silicon purification, an experiment was done with aqua regia (50°C, liquid/solid of 10/1, 3h) and prior to leaching; samples were etched with hydrofluoric acid and the results are shown in Table 3.

The results showed that, silicon etching had a positive effect only on the removal of Al from silicon. As mentioned earlier, Al particles were surrounded and covered with an oxide layer and the treatment of silicon with HF generated H_3AlF_6 complex and this dissolved the oxide layer and improved the removal of Al.

Table 3. The effect of preliminary etching on the purification of silicon.

Element	Impurity concentration in Si (ppm)	
	Without etching	With etching
Fe	2174	3001.6
Ca	20.4	40.6
Al	47.6	28

CONCLUSION

An effective leaching time of 2 h and 3 h was obtained for the removal of iron and calcium, respectively, but in the case of aluminum, time had no significant effect on the removal of Al.

Aqua regia is a very strong oxidizing agent, thus during leaching, Al particles were surrounded with an oxide layer and the leaching solution had no effect on the removal of Al after about 1 h.

At higher temperatures, a decrease in the purification of iron was observed, while an increase was seen in the removal of calcium at higher temperatures. In the case of Al, increase in temperature had no significant effect on the purification of silicon.

Silicon etching had a positive effect only on the removal of Al from silicon because treatment of silicon with HF generated H_3AlF_6 complex and this dissolved the oxide layer and improved the removal of Al.

To remove all harmful impurities from silicon, a combination of several refining processes will be needed. This is because of the different behaviour and their characteristics of the various impurities present.

Date of submission: December 2006

Date of acceptance: May 2007

REFERENCES

- Dietl, J 1983, 'Hydrometallurgical purification of metallurgical grade silicon', *Solar Cells*, vol. 10, no. 2, pp. 145-154.
- Habashi, F 1997, *Handbook of extractive metallurgy*, vol. IV, Wiley-VCH.
- Hunt, LP, Dosaj, VD, McCormick, JR & Crossman, LD 1976, 'Purification of metallurgical grade silicon to solar grade quality', in *Proceedings of Solar Energy, Proc. Int. Symp.*, Electro-chemical Society, New York, p. 200.
- Lian, SH, Kammel, R & Kheiri, MJ 1992, 'Preliminary study of hydro-metallurgical refining of MG-silicon with attrition

- grinding', *Solar Energy Materials and Solar Cells*, vol. 26, no. 1, pp. 269–276.
- Margarido, F, Martins, JP, Figueiredo, MO & Bastos, MH 1993, 'Refining of Fe-Si alloys by acid leaching', *Hydrometallurgy*, vol. 32, no. 1, pp. 1–8.
- Morita, K & Miki, T 2003, 'Thermodynamics of solar grade silicon refining', *Journal of Intermetallics*, vol. 11, nos. 11–12, pp. 1111–1117.
- Norman, CE, Thomas, RE & Absi, EM 1985, 'Solar grade silicon substrates by a powder-to-ribbon process', *Can. J. Phys.*, vol. 63, pp. 859–862.
- Santos, IC, Goncalves, AP, Santos, CS, Almeida, M, Afonso, MH & Cruz, MJ 1990, 'Purification of Metallurgical Grade Silicon by Acid Leaching', *Hydrometallurgy*, vol. 23, nos. 2–3, pp. 237–246.

Fourth Order Centred Total Variation Diminishing Scheme for Hyperbolic Conservation Laws

Y. H. Zahran¹

A new fourth order accuracy centred finite difference scheme for the solution of hyperbolic conservation laws is presented. A technique of making the fourth order total variation diminishing (TVD) scheme is also exhibited. The resulting scheme could avoid the spurious oscillations and preserve fourth-order accuracy in smooth parts. In addition the extension of the TVD scheme to the nonlinear scalar hyperbolic conservation laws are discussed. For nonlinear systems the TVD constraint was applied by solving shallow water equations. The performance of the scheme was assessed by solving test problems. Numerical results are presented and compared with exact solutions and other methods.

Key words: conservation laws; difference schemes; TVD; MUSCL; hyperbolic conservation laws; centred schemes

In recent years, much research was done in developing and implementing modern high resolution methods for approximating solutions of hyperbolic conservation laws.

Among the variety of methods for approximating solutions of such problems, I focus on finite difference methods which can be divided into two main categories, namely upwind schemes and centred schemes.

The prototype of upwind schemes is the first order Godunov scheme in which a piecewise constant interpolated (which is constructed based on previously computed cell averages) is evolved exactly to the next time step according to the conservation laws. This evolution involves a solution of Riemann Problems (RP) on the boundaries of each cell which is interpreted as an up-winding procedure, as one has to differ between the left-going and right-going waves in order to compute the inter-cell flux in the non-smooth regions.

An important issue is to how to generalize the first order Godunov method to second or higher order accuracy. Van Leer (1977, p. 263) proposed his monotone upwind schemes for conservation laws (MUSCL) approach whereby the piecewise constant cell average states in the Godunov method are replaced by reconstructed states that admit spatial variation within each cell. A class of second order Godunov-type (upwind) methods based on this approach have been constructed. Examples are MUSCL-Hancock schemes (Van Leer 1977, p. 263).

Centred (non-upwind or symmetric) schemes do not explicitly use the wave propagation information. The main advantage of centred over upwind schemes is that they do not require the solutions of Riemann problems or the

computation of characteristic velocities of the system. These features make the centred schemes approach very attractive for these systems for which the solution to the Riemann problem is complicated or when there is no simple analytical expression for the eigenvalues of the Jacobian matrix.

It is well known that when using a second (or higher) order accurate scheme, accuracy is gained in smooth parts of the solution, but the waves are accompanied by spurious oscillations and near discontinuities overshoots or undershoots are accompanied by spurious oscillations.

This problem has frustrated people for many years until the concept and theory of total variation diminishing (TVD) scheme was introduced by Harten (1983, p. 357). The main property of the TVD scheme is that it can be second (or higher) order and oscillations be free across discontinuities.

In this paper we use the MUSCL-Hancock (upwind) approach to construct, for linear case, fourth order centred scheme, whereby the Godunov first order upwind scheme is replaced by the second order centred scheme presented by Zahran (2004, p. 9), thus eliminating the need for the RP altogether. TVD version of this scheme was then constructed; this required the formulation of TVD conditions that are suitable for the scheme. Ways of extending the scheme to nonlinear scalar case are also presented. Some numerical results are also presented. The extension of the third order to nonlinear hyperbolic conservation laws was validated by solving a test problem for shallow water equations.

The paper firstly reviews briefly the general framework of the upwind and centered schemes. The fourth order

¹ Physics and Mathematics Department, Faculty of Engineering, Suez Canal University, Port Said, Port Fouad, P. O. Box 42523, Egypt
E-mail : yousef_hashem_zahran@yahoo.com

accuracy centred scheme following the MUSCL-Hancock approach was also constructed and a TVD version of the scheme was developed. Furthermore, the previous scheme to nonlinear scalar problems were extended. Subsequently, the scheme for constant coefficients linear hyperbolic conservation laws was elaborated. In addition, nonlinear systems typically the shallow water equations were discussed. Finally, numerical tests on the linear equations with different initial conditions, nonlinear Burger equations and shallow water equations were brought to light. Numerical results were presented and compared with exact solutions. The efficiency of the scheme was shown numerically by comparison with other schemes.

REVIEW OF THE DIFFERENCE SCHEMES

Consider the hyperbolic conservation law:

$$U_t + F(U)_x = 0, \quad -\infty < x < \infty, \quad t \geq 0 \quad (1)$$

along with initial and boundary conditions. Where U is the vector of m unknown conservative variables and $F(U)$ is the corresponding vector of fluxes.

Consider now a control volume in $x-t$ space $I_j \times (t^n, t^{n+1})$ of dimension. $\Delta x = x_{j+1/2} - x_{j-1/2}$, $\Delta t = t^{n+1} - t^n$, where $I_j = (x_{j-1/2}, x_{j+1/2})$. Integrating Equation 1 on this control volume produces the conservative formula:

$$U_j^{n+1} = U_j^n - \lambda(F_{j+1/2}^n - F_{j-1/2}^n), \quad \lambda = \frac{\Delta t}{\Delta x} \quad (2)$$

where, $U_j^n, F_{j+1/2}^n$ are given by:

$$U_j^n = \frac{1}{\Delta x} \int_{x_{j-1/2}}^{x_{j+1/2}} U(x, t^n) dx \quad \text{and} \quad F_{j+1/2}^n = \frac{1}{\Delta t} \int_{t^n}^{t^{n+1}} F[U(x_{j+1/2}, t) dt] \quad (3)$$

Numerical methods could be constructed based on the control volume (Equation 2) by finding numerical fluxes that are approximations to the time integral average of the fluxes at the control volume boundaries given in Equation 3. The numerical scheme will then evolve in time integral averages in control volumes. Next, the two classical ways of finding a numerical flux are briefly reviewed.

Upwind Difference Schemes

The prototype of such upwind schemes is the Godunov scheme. Godunov introduced the idea of computing the numerical flux in Equation 2 by evaluating Equation 3 in terms of the solution $U^*(x/t)$ of a local initial value problem called the RP:

$$U_t + F(U)_x = 0, \quad U(x, 0) = \begin{cases} U_j^n, & x < x_{j+1/2} \\ U_{j+1}^n, & x > x_{j+1/2} \end{cases} \quad (4)$$

evaluated at the cell interface $x_{j+1/2}$.

Conventionally, the initial data $U(x, 0)$ in the RP is piecewise constant and consists of two constant states of the form (Equation 3) separated by a discontinuity. Such distribution of the initial data is traditionally associated with a first order accurate Godunov type scheme with numerical flux:

$$F_{j+1/2} = F[U^*(0)] \quad (5)$$

obtained by evaluating the flux (Equation 3) with integrand $F[U^*(x/t)]$.

Van Leer (1977, p. 263) introduced the idea of modifying the piecewise constant data in the Godunov first order upwind method, as a way to achieve a higher order of accuracy. This approach has become known as MUSCL scheme and has been used to construct high order upwind schemes. A first step common to all MUSCL scheme is the data reconstruction procedure.

Data Reconstruction

The simplest way of modifying the piecewise constant data (U_j^n) is to replace the U_j^n , understood as integral averages in cells I_j , by piecewise linear functions $U_j(x)$, namely (Toro & Billett 2000, p. 47):

$$U_j(x) = U_j^n + \frac{(x-x_j)}{\Delta x} \Delta_j, \quad x \in (0, \Delta x) \quad (6)$$

where, Δ_j is suitably chosen slope of $U_j(x)$ in the cell I_j . The center of the cell x_j in local co-ordinates is $x = 1/2 \Delta x$ and $U_j(x_j) = U_j^n$.

The boundary extrapolated values are:

$$U_j^L(x) = U_j(0) = U_j^n - \frac{1}{2} \Delta_j, \quad U_j^R(x) = U_j(\Delta x) = U_j^n + \frac{1}{2} \Delta_j \quad (7)$$

A possible choice of the slope Δ_j in Equation 6 is:

$$\Delta_j = \frac{1}{2} (1+\omega) \Delta_{j-1/2} U + \frac{1}{2} (1-\omega) \Delta_{j+1/2} U \quad (8)$$

where, ω is a free parameter in the real interval $(-1, 1)$. For $\omega = 0$, Δ_j is a central difference approximation to the first spatial derivative. Here $\Delta_{j+1/2} u = u_{j+1} - u_j$.

MUSCL-Hancock approach. Having modified the data there are several ways of using the Godunov first order upwind method to obtain high order schemes. One possible choice is the MUSCL-Hancock approach (Van Leer 1985, p. 1):

This has three steps, namely (Toro 1998, p. 323):

- (i) Data reconstruction as in Equation 6 with boundary extrapolated values as in Equation 7.

(ii) Evolution of \bar{U}_j^L, \bar{U}_j^R by a time $1/2\Delta t$ according to:

$$\begin{aligned}\bar{U}_j^L &= U_j^L + \frac{1}{2}\lambda[F(U_j^L) - F(U_j^R)] \\ \bar{U}_j^R &= U_j^R + \frac{1}{2}\lambda[F(U_j^L) - F(U_j^R)]\end{aligned}\quad (9)$$

(iii) Solution of the piecewise constant data RP for the appropriate conservation laws with initial data $\bar{U}_j^R, \bar{U}_{j+1}^L$ to find the similarity solution $U_{j+1/2}(x/t)$.

In the conventional MUSCL-Hancock scheme, the inter-cell numerical flux $F_{j+1/2}$ is then obtained in exactly the same way as in the Godunov first order upwind method, namely:

$$F_{j+1/2} = F[U_{j+1/2}^*(0)] \quad (10)$$

Centered Schemes

Centered (non-upwind or symmetric) schemes do not explicitly utilize wave propagation of information and are thus simpler and more generally applicable. Commonly, the numerical fluxes can be computed explicitly as algebraic functions of the initial condition in Equation 4, namely:

$$F_{j+1/2} = F_{j+1}(U_{j+1/2}^n, U_{j+1}^n)$$

For examples, first order Lax-Friedrichs (L×F) and second order Lax-Wendroff (L–W); in Zahran (2004, p. 9), second order centered scheme was presented.

For the scalar hyperbolic conservation law, namely:

$$u_t + f(u)_x = 0 \quad (11)$$

Here, u is the unknown function, and $f(u)$ is the physical flux. First let us consider the linear case $f(u) = au$, so that $f(u) = a$ is a constant wave propagation speed.

The conservative numerical scheme introduced in Zahran (2004, p. 9) has the form:

$$U_j^{n+1} = U_j^n - \lambda(F_{j+1/2}^n - F_{j-1/2}^n) \quad (12a)$$

with the numerical flux:

$$F_{j+1/2} = \frac{1}{2}(au_j + au_{j+1}) - \frac{1}{2}|a|\Delta_{j+1/2}u + |a|\left\{A_0\Delta_{j+1/2}u + A_1\Delta_{j+L+1/2}u + A_2\Delta_{j+M+1/2}u\right\} \quad (12b)$$

where,

$$A_0 = \frac{1}{2} - \frac{|c|}{4}, A_1 = -\frac{1}{8} - \frac{|c|}{8}, A_2 = \frac{1}{8} - \frac{|c|}{8}, \quad (12c)$$

$L = -1, M = 1$ for $c > 0$ and $L = 1, M = -1$ for $c < 0$. Here $c = \frac{\Delta t}{\Delta x}a$ is the Courant number.

The above flux includes five point second order scheme. The scheme is stable for $|c| \leq \sqrt{2}$.

In the next section the MUSCL-Hancock approach was used to construct centred scheme, whereby the Godonuv first order upwind method is replaced by the second order centred scheme (Equation 12), thus eliminating the need of the RP altogether.

CENTERED MUSCL-HANCOCK METHOD

Here the MUSCL-Hancock scheme is modified, as mentioned in the last section, by replacing Godunov first order upwind method in step (iii) by the second order centred scheme (Equation 12). In this way, the role of the RP is eliminated altogether. Now, instead of solving the RP with data $(\bar{U}_j^R, \bar{U}_{j+1}^L)$ to find the Godunov first order upwind flux, I evaluated a centered flux $F_{j+1/2}^C$. For the linear equation (Equation 11), case $F_{j+1/2}^C$ is given by Equation 12b, and thus we have:

$$F_{j+1/2}^C = \frac{1}{2}a(\bar{u}_j^R + \bar{u}_{j+1}^L) - \frac{1}{2}a(\bar{u}_{j+1}^L - \bar{u}_j^R) + a\left\{A_0(\bar{u}_{j+1}^L - \bar{u}_j^R) + A_1(\bar{u}_j^L - \bar{u}_{j-1}^R) + A_2(\bar{u}_{j+2}^L - \bar{u}_{j+1}^R)\right\} \quad (13)$$

where, \bar{U}_j^R, \bar{U}_j^L are given by Equation 9.

Direct substitution of this flux into the conservative formula (Equation 12a) gives a seven point centered MUSCL-Hancock scheme, namely:

$$U_j^{n+1} = \sum_{-3}^3 b_k u_{j+k}^n \tag{14}$$

with coefficients:

$$\left. \begin{aligned} b_{-3} &= \frac{1}{192} \{-6c + 6c^3 + 6c\omega - 6c^3\omega\}, & b_{-2} &= \frac{1}{192} \{28c + 24c^2 - 12c^3 + 12c\omega - 12c^3\omega\} \\ b_{-1} &= \frac{1}{192} \{-18c + 14c^3 + 102c\omega - 6c^3\omega\}, & b_0 &= \frac{1}{192} \{192 + 120c - 48c^2 - 24c\omega^3 - 180c\omega + 36c^3\omega\} \\ b_1 &= \frac{1}{192} \{-178c + 18c^3 + 102c\omega - 6c^3\omega\}, & b_2 &= \frac{1}{192} \{12c + 24c^2 + 4c^3 - 12c\omega - 12c^3\omega\} \\ b_3 &= \frac{1}{192} \{6c - 6c^3 - 6c\omega + 6c^3\omega\} \end{aligned} \right\} \tag{15}$$

Theorem 1. Scheme (Equations 14 – 15) is third order accuracy in space and time for any value ω and it is fourth order accuracy in space and time when:

$$\omega = \frac{64c^2 - 32c^2 - 256c + 157}{384 - 192c^2} \tag{16}$$

Proof. It can be shown (Roe 1981) that a scheme for the linear equation (Equation 11) of the form (Equation 14) is p-th order accurate in space and time if and only if:

$$\sum k^q b_k = (-c)^q, 0 \leq q \leq p \tag{17}$$

Application of condition (Equation 17) to the scheme (Equations 14 – 15) produced the desired result. It is well known that the difference schemes that are second (or higher) order accurate produce spurious oscillations behind the waves and near discontinuities. This problem has frustrated people for many years until the concept and theory of TVD schemes were introduced by Harten (1983, p. 357). The main property of TVD scheme is that it can be second (or higher) order accurate and free of oscillation. A TVD version of this centre scheme will be constructed in the next section.

TVD ANALYSIS FOR FOURTH ORDER SCHEME

Here I propose TVD criteria that are suitable for constructing TVD schemes based on the centred fourth order scheme (Equations 14 – 16). To this end I consider the model of hyperbolic conservation law:

$$u_t + f(u)_x = 0, \quad f(u) = au \tag{18}$$

where, a is constant.

The fourth order finite difference centered scheme constructed in the last section may be written in conservative form as:

$$u_j^{n+1} = u_j^n - \lambda (F_{j+1/2}^n - F_{j-1/2}^n) \tag{19}$$

with numerical flux:

$$F_{j+1/2}^n = \frac{1}{2}(f_j + f_{j+1}) - \frac{1}{2}|a|\Delta_{j+1/2} u + |a|\{A_0\Delta_{j+1/2} u + A_1\Delta_{j+L+1/2} u + A_2\Delta_{j+M+1/2} u\} + |a|\{A_3\Delta_{j+S+1/2} u + A_4\Delta_{j+Q+1/2} u\} \tag{20}$$

where,

$$\left. \begin{aligned} A_0 &= \frac{1}{192} \{59 + 96\omega + 48c + 8c^2 - 48c^2\omega\}, & A_1 &= \frac{1}{192} \{176 + 24c - 36\omega + 12c^2\omega\} \\ A_2 &= \frac{1}{192} \{24 + 24c - 8c^3 - 24c\omega\}, & A_3 &= \frac{1}{192} \{-6 + 6c^2 + 6c\omega - 6c^2\omega\} \\ A_4 &= \frac{1}{192} \{6 + 6c^2 - 6\omega + 6c^2\omega\} \end{aligned} \right\} \tag{21}$$

$L = -1, M = 1, S = -2, Q = 2$; for $c > 0$ and $L = 1, M = -1, S = 2, Q = -2$ for $c < 0$.

We assume the scheme (Equation 19) can be expressed as:

$$u_j^{n+1} = u_j^n - B_{j-\frac{1}{2}} \Delta_{j-\frac{1}{2}} u + C_{j+\frac{1}{2}} \Delta_{j+\frac{1}{2}} u \quad (22a)$$

where $B_{j+\frac{1}{2}}$ and $C_{j+\frac{1}{2}}$ are data dependent coefficients i.e., functions of the set $\{u_j^n\}$.

To apply the TVD concept, we use Harten's theorem (Harten 1983, p. 357), which states that : the scheme Equation 22a is TVD provided that:

$$B_{j+\frac{1}{2}} \geq 0, \quad C_{j+\frac{1}{2}} \geq 0 \quad B_{j+\frac{1}{2}} + C_{j+\frac{1}{2}} \leq 1 \quad (22b)$$

Imposing a TVD constraint on Equation 20 via flux limiter functions gives:

$$F_{j+\frac{1}{2}} = \frac{1}{2}(f_j + f_{j+1}) - \frac{1}{2}|a|\Delta_{j+\frac{1}{2}}u + |a|\{A_0\Delta_{j+\frac{1}{2}}u + A_1\Delta_{j+L+\frac{1}{2}}u\}\phi_j + |a|\{A_2\Delta_{j+M+\frac{1}{2}}u + A_3\Delta_{j+S+\frac{1}{2}}u + A_4\Delta_{j+Q+\frac{1}{2}}u\}\phi_{j+M} \quad (23)$$

where, ϕ_j and ϕ_{j+M} are flux limiter functions.

Theorem 2. Schemes (Equation 19 and Equation 23) is TVD for $|c| \leq 1$ if the limiter function is determined by:

$$\phi_j \leq \frac{(1-|c|r_j)}{\eta(A_1r_j + A_0 - A_2 - A_3r_{j-2}^*r_j + \frac{A_4}{r_j^{**}}r_j)}, \quad (24)$$

$$\phi_j \leq \frac{(1-|c|) + \eta\left(\frac{A_2}{r_{j+1}^*} + A_3r_j + \frac{A_4}{r_{j+1}^{**}}\right)}{\eta(A_1r_j + A_0)}, \quad (25)$$

$$\phi_j \leq \frac{\left(\frac{A_2}{r_{j+1}^*} + A_3r_j + \frac{A_4}{r_{j+1}^{**}}\right)}{(A_1r_j + A_0)}, \quad (26)$$

$$\phi_j \geq 0 \quad (27)$$

where,

$$r_j = \frac{\Delta_{j+L+\frac{1}{2}}u}{\Delta_{j+\frac{1}{2}}u}, \quad r_j^* = \frac{\Delta_{j+L+\frac{1}{2}}u}{\Delta_{j+M+\frac{1}{2}}u}, \quad r_j^{**} = \frac{\Delta_{j+L+\frac{1}{2}}u}{\Delta_{j+Q+\frac{1}{2}}u} \quad (28)$$

and η is defined by:

$$\eta = \begin{cases} 1-|c| & \text{for } 0 \leq |c| < \frac{1}{2} \\ |c| & \text{for } \frac{1}{2} \leq |c| < 1 \end{cases} \quad (29)$$

Proof. Firstly, consider the method with Courant $0 \leq c \leq 1$.

From Equation 19 and Equation 23 the numerical method is:

$$u_j^{n+1} = u_j^n - c \left(\Delta_{j-\frac{1}{2}} u^n + A_0 \Delta_{j+\frac{1}{2}} u^n \phi_j + A_1 \Delta_{j+\frac{1}{2}} u^n \phi_j - A_0 \Delta_{j-\frac{1}{2}} u^n \phi_{j-1} - A_1 \Delta_{j-\frac{3}{2}} u^n \phi_{j-1} \right) - c \left(A_2 \Delta_{j+\frac{3}{2}} u^n \phi_{j+1} + A_3 \Delta_{j-\frac{3}{2}} u^n \phi_{j+1} + A_4 \Delta_{j-\frac{5}{2}} u^n \phi_{j+1} \right) + c \left(A_2 \Delta_{j+\frac{1}{2}} u^n \phi_j + A_3 \Delta_{j-\frac{3}{2}} u^n \phi_j + A_4 \Delta_{j+\frac{3}{2}} u^n \phi_j \right) \quad (30)$$

This is equivalent to Harten's theorem (Equation 22), with the choice:

$$B_{j-\frac{1}{2}} = c \left(1 + \frac{A_0}{r_j} \phi_j + A_1 \phi_j - A_0 \phi_{j-1} - A_1 r_{j-1} \phi_{j-1} \right) + c \left(\frac{A_0}{r_j^*} \phi_{j+1} + A_3 r_{j-1} \phi_{j+1} + \frac{A_4}{r_j^{**}} \phi_{j+1} \right) + c \left(-\frac{A_2}{r_j} \phi_j - A_3 r_{j-2}^* \phi_j - \frac{A_4}{r_j^{**}} \phi_j \right) \quad (31)$$

$$C_{j+\frac{1}{2}} = 0 \quad (32)$$

I apply condition, Equation 22 to Equation 31 i.e.,

$$0 \leq c \left(1 + \frac{A_0}{r_j} \phi_j + A_1 \phi_j - A_0 \phi_{j-1} - A_1 r_{j-1} \phi_{j-1} \right) + c \left(\frac{A_2}{r_j^*} \phi_{j+1} + A_3 r_{j-1} \phi_{j+1} + \frac{A_4}{r_j^{**}} \phi_{j+1} \right) + c \left(-\frac{A_2}{r_j^*} \phi_j - A_3 r_{j-2}^* \phi_j - \frac{A_4}{r_j^{**}} \phi_j \right) \leq 1 \quad (33)$$

one way to satisfy these inequalities is by imposing:

$$\left(\frac{A_0}{r_j} + A_1 - \frac{A_2}{r_j} - A_3 r_{j-2}^* - \frac{A_4}{r_j^{**}} \right) \phi_j - \left(A_0 + A_1 r_{j-1} \right) \phi_{j-1} + \left(\frac{A_2}{r_j^*} + A_3 r_{j-1} + \frac{A_4}{r_j^{**}} \right) \phi_{j+1} \leq \frac{1-c}{c} \quad (34)$$

$$\left(A_0 + A_1 r_{j-1} \right) \phi_{j-1} - \left(\frac{A_2}{r_j^*} + A_3 r_{j-1} + \frac{A_4}{r_j^{**}} \right) \phi_{j+1} - \left(\frac{A_0}{r_j} + A_1 - \frac{A_2}{r_j} - A_3 r_{j-2}^* - \frac{A_4}{r_j^{**}} \right) \phi_j \leq 1 \quad (35)$$

from Equation 34 we have:

$$0 \leq \left(\frac{A_0}{r_j} + A_1 - \frac{A_2}{r_j} - A_3 r_{j-2}^* - \frac{A_4}{r_j^{**}} \right) \phi_j \leq \frac{1-c}{c} \quad (36)$$

$$0 \leq \left(A_0 + A_1 r_{j-1} \right) \phi_{j-1} - \left(\frac{A_2}{r_j^*} + A_3 r_{j-1} + \frac{A_4}{r_j^{**}} \right) \phi_{j+1} \leq \frac{1-c}{c} \quad (37)$$

and from Equation 35 we get:

$$0 \leq \left(A_0 + A_1 r_{j-1} \right) \phi_{j-1} - \left(\frac{A_2}{r_j^*} + A_3 r_{j-1} + \frac{A_4}{r_j^{**}} \right) \phi_{j+1} \leq 1 \quad (38)$$

$$0 \leq \left(\frac{A_0}{r_j} + A_1 - \frac{A_2}{r_j} + A_3 r_{j-2}^* - \frac{A_4}{r_j^{**}} \right) \phi_j \leq 1 \quad (39)$$

from Equation 36, the following is derived:

$$\phi_j \leq \frac{(1-c)r_j}{c \left(A_0 + A_1 r_j - A_2 - A_3 r_{j-2}^* + \frac{A_4}{r_j^{**}} r_j \right)} \quad (40)$$

and from Equation 39, the following is obtained:

$$\phi_j \leq \frac{r_j}{c \left(A_0 + A_1 r_j - A_2 - A_3 r_{j-2}^* + \frac{A_4}{r_j^{**}} r_j \right)} \quad (41)$$

from Equations 37 and 38, I acquired:

$$\phi_j \leq \frac{1-c + c \left(\frac{A_2}{r_{j+1}^*} + A_3 r_j + \frac{A_4}{r_{j+1}^{**}} \right)}{c(A_0 + A_1 r_j)} \phi_{j+2}, \quad (42)$$

$$\phi_j \leq \frac{1 + \left(\frac{A_2}{r_{j+1}^*} + A_3 r_j + \frac{A_4}{r_{j+1}^{**}} \right)}{(A_0 + A_1 r_j)} \phi_{j+2} \quad (43)$$

and

$$\phi_j \geq \frac{\frac{A_2}{r_{j+1}^*} + A_3 r_j + \frac{A_4}{r_{j+1}^{**}}}{(A_0 + A_1 r_j)} \phi_{j+2} \quad (44)$$

$$\phi_j \geq 0 \quad (45)$$

then from Equations 40 and 41 the following is secured:

$$\Phi_j \leq \frac{(1-|c|)r_j}{\eta \left(A_1 r_j + A_0 - A_2 - A_3 r_{j-2}^* + \frac{A_4}{r_j^{**}} r_j \right)} \quad (46)$$

$$\Phi_j \leq \frac{(1-|c|) + \eta \left(\frac{A_2}{r_{j+1}^*} + A_3 r_j + \frac{A_4}{r_{j+1}^{**}} \right)}{\eta (A_1 r_j + A_0)} \Phi_{j+2} \quad (47)$$

$$\Phi_j \geq \frac{\frac{A_2}{r_{j+1}^*} + A_3 r_j + \frac{A_4}{r_{j+1}^{**}}}{(A_1 r_j + A_0)} \Phi_{j+2} \quad (48)$$

where, η is defined by Equation 29. The analysis for $-1 \leq c \leq 0$ goes through in exactly the same way, but c is replaced by $|c|$ and Φ_{j+2} is replaced by Φ_{j-2} . Finally, by setting $\Phi_{j+2} = 1$ or $\Phi_{j-2} = 1$ the theorem is established (Shi & Toro 1996, p. 343).

By applying the last theorem to the scheme (Equation 19 and Equation 23), the flux limiter can be defined as:

$$\Phi_j = \begin{cases} \frac{(1-|c|)r_j}{\eta \left(A_1 r_j + A_0 - A_2 - A_3 r_{j-2}^* + \frac{A_4}{r_j^{**}} r_j \right)}, & 0 \leq r_j \leq r^L \\ 1 & r^L \leq r_j \leq r^R \\ \frac{(1-|c|) + \eta \left(\frac{A_2}{r_{j+1}^*} + A_3 r_j + \frac{A_4}{r_{j+1}^{**}} \right)}{\eta (A_1 r_j + A_0)}, & r_j \leq r^R \\ 0 & r_j \leq 0 \end{cases} \quad (49)$$

where,

$$r^L = \frac{\eta(A_0 - A_2 - A_3 r_{j-2}^*)}{1-|c| - \eta A_1 - \eta \frac{A_4}{r_j^{**}}}, \quad r^R = \frac{1-|c| - \eta \left(A_0 - \frac{A_2}{r_{j+1}^*} - \frac{A_4}{r_{j+1}^{**}} \right)}{\eta(A_1 - A_3)} \quad (50)$$

Therefore the scheme (Equation 19 and Equation 23) becomes TVD.

EXTENSION TO NONLINEAR SCALAR HYPERBOLIC CONSERVATION LAWS

To extend the scheme (Equation 19 and Equation 23) to nonlinear scalar problems, I consider the equation:

$$u_t + f(u)_x = 0, \quad (51)$$

Define the wave speed,

$$a_{j+\frac{1}{2}} = \begin{cases} \frac{\Delta_{j+\frac{1}{2}} f}{\Delta_{j+\frac{1}{2}} u} & \Delta_{j+\frac{1}{2}} u \neq 0 \\ \frac{\partial f}{\partial u} \Big|_{u_j} & \Delta_{j+\frac{1}{2}} u = 0 \end{cases} \quad (52)$$

Now I re-define the r_j in Equation 28 as:

$$r_j = \frac{|a_{j+L+\frac{1}{2}}| \Delta_{j+L+\frac{1}{2}} u}{|a_{j+\frac{1}{2}}| \Delta_{j+\frac{1}{2}} u}, \quad r_j^* = \frac{|a_{j+L+\frac{1}{2}}| \Delta_{j+L+\frac{1}{2}} u}{|a_{j+M+\frac{1}{2}}| \Delta_{j+M+\frac{1}{2}} u}, \quad r_j^{**} = \frac{|a_{j+L+\frac{1}{2}}| \Delta_{j+L+\frac{1}{2}} u}{|a_{j+Q+\frac{1}{2}}| \Delta_{j+Q+\frac{1}{2}} u} \quad (53)$$

Here $c_{j+1/2} = \frac{\Delta t}{\Delta x} a_{j+1/2}$. Unlike the constant coefficient case, $a_{j+1/2}$ and $a_{j-1/2}$ are not always the same sign. Then the numerical flux (Equation 23) takes the form:

$$F_{j+1/2} = \frac{1}{2}(f_j + f_{j+1}) - \frac{1}{2}|a_{j+1/2}|\Delta_{j+1/2}u + |a_{j+1/2}|\left\{A_0\Delta_{j+1/2}u + A_1\Delta_{j+L+1/2}u\right\}\phi_{j+} + |a_{j+1/2}|\left\{A_2\Delta_{j+M+1/2}u + A_3\Delta_{j+S+1/2}u + A_4\Delta_{j+Q+1/2}u\right\}\phi_{j+M} \quad (54)$$

After considering all the possible combinations of the signs of $a_{j+1/2}$ and $a_{j-1/2}$, a set of sufficient conditions on ϕ still can be of the form similar to Equation 49 by replacing (c) by $a_{j+1/2}$.

APPLICATION ON LINEAR HYPERBOLIC SYSTEMS

In this section we extend the scalar schemes (Equation 19 and Equation 23) to solve the initial value problem for linear hyperbolic systems with constant coefficients:

$$U_t + AU_x = 0, \quad U(x,0) = U_0(x) \quad (55)$$

where, U is a column vector of m conserved variables and A is an $m \times m$ constant matrix. This is a system of conservation laws with flux function $F(U) = AU$ which is hyperbolic if A is diagonalizable with real eigenvalues, i.e. the matrix A can be written as:

$$A = R \Omega R^{-1} \quad (56)$$

Where, $\Omega = \text{diag}(\lambda^{(1)}, \lambda^{(2)}, \dots, \lambda^{(m)})$ is the diagonal matrix of eigenvalues of A and $R = (r^{(1)}, r^{(2)}, \dots, r^{(m)})$ is the matrix of right eigenvectors of A .

Equation 56 means $AR = R \Omega$, i.e.:

$$Ar^{(p)} = \lambda^{(p)} r^{(p)}, \quad p = 1, 2, \dots, m \quad (57)$$

The natural way to extend the scalar scheme to linear systems is obtained by defining expressions for the flux differences $\Delta_{j+1/2}F = A\Delta_{j+1/2}U$. This can be done by diagonalizing the system, solving local RPs with left and right states U_j^n and U_{j+1}^n , i.e.:

$$U(x,0) = \begin{cases} U_j^n, & x < 0 \\ U_{j+1}^n, & x > 0 \end{cases} \quad (58)$$

and letting

$$\alpha_{j+1/2} = R_{j+1/2}^{-1} \Delta_{j+1/2}U \quad (59)$$

where, $R_{j+1/2}$ is the matrix of right eigenvectors at the interface $(j + 1/2)$, which for the linear constant coefficient case is of course constant; $\alpha_{j+1/2}$ is called the wave strength vector with components $\alpha_{j+1/2}^{(p)}$, ($p = 1, 2, \dots, m$) across the p -th wave travelling at speed $\lambda_{j+1/2}^{(p)}$ in the $(j + 1/2)$ intercell. Then I have:

$$\Delta_{j+1/2}U = \sum_{p=1}^m \alpha_{j+1/2}^{(p)} r_{j+1/2}^{(p)} \quad (60)$$

Since $F(U) = AU$, this leads to:

$$\Delta_{j+1/2}F = A\Delta_{j+1/2}U = \sum_{p=1}^m \alpha_{j+1/2}^{(p)} Ar_{j+1/2}^{(p)} = \sum_{p=1}^m \alpha_{j+1/2}^{(p)} \lambda_{j+1/2}^{(p)} r_{j+1/2}^{(p)} \quad (61)$$

Note that the single jump $\Delta_{j+q+1/2}F = |a_{j+q+1/2}|\Delta_{j+q+1/2}U$ in the scalar scheme (Equation 54) with the appropriate interpretation for $|a_{j+q+1/2}|$ is now substituted by a summation of jump (Equation 61), which gives a natural extension to linear systems with constant coefficients.

NONLINEAR HYPERBOLIC SYSTEMS

Let the nonlinear system of equations be:

$$U_t + F(U)_x = 0 \quad (62)$$

where, $F(U)$ is a vector flux such that $A(U) = \frac{\partial F}{\partial U}$ is the Jacobian matrix.

A possible strategy for solving systems of nonlinear equations is to linearize the nonlinear system of equations (Equation 62) locally at each cell interface by an approximate of the Jacobian matrix $A(U)$ and then implement the method of the last section using the linearized system:

$$U_t + \bar{A}U_x = 0 \quad (63)$$

where, \bar{A} is a linearized constant matrix depending only on the local data U_j^n and U_{j+1}^n , i.e.,

$\bar{A} = \bar{A}(U_j^n, U_{j+1}^n)$. Popular example of this approach is Roe's approximation (Roe 1981). Roe's matrix

$\bar{A}(U_j^n, U_{j+1}^n)$ is assumed to satisfy the following properties :

- i) $\bar{A}\Delta_{j+1/2}U = \Delta_{j+1/2}F$
- (ii) \bar{A} is diagonalizable with real eigenvalues ;
- (iii) $A \rightarrow F'(\bar{U})$ smoothly as $U_j^n, U_{j+1}^n \rightarrow \bar{U}$. Denoting the Roe eigenvalues, eigen vectors and wave strengths as $\bar{\lambda}_{j+1/2}^{(p)}, \bar{r}_{j+1/2}^{(p)}, \bar{\alpha}_{j+1/2}^{(p)}$ ($p = 1, 2, \dots, m$) respectively, then applying the fourth order scheme of the last section, I solved the original nonlinear systems in a straightforward manner.

Shallow Water Equations

The one-dimensional shallow water equations as atypical nonlinear system of conservation laws, represents the motion of a free surface flow in a channel, take the form (Vella 1989, p. 830):

$$U_t + F(U)_x = 0 \quad (64a)$$

where,

$$U = (S, Su)^T, F(U) = (S, Su^2 + S^2)^T \quad (64b)$$

where, S is the cross section of the flow, u velocity. With initial conditions:

$$U(x, t_0) = \begin{cases} U_L & x < x_0 \\ U_R & x > x_0 \end{cases} \quad (64c)$$

Equations 64 can be written in the form:

$$U_t + A(U)U_x = 0, \quad A(U) = \frac{\partial F}{\partial U} \quad (65)$$

where, $A(U)$ is the Jacobian matrix such that:

$$A = \begin{pmatrix} 0 & 1 \\ 2S - u^2 & 2u \end{pmatrix} \quad (66)$$

The system (Equations 64 – 66) is hyperbolic with eigen values:

$$\lambda^{(1)} = u - C, \quad \lambda^{(2)} = u + C \quad (67)$$

where $C = \sqrt{2S}$ denotes the sound speed. The corresponding right eigenvectors of the Jacobian A are found to be:

$$r^{(1)} = (1, u - C)^T, \quad r^{(2)} = (1, u + C)^T \quad (68)$$

Linearization of Shallow Water Equations

The nonlinear system of Equations 64 can be linearized as:

$$U_t + \bar{A}U_x = 0 \tag{69}$$

where, \bar{A} is an approximate Jacobian matrix of A with eigenvalues $\bar{\lambda}^{(p)}$ and eigen vectors $\bar{r}^{(p)}$ such that:

$$\bar{A}\Delta U = \Delta F \tag{70}$$

The approximate matrix Jacobian \bar{A} satisfying Equation 70 can be written as:

$$\bar{A}(U_j, U_{j+1}) = \begin{pmatrix} 0 & 1 \\ \bar{C}^2 - \bar{u}^2 & 2\bar{u} \end{pmatrix} \tag{71a}$$

where, \bar{C} and \bar{u} are given by:

$$\bar{C} = \sqrt{S_j + S_{j+1}} \tag{71b}$$

$$\bar{u} = \frac{u_{j+1}\sqrt{S_{j+1}} + u_j\sqrt{S_j}}{\sqrt{S_{j+1}} + \sqrt{S_j}} \tag{71c}$$

The eigenvalues and eigen vectors of the linearized matrix \bar{A} are:

$$\bar{\lambda}^{(1)} = \bar{u} - \bar{C}, \quad \bar{\lambda}^{(2)} = \bar{u} + \bar{C}, \quad \bar{r}^{(1)} = (1, \bar{u} - \bar{C})^T, \quad \bar{r}^{(2)} = (1, \bar{u} + \bar{C})^T \tag{72}$$

The wave strengths are:

$$\bar{\alpha}^1 = 0.5\Delta S + \frac{1}{2\bar{C}}(\bar{u}\Delta S - \Delta Su), \quad \bar{\alpha}^2 = 0.5\Delta S - \frac{1}{2\bar{C}}(\bar{u}\Delta S - \Delta Su) \tag{73}$$

where, $\Delta pq = \bar{p}\Delta q + \bar{q}\Delta p$.

NUMERICAL EXPERIMENTS

In this section some numerical experiments are presented to show the performance of my method. For all calculations, transmissive boundary conditions are used.

Example 1.

The approximate solution of the linear equation was considered:

$$u_t + u_x = 0, \quad -1 < x < 1, \quad t \geq 0 \tag{74}$$

$$u(x, 0) = \sin^4(\pi x) \tag{75}$$

with periodic condition on $[-1, 1]$. This test is used to check the convergence rate of the scheme. I compared my fourth order scheme with Balaguer’s fourth order scheme (Balaguer & Conde 2005, p. 455). Here the Balaguer fourth order scheme will be referred to as BG and the fourth order scheme (Equation 19 and Equation 23) will be referred to as FD4.

Table 1 shows the L^1 and L^∞ errors at large time $t = 10$. Several runs with different grid sizes were performed. Here, N denotes the total number of spatial cells. The author regarded $\Delta t = 0.8 \Delta x$. From Table 1 it was noted that the fourth order scheme (Equations 19 – 23) was more accurate than the Balaguer scheme. Moreover, the magnitude of the errors of FD4 were much smaller than of BG scheme, even on coarsest mesh.

Table 1. L^1 and L^∞ errors at large time $t = 10$.

N	BG L ¹ error	BG L ¹ order	FD4 L ¹ error	FD4 L ¹ order	BG L [∞] error	BG L [∞] order	FD4 L [∞] error	FD4 L [∞] order
80	2.431E-4		6.528E-5		2.936e-4		1.004E-4	
160	1.363E-5	4.16	3.224E-6	4.34	1.636E-5	4.17	4.953E-6	4.34
320	8.262E-7	4.04	1.633E-7	4.30	1.076E-6	3.93	2.526E-7	4.29
640	5.110E-8	4.01	8.379E-9	4.28	6.462E-8	4.06	1.287E-8	4.30

Example 2.

The author considered Equation 74 with the initial condition (Balagur & Conde 2005, p. 455):

$$u(x,0) = \begin{cases} \frac{1}{6}[G(x, z - \delta) + G(x, z + \delta) + 4G(x, z)], & -0.8 \leq x \leq -0.6 \\ 1, & -0.4 \leq x \leq -0.2 \\ 1 - |10(x - 0.1)| & 0 \leq x \leq 0.2 \\ \frac{1}{6}[F(x, a - \delta) + F(x, a + \delta) + 4F(x, a)], & 0.4 \leq x \leq 0.6 \\ 0, & \text{otherwise} \end{cases} \quad (76)$$

with periodic boundary condition on $[-1,1]$.

Where, $G(x, z) = \exp[-\beta(x - z)^2]$, $F(x, a) = \{\max(1 - \alpha^2(x - a)^2)\}^{1/2}$. The constants are taken as $a = 0.5$, $z = -0.7$, $\delta = 0.005$, $\alpha = 10$ and $\beta = (\log 2)/36\delta^2$.

This initial condition consists of several shapes which are difficult for numerical methods to resolve correctly. Some of these shapes are not smooth and the others are smooth but extremely sharp.

Figure 1 shows the numerical results at $t = 20$ obtained by FD4 scheme with mesh size of 200 cells and $\Delta t = 0.8\Delta x$. The exact solution is shown by the solid line and numerical solution shown by symbols. Comparing the results in Figure 1 and Figure 4.1 in Balagur & Conde (2005, p. 455), I noticed that the accuracy of FD4 scheme was higher overall than that of the BG scheme. In particular, FD4 provided better resolution of the discontinuous square pulse. I also noted that the resolution of the left peak in the FD4 scheme was sharper than the BG scheme. I observed that my method was more accurate and economic since for the FD4 scheme, I considered $\Delta t = 0.8\Delta x$ and 200 cells while for the BG scheme, $\Delta t = 0.45\Delta x$ and 500 cells.

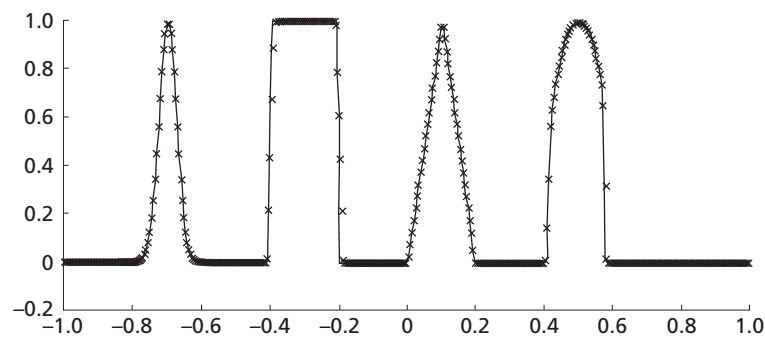


Figure 1. Solution of the Equation 74 (with Equation 76 and the FD4 scheme at $t = 20$).

Example 3. In this example I approximated the solution of the inviscid Burger equation:

$$u_t + \left(\frac{u^2}{2}\right)_x = 0, \quad (77)$$

with the smooth periodic data:

$$u(x,0) = 1 + 0.5 \sin \pi x, \quad -1 \leq x \leq 1 \quad (78)$$

It is well known that the solution of Equation 77 and Equation 78 develops a shock discontinuity at the critical time $t = 1.1$. Using $N = 80$ and $\Delta t = 0.8 \Delta x$. Figure 2 shows the results obtained by the scheme (Equation 19 and Equation 54)

at $t = 1.1$. Note that the numerical solutions in Figure 2, using the fourth order scheme (Equation 19 and Equation 54), are almost indistinguishable from the exact solutions. Comparing the results in Figure 2 with the results in Figure 4.3 in Balagur & Conde (2005, p. 455) with $\Delta t = 0.33\Delta x$, I noticed that my scheme was more accurate than the BG scheme and saved more time.

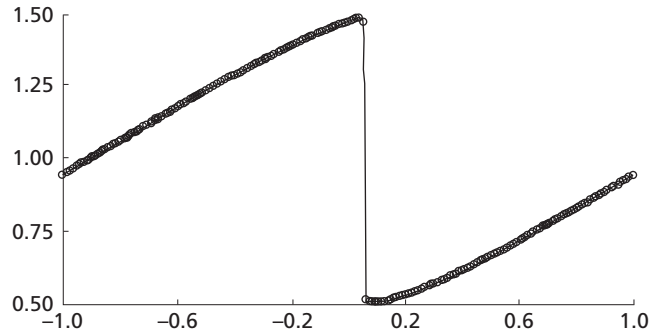


Figure 2. Solution of the Equation 77 with Equation 78 : (a) at $t = 1.1$.

Example 4. Here I apply my scheme developed in this paper to Buckley–Leverett’s problem, whose flux is non-convex (Balagur & Conde 2005, p. 455):

$$\frac{\partial u}{\partial t} + \frac{\partial f(u)}{\partial x} = 0, \quad -1 \leq x \leq 1, \quad f(u) = \frac{4u^2}{4u^2 + (1-u)^2} \quad (79a)$$

subject to the initial condition:

$$u_0(x) = \begin{cases} 1 & x \in [-0.50, 0], \\ 0 & \text{otherwise} \end{cases} \quad (79b)$$

Similarly to Balagur & Conde (2005), I have computed the solution at $t = 0.4$ with my scheme (Equation 19 and Equation 54). Figure 3 shows the results obtained with $N = 80$ and $\Delta t = 0.8 \Delta x$. Comparing the results with Figure 4.4 in Balagur & Conde (2005) (with $\Delta t = 0.25 \Delta x$) I noticed that my scheme was more efficient than the BG scheme.

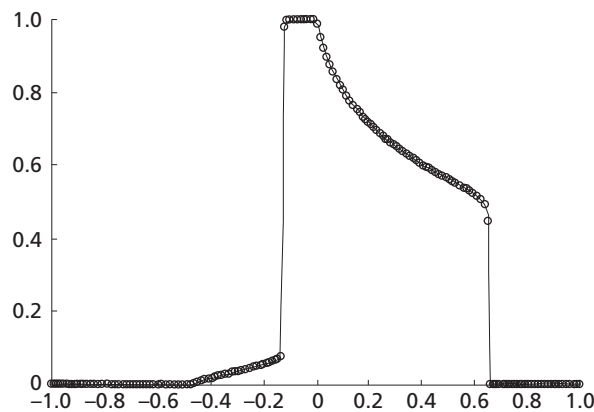


Figure 3. Solution of the Equation 79 at $t = 0.4$.

Example 5. Here, we discuss numerical test results of the solution of the RP (Equation 64) with initial data 9:

$$U_L = (0.597, 0)^T, \quad U_R = (0.004166, 0)^T \quad (80)$$

The numerical experiments were performed using the linearized system (Equations 69 – 73) and the scheme (Equation 19 and Equation 23). Figure 4 shows the exact solution in full lines for the cross section $S(x,t)$ and the velocity $u(x,t)$ together with the numerical solution, shown in symbols. I regard $\Delta x = 0.01$ and the Courant number used is 0.9. Note that the results showed good approximation in the smooth parts and the discontinuities were absolutely sharp and their positions were exact.

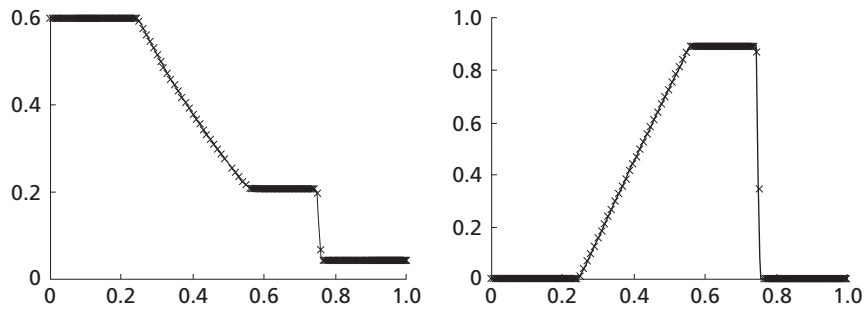


Figure 4. Solution of shallow water equation using the scheme (Equation 19 and Equation 23) using the linearized method.

Date of submission: December 2006

Date of acceptance: June 2007

REFERENCES

- Balagur, A & Conde, C 2005, 'Fourth order non-oscillatory upwind and central schemes for hyperbolic conservation laws', *SIAM J. Numer. Anal.*, vol. 43, no. 2, pp. 455–473
- Harten, A 1983, 'High resolution scheme for hyperbolic conservation laws' *J. Comput. Phys.*, vol. 83, pp. 357–393
- Roe, PL 1981, 'Numerical algorithms for linear wave equation', *Technical Report 81047*, Royal Aircraft Establishments Bedford, U.K.
- Shi, J & Toro, EF 1996, 'Fully discrete high order shock capturing numerical schemes', *Int. J. Numer. Methods Fluids*, vol. 23, pp. 241–269.
- Toro, EF 1998, 'Primitive, conservative and adaptive schemes for hyperbolic conservation laws', in *Numerical methods for wave propagation*, eds EF Toro & JF Clarke, Kluwer Academic Publishers, pp. 323–358.
- Toro, EF & Billett, SJ 2000, 'Centered TVD schemes for hyperbolic conservation laws', *IMA J. Numerical Analysis*, vol. 20, pp. 47–79.
- Van Leer, B 1977, 'Towards the ultimate conservative difference schemes III. Upstream-centered finite difference schemes for ideal compressible flow', *J. Comput. Phys.*, vol. 23, pp. 263–275.
- Van Leer, B 1985, 'On the relation between the upwind differencing schemes of Godunov, Enguist, Osher and Roe', *SIAM J. Sci. Stat. Comput.*, vol. 5, pp. 1–20.
- Vila, JP 1989, 'An analysis of class of second order accurate Godunov type schemes', *SIAM J. Num. Anal.*, vol. 26, pp. 830–853.
- Zahran, YH 2004, 'A family of TVD second order schemes of nonlinear scalar conservation laws', *J. Comptes Rendus de l'Acad. Bulgare de Sci.*, vol. 57, no 2, pp. 9–18.

Stability of Marangoni Convection in Superposed Fluid and Porous Layers

N. M. Arifin^{1,*}, N. F. M. Mokhtar¹, R. Nazar² and I. Pop³

Linear stability analysis was used to investigate the onset of Marangoni convection in a two-layer system. The system comprised a saturated porous layer over which was a layer of the same fluid. The fluid was heated from below and the upper free surface was deformable. At the interface between the fluid and the porous layer, the Beavers-Joseph slip condition was used and in the porous medium the Darcy law was employed to describe the flow. Predictions for the onset of convection were obtained from the analysis by the perturbation technique. The effect of surface deformation and depth ratio, ζ (which is equal to the depth of the fluid layer/depth of the porous layer) on the onset of fluid motion was studied in detail.

Key words: Marangoni convection; porous medium; stability; flow; surface deformation; depth ratio

The problem of thermoconvective instability in a horizontal convection has been studied extensively by many researchers. The first theoretical study on steady Marangoni convection in a horizontal fluid layer was done by Pearson (1958). The convective instability of a fluid overlying a porous region saturated with the fluid, subject to a uniform temperature gradient has been investigated extensively by several authors (Nield 1977, 1998; Nield & Bejan 2006; Straughan 2001; Taslim & Narusawa 1989). Nield (1977) considered a layered model and employed an empirical interfacial condition at the fluid-porous interface suggested by Beavers and Joseph (1967). Chen and Chen (1988) produced a classical paper in which they studied the thermal convection in a two-layer system composed of a porous layer saturated with fluid over which lay the same fluid. The work of Chen and Chen (1988) employed the fundamental model for convection in a porous-fluid-layer system developed originally by Nield (1977).

McKay (1998) examined the onset of Bénard convection in a layer of fluid on top of a saturated porous layer. He reported that the relative thickness of the two layers determines whether this convection is concentrated in the fluid layer or in the porous layer. The presence of thin porous layers was found to have a small destabilizing influence on the system. Shivakumara *et al.* (2006) studied the onset of Marangoni convection in a composite porous-layer system and Beavers-Joseph slip condition is used at the interface and Darcy law is employed to describe the flow in the porous medium. They showed that the linear stability curves for the onset of Marangoni convection depend on the parameter ζ , that is the ratio of the fluid layer depth to the porous layer depth. They interpreted their findings by showing that for a small ζ , the instability

was initiated in the porous medium, whereas for a larger ζ , the instability was controlled by the fluid layer. They also suggested that regular perturbation technique with small wave number a , as a perturbation parameter, can be conveniently used in solving convective instability problems in the case of insulating boundaries.

In this paper, we extend the work of Shivakumara *et al.* (2006) to the problem of the Marangoni convection in a composite porous-fluid-layer in the case of deformable free surface. We use a regular perturbation technique to obtain the asymptotic solutions of the long-wavelength.

Basic Equations

Consider an infinite horizontal porous layer of thickness d_p underlying a liquid layer of thickness d_f . The physical configuration is shown in Figure 1. The lower boundary is subject to a fixed heat flux, while the upper surface of the fluid is free and is assumed to be deformable.

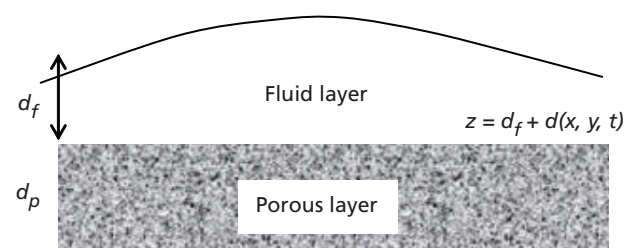


Figure 1. A Physical model.

Based on the above assumptions together with the Boussinesq approximation (Nield & Bejan 2006), the

¹ Department of Mathematics, Faculty of Science, Universiti Putra Malaysia, 43400 UPM Serdang, Selangor

² School of Mathematical Sciences, Faculty of Science and Technology, Universiti Kebangsaan Malaysia, 43600 UKM Bangi, Selangor

³ Faculty of Mathematics, University of Cluj, R-3400 Cluj, CP 253, Rumania

* Corresponding author (e-mail: norihan@fsas.upm.edu.my)

governing equations for continuity, momentum and energy in the fluid layer are as follows, respectively:

$$\nabla \cdot u_f = 0, \quad (1)$$

$$\rho_o \left(\frac{\partial}{\partial t} + u_f \cdot \nabla \right) u_f = -\nabla p_f + \mu \nabla^2 u_f, \quad (2)$$

$$\left(\frac{\partial}{\partial t} + u_f \cdot \nabla \right) T_f = \kappa_f \nabla^2 T_f \quad (3)$$

and for the porous layer, the equations are:

$$\nabla \cdot u_p = 0 \quad (4)$$

$$\frac{\rho_o}{\phi} \frac{\partial u_p}{\partial t} = -\nabla_p p_p - \frac{\mu}{K} u_p, \quad (5)$$

$$H \frac{\partial T_p}{\partial t} + (u_p \cdot \nabla_p) T_p = \kappa_p \nabla_p^2 T_p \quad (6)$$

where u is the velocity vector, T is the temperature, p is the pressure, K is the permeability of the porous medium, H is the ratio of heat capacity, μ is the fluid viscosity, ϕ is the porosity, while κ and ρ_o are the thermal diffusivity and reference fluid density, respectively. The subscripts f and p refer to the quantities in the fluid and porous layers, respectively. Since the fluid layer is very thin or under microgravity conditions, convection occurs due to surface tension effect rather than buoyancy effect. Therefore, the buoyancy forces are neglected in Equations 2 and 5. When motion occurs, the upper free surface of the layer would be deformable with its position at:

$$z = d_f + \delta(x, y, t).$$

We may introduce the infinitesimal disturbances to the governing equations by setting $(u_f, u_p, \rho, p, \mu, T_f, T_p) = (0, 0, \bar{\rho}, \bar{p}, \bar{\mu}, \bar{T}_f, \bar{T}_p) + (u'_f, u'_p, \rho', p', \mu', T'_f, T'_p)$, where the primed quantities are the perturbed ones over their equilibrium counterparts. The variables are then non-dimensionalized using $d_f, d_f^2/\kappa_f, \kappa_f/d_f, \Delta T_f$ as the units of length, time, velocity and temperature, respectively, in the fluid layer and $d_p, d_p^2/\kappa_p, \kappa_p/d_p, \Delta T_p$ as the corresponding characteristic quantities in the porous layer. Then the linearized equations involving only the z -dependent part of the z -component of the perturbation to the velocity, denoted by $w(z)$, and the z -dependent part of the perturbation to the temperature, denoted by $\theta(z)$, in dimensionless forms for the fluid layer are

$$\left(\frac{1}{P_r} \frac{\partial}{\partial t} - \nabla^2 \right) \nabla^2 w_f = 0, \quad (7)$$

$$\left(\frac{\partial}{\partial t} - \nabla^2 \right) \theta_f = w_f \quad (8)$$

and for the porous layer are:

$$\left(\frac{Da}{P_r} \frac{\partial}{\partial t} + 1 \right) \nabla_p^2 w_p = 0 \quad (9)$$

$$\left(H \frac{\partial}{\partial t} - \nabla_p^2 \right) \theta_p = w_p \quad (10)$$

For the fluid layer, $P_r = \nu/\kappa_f$ is the Prandtl number, $\nabla^2 = \frac{\partial}{\partial x^2} + \frac{\partial}{\partial y^2} + \frac{\partial}{\partial z^2}$ is the Laplacian operator and for the porous layer, $P_{rp} = \nu/\kappa_p \phi$ is the Prandtl number, $Da = K/d_p^2$ is the Darcy number and $\nabla_p^2 = \frac{\partial}{\partial x_p^2} + \frac{\partial}{\partial y_p^2} + \frac{\partial}{\partial z_p^2}$.

The linearized perturbed boundary conditions in dimensionless forms at the deformable surface at $z = 1$, lead to:

$$w_f = \frac{\partial \delta}{\partial z} = 0, \quad (11)$$

$$\frac{\partial \delta_f}{\partial z} = 0, \quad (12)$$

$$P_r \left(\frac{\partial w_f}{\partial z} + 3 \nabla_h^2 \frac{\partial w_f}{\partial z} \right) C_r - \nabla_h^4 \delta - \nabla_h^2 \delta B_o = 0, \quad (13)$$

$$P_r \frac{\partial^2 w_f}{\partial z^2} + M \left(\nabla_h^2 \theta_f - \nabla_h^2 \delta \right) = 0, \quad (14)$$

$$\frac{\partial \theta_f}{\partial z} + B_i (\theta_f - \delta) = 0 \quad (15)$$

where $M = \sigma_T \Delta T_f d_f / \mu \kappa_f$ is the Marangoni number, $B_i = qd/k$ is the Biot number, $C_r = \sigma_T d_f / \mu k$ is the Crispation number, $B_o = \rho_o g d^2 / \sigma_T$ is the Bond number, $\nabla_h^2 = (\partial^2 / \partial x^2) + (\partial^2 / \partial y^2)$ is the horizontal Laplacian operator, σ_T is the rate of change of the surface tension with respect to temperature and q is the heat transfer coefficient between the free surface and the gas. At the porous-fluid interface ($z = 0$) the boundary conditions are:

$$w_f = \frac{\delta}{\varepsilon_T} w_p \quad (16)$$

$$\theta_f = \frac{\varepsilon_T}{\zeta} \theta_p \quad (17)$$

$$\frac{\partial \theta_f}{\partial z} = \frac{\partial \theta_p}{\partial z_p} \quad (18)$$

$$\begin{aligned} \frac{\partial^2 w_f}{\partial z^2} - \chi \nabla_h^2 w_f &= \frac{\beta \zeta}{\sqrt{Da}} \frac{\partial w_f}{\partial z} \\ \frac{\beta \zeta^3}{\varepsilon_T} \left[\frac{1}{\sqrt{Da}} \right] \frac{\partial w_p}{\partial z_p} & \end{aligned} \quad (19)$$

$$\begin{aligned} \left(3 \nabla_p^2 + \frac{\partial^2}{\partial z^2} \right) \frac{\partial w_f}{\partial z} - \frac{\partial}{\partial t} \frac{1}{P_r} \left(\frac{\partial w_f}{\partial z} \right) &= \\ - \frac{\zeta^4}{\varepsilon_T} \left[\frac{1}{\sqrt{Da}} \right] \frac{\partial w_p}{\partial z_p} - \frac{1}{P_r} \frac{\partial}{\partial t} \left(\frac{\partial w_p}{\partial z_p} \right) & \end{aligned} \quad (20)$$

where χ is a constant taking the value zero for Beavers-Joseph condition and the value one for Jones condition

(Shivakumara *et al.* 2006), $\varepsilon_T = \kappa_f/\kappa_p$ is the ratio of thermal diffusivities and β is the slip parameter. At the lower boundary ($z_p = -1$), the boundary conditions are:

$$w_p = 0 \quad (21)$$

$$\frac{\partial \theta_p}{\partial z_p} = 0 \quad (22)$$

The perturbation quantities in terms of normal modes are expressed as:

$$(w_f, \theta_f, \delta) = [W_f(z), \Theta_f(z), \eta] \exp [i(a_x x + a_y y) + \omega t] \quad (23)$$

$$(w_p, \theta_p) = [W_p(z_p), \Theta_p(z_p)] \exp [i(\tilde{a}_x x + \tilde{a}_y y) + \omega_p t] \quad (24)$$

where $a = \sqrt{a_x^2 + a_y^2}$ is the dimensionless wave number in the fluid layer, while $a_p = \sqrt{\tilde{a}_x^2 + \tilde{a}_y^2}$ is the dimensionless wave number in the porous layer. By substituting Equations 23 and 24 into Equations 7–10, and setting $\omega = \omega_p = 0$ to obtain the equations relevant to marginal stability, the governing equations of the perturbed state become:

$$(D^2 - a^2)^2 W_f = 0, \quad (25)$$

$$(D^2 - a^2) \Theta_f = -W_f, \quad (26)$$

$$(D_p^2 - a_p^2) W_p = 0, \quad (27)$$

$$(D_p^2 - a_p^2) \Theta_p = -W_p \quad (28)$$

where D and D_p denote differentiation with respect to z and z_p , respectively. If matching of the solutions in the two layers is to be possible, the wave numbers in the fluid and porous layer must be the same, so that we have $a/d_f = a_p/d_p$ and hence $\zeta = a/d_p$. Using Equations 23 and 24, the boundary conditions given by Equations 11–22 now take the form,

at $z = 1$:

$$W_f = 0, \quad (29)$$

$$D\Theta_f = 0, \quad (30)$$

$$P_r C_r [(D^2 + a^2)DW_f] - a^2(a^2 + B_o)\eta = 0, \quad (31)$$

$$P_r (D^2 + a^2)W_f + a^2 M (P_r \Theta_f - \eta) = 0, \quad (32)$$

$$P_r D\Theta_f + B_i (P_r \Theta_f - \eta) = 0 \quad (33)$$

at $z = 0$:

$$W_f = \frac{\zeta}{\varepsilon_T} W_p, \quad (34)$$

$$D\Theta_f = D_p \Theta_p, \quad (35)$$

$$\Theta_f = \frac{\varepsilon_T}{\zeta} \Theta_p, \quad (36)$$

$$\left(D^2 + \chi a^2 - \frac{\beta \zeta D}{\sqrt{Da}} \right) W_f = - \frac{\beta \zeta^3}{\varepsilon_T \sqrt{Da}} D_p W_p, \quad (37)$$

$$\left[D^2 + 3a^2 \right] DW_f = - \frac{\zeta^4}{\varepsilon_T Da} D_p W_p \quad (38)$$

and at $z_p = -1$:

$$W_p = 0, \quad (39)$$

$$D_p W_p = 0 \quad (40)$$

The free surface deflection given by Equation 31 is:

$$\eta = \frac{P_r C_r (D^2 + a^2) DW_f}{a^2 (a^2 + B_o)} \quad (41)$$

Long Wavelength Asymptotic Analysis

As the fluid is subjected to a uniform heat flux below and above ($B_i = 0$), the critical wave number is vanishing, $a_c \rightarrow 0$. When both boundaries are insulated to temperature perturbations, the long wavelength ($a_c \rightarrow 0$) approximation is usually invoked to find the solution for the eigenvalue problem in a closed form using regular perturbation technique with wave number a as a perturbation parameter. To study the validity of small wave number analysis, the dependent variables in both the fluid and porous layers are now expanded in powers of a^2 in the form:

$$(W_f, \Theta_f) = \sum_{i=0}^N (a^2)^i (W_{fi}, \Theta_{fi}), \quad (42)$$

$$(W_p, \Theta_p) = \sum_{i=0}^N \left(\frac{a_p^2}{\zeta^k} \right)^i (W_{pi}, \Theta_{pi}) \quad (43)$$

Substitution of Equations 42 and 43 into Equations 25–28 and collecting the terms of 0th order, we obtain:

$$D^4 W_{f0} = 0 \quad (44)$$

$$D^2 \Theta_{f0} = -W_{f0} \quad (45)$$

$$D_p^2 W_{p0} = 0 \quad (46)$$

$$D_p^2 \Theta_{p0} = -W_{p0} \quad (47)$$

and the boundary conditions (Equations 29–40) become:

$$D^2 W_{f1} - \frac{\alpha\zeta}{\sqrt{Da}} DW_{f1} = - \frac{\alpha\zeta}{\varepsilon_T \sqrt{Da}} D_p W_{p1}, \quad (66)$$

at $z = 1$:

$$D^3 W_{f1} = - \frac{\zeta^2}{\varepsilon_T Da} D_p W_{p1} \quad (67)$$

at $z = 0$:

$$W_{f0} = D\Theta_{f0} = D^2 W_{f0} = 0 \quad (48)$$

and at $z_p = -1$:

$$W_{f0} = \frac{\zeta}{\varepsilon_T} W_{p0}, \quad (49)$$

$$W_{p1} = 0, \quad (68)$$

$$\Theta_{f0} = \frac{\varepsilon_T}{\zeta} \Theta_{p0}, \quad (50)$$

$$D_p \Theta_{p1} = 0 \quad (69)$$

$$D\Theta_{f0} = D_p \Theta_{p0}, \quad (51)$$

$$D^2 W_{f0} - \frac{\alpha\zeta}{\sqrt{Da}} DW_{f0} = - \frac{\alpha\zeta^3}{\varepsilon_T \sqrt{Da}} D_p W_{p0}, \quad (52)$$

$$D^3 W_{f0} = - \frac{\zeta^4}{\varepsilon_T \sqrt{Da}} D_p W_{p0} \quad (53)$$

and at $z_p = -1$:

$$W_{p0} = D_p \Theta_{p0} = 0 \quad (54)$$

The solution to the zeroth order equations is given by:

$$W_{f0} = 0, \quad \Theta_{f0} = \frac{\varepsilon_T}{\zeta}, \quad W_{p0} = 0, \quad \Theta_{p0} = 1 \quad (55)$$

The terms of order a^2 are:

$$D^4 W_{f1} = 0, \quad (56)$$

$$D^2 \Theta_{f1} - \frac{\varepsilon_T}{\zeta} = -W_{f1}, \quad (57)$$

$$D_p^2 \Theta_{p1} = 0, \quad (58)$$

$$D_p^2 \Theta_{p1} - 1 = -W_{p1} \quad (59)$$

and the corresponding boundary conditions are:

at $z = 1$:

$$W_{f1} = D\Theta_{f1} = 0, \quad (60)$$

$$P_r D^2 W_{f1} + M \left(P_r \frac{\varepsilon_T}{\zeta} - \eta \right) = 0, \quad (61)$$

$$P_r C_r D^3 W_{f1} - B_0 \eta = 0 \quad (62)$$

at $z = 0$:

$$W_{f1} = \frac{1}{\zeta \varepsilon_T} W_{p1}, \quad (63)$$

$$\Theta_{f1} = \frac{\varepsilon_T}{\zeta^3} \Theta_{p1}, \quad (64)$$

$$D\Theta_{f1} = \frac{1}{\zeta^2} D_p \Theta_{p1}, \quad (65)$$

We used the symbolic algebra package MAPLE 10 running on a Pentium PC to carry out much of the tedious algebraic manipulations to obtain the critical Marangoni number Mc . The three boundary conditions involving $D\Theta_{f1}$ and $D_p \Theta_{p1}$ and the differential equations involving $D^2 \Theta_{f1}$ and $D_p^2 \Theta_{p1}$ yield:

$$\int_0^1 W_{f1} dz + \frac{1}{\zeta^2} \int_0^1 W_{p1} dz_p = \frac{\varepsilon_T}{\zeta} + \frac{1}{\zeta^2} \quad (70)$$

The differential Equations 56–59 have general solutions of the form:

$$W_{f1} = -\frac{1}{6} z^3 c_1 + \frac{1}{2} c_2 z^2 + c_3 z + c_4, \quad (71)$$

$$\Theta_{f1} = -\frac{1}{120} z^5 c_1 - \frac{1}{24} z^4 c_2 - \frac{1}{6} z^3 c_3 - \frac{1}{2} (T + c_4) z^2 + z r_1 + r_2, \quad (72)$$

$$W_{p1} = z_p s_1 + s_2, \quad (73)$$

$$\Theta_{p1} = -\frac{1}{6} z_p^3 s_1 + \frac{(1-s_2)}{2} z_p^2 + z_p g_1 + g_2. \quad (74)$$

where $c_1 - c_4$, T , r_1 , r_2 , s_1 , s_2 , g_1 and g_2 are constants. These constants are determined using the corresponding boundary conditions. Thus, W_{f1} and W_{p1} are determined and their expressions can be substituted into Equation 62 to obtain the critical Marangoni number, Mc as:

$$Mc = \frac{48 B_0 \zeta (\varepsilon_T \zeta + 1) A_1}{\varepsilon_T A_2 + C_r A_3} \quad (75)$$

where,

$$A_1 = 9\sqrt{Da} \beta \zeta^4 + 3\beta^2 \zeta^2 Da + 18Da^{3/2} \beta \zeta + \beta^2 \zeta^5 + 3\beta^2 \zeta Da + 18\zeta^3 Da,$$

$$A_2 = \varepsilon_T B_0 \left(12\sqrt{Da} \beta \zeta^6 + 72Da^{3/2} \zeta^3 \beta + \beta^2 \zeta^7 + 432\varepsilon_T Da^2 + 36Da\beta^2 + 12\beta^2 \zeta^4 Da + 48Da\beta^2 \zeta^3 + 360Da^{3/2} \beta \zeta^2 + 36Da\zeta^5 + 432Da^2 \zeta + 288\varepsilon_T Da^{3/2} \beta \zeta \right)$$

$$A_3 = (1 + \varepsilon_T \zeta) \left(72\zeta^6 \beta^2 + 864\zeta^4 Da + 576\zeta^5 \beta \sqrt{Da} \right)$$

When $C_r = 0$, expression (Equation 75) can be reduced to the result of Shivakumara *et al.* (2006) for the non-deformable case.

RESULTS AND DISCUSSION

The onset of Marangoni convection corresponding to a vanishing small wave number in a two-layer system comprising an incompressible fluid saturated porous layer over which lies a layer of the same fluid, was investigated theoretically. As the fluid was subjected to a uniform heat flux below and above ($B_i = 0$), the critical wave number (a_c) vanished. The regular perturbation technique was used to obtain the analytical expression for the critical Marangoni numbers, M_c for long wavelength ($a \rightarrow 0$). The critical Marangoni number M_c depended on the depth ratio $\zeta = d_f/d_p$, Crispation number C_r , Bond number B_o , Darcy number Da and slip parameter β . Before presenting the numerical results, it was helpful to specify the range for parameters B_o and C_r which were respectively given as $10^{-3} \leq B_o \leq 1$ and $10^{-6} \leq C_r \leq 10^{-2}$ for most fluid layers of depths ranging from 0.01 cm to 0.1 cm and were in contact with air (Palmer and Berg 1972).

Figure 2 shows the critical Marangoni number M_c as a function of the depth ratio, ζ for different values of the Crispation number C_r with $B_o = 0.1$, $Da = 3 \times 10^{-6}$, $\beta = 1$ and $\varepsilon_T = 0.725$. As $\zeta \rightarrow \infty$ and $C_r \rightarrow 0$, the critical Marangoni number M_c attained a constant value 48, which is the exact value known for the case of a single fluid layer (Pearson 1958). We note that M_c increases for $0.7 < \zeta < 0.8$, at which maximum values of M_c were reached and then decreased for $\zeta > 0.8$. Also, we found that M_c decreased as the value of C_r increased. Consequently, the degree of free surface deformation had destabilizing effect on the system. The critical Marangoni number M_c as a function of the depth ratio ζ was plotted in Figure 3 for a variety of Bond number B_o with $C_r = 0.001$, $Da = 3 \times 10^{-6}$, $\beta = 1$ and $\varepsilon_T = 0.725$. It showed that as the value of B_o increased, the system became more stable.

To examine the effect of Darcy number Da , the critical Marangoni number M_c is shown in Figure 4 as a function of the depth ratio ζ with $C_r = 0.0001$, $B_o = 0.1$, $\beta = 1$ and $\varepsilon_T = 0.725$. As expected, the critical Marangoni number M_c increased with decrease in the Darcy number Da . The variation in Da had a significant effect on values of $\zeta < 2$ while the curves of different Da merged into one when $\zeta > 2$.

In all of the cases above, we used the values of the parameters similar to Shivakumara *et al.* (2006) and we also recovered their results for the case of $C_r = 0$.

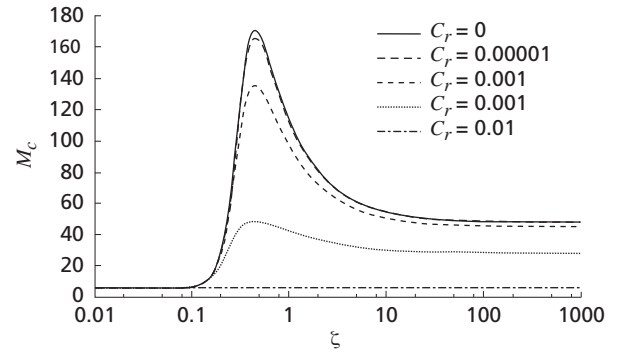


Figure 2. The critical Marangoni number M_c are plotted for ζ different values of C_r in the case of $B_o = 0.1$, $Da = 3 \times 10^{-6}$, $\beta = 1$ and $\varepsilon_T = 0.725$.

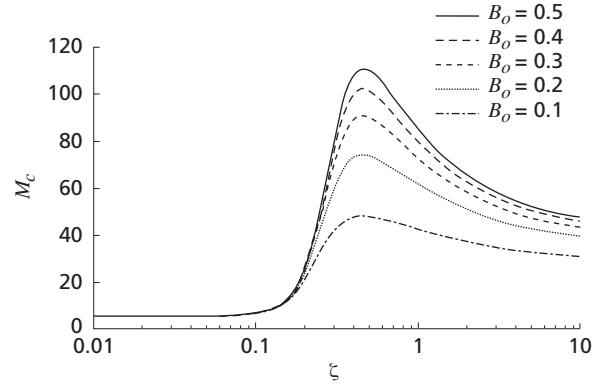


Figure 3. The critical Marangoni number M_c are plotted for ζ different values of B_o in the case of $C_r = 0.001$, $Da = 3 \times 10^{-6}$, $\beta = 1$ and $\varepsilon_T = 0.725$.

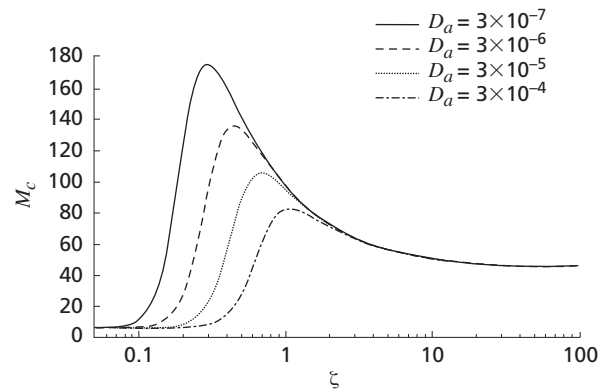


Figure 4. The critical Marangoni number M_c are plotted for ζ different values of Da in the case of $C_r = 0.0001$, $B_o = 0.1$, $\beta = 1$ and $\varepsilon_T = 0.725$.

CONCLUSION

In this paper, we have investigated the stability of Marangoni convection in a fluid overlying a porous medium. We have considered the deformable case, and the patterns of the output were in excellent agreement with those of Shivakumara *et al.* (2006) for the case of $C_r = 0$. The effect of the Crispation number C_r generally enhanced the deformation of the free surface and clearly produced a destabilizing effect on the onset of Marangoni convection instability. The system was more stable at smaller values of the Darcy number Da , and higher for the Bond number B_o .

ACKNOWLEDGMENTS

Gratefully acknowledge the financial support received (Fundamental Research Grant Scheme) from the Ministry of Higher Education, Malaysia.

Date of submission: March 2007

Date of acceptance: June 2007

REFERENCES

- Beavers, GS & Joseph, DD 1967, 'Boundary conditions at a naturally permeable wall', *Journal of Fluid Mechanics*, vol. 30, pp. 197–207.
- Chen, F & Chen, CF 1988, 'Onset of finger convection in a horizontal porous layer underlying a fluid layer', *ASME Journal of Heat Transfer*, vol. 110, pp. 403–409.
- McKay, G 1998, 'Onset of buoyancy-driven convection in superposed reacting fluid and porous layers', *Journal of Engineering Mathematics*, vol. 33, pp. 320–337.
- Nield, DA 1977, 'Onset of convection in a fluid layer overlying a layer of a porous medium', *Journal of Fluid Mechanics*, vol. 81, pp. 513–522.
- Nield, DA 1998, 'Modelling the effect of surface tension on the onset of natural convection in a saturated porous medium', *Transport in Porous Media*, vol. 31, pp. 365–368.
- Nield, DA & Bejan, A 2006, *Convection in porous media*, 3rd edn, Springer-Verlag, New York, USA.
- Palmer, HJ & Berg, JC 1972, 'Hydrodynamics stability of surfactant solution heated from below', *Journal of Fluid Mechanics*, vol. 51, pp. 385–402.
- Pearson, JRA 1958, 'On convection cell induced by surface tension', *Journal of Fluid Mechanics*, vol. 4, pp. 489–500.
- Shivakumara, IS, Suma, SP & Chavaraddi, KB 2006, 'Onset of surface-tension-driven convection in superposed layers of fluid and saturated porous medium', *Archives of Mechanics*, vol. 58, pp. 71–92.
- Straughan, B 2001, 'Surface-tension-driven convection in a fluid overlying a porous layer', *Computational Physics*, vol 170, pp. 320–337.
- Taslim, ME & Narusawa, V 1989 'Thermal stability of horizontally superposed porous and fluid layers', *ASME Journal of Heat Transfer*, vol. 111, pp. 357–362.

Enhancing Animal Protein Supplies in Malaysia: Opportunities and Challenges[†]

C. Devendra*

The increased human demand for animal proteins in Malaysia is led by several factors: population growth, urbanisation, income growth and changing consumer preferences. Meeting the projected increased demand in the future is an awesome and challenging task. Presently, the non-ruminant poultry and pig industries, mainly private sector led, make the most significant contribution to total animal protein supplies, and inefficient ruminant production systems lag well behind. The strategy for promoting productivity growth to increase animal protein supplies from ruminants requires concerted efficient natural resource management that can target specific production systems. Two distinct economic opportunities are the development of oil palm-based cattle and goat production. The value addition to oil palm cultivation due to the beneficial crop-animal-soil interactions are enormous. The prerequisites are inter-disciplinary efforts, holistic systems, participatory community-based research and development that are needs-based and address constraints, increased research investments, institutional commitment and a policy environment that can enhance total factor productivity in the future.

Key words: Animal protein supplies, natural resources, productivity, oil palm, opportunities, challenges, Malaysia

Improved animal production and productivity enhancement in Malaysia is justified by the direct response to the need for more animal proteins. This need is associated with several demand-driven factors and include inadequate animal protein supplies; rising income, which encourage people to diversify their diets to include a variety of meats; eggs and dairy products, including the substitution of calories in livestock for low-priced starch calories.

Animal food products provide high quality animal proteins and energy, and also precious micronutrients such as calcium, iron and Vitamin A. The demand for more protein supplies provides major opportunities for the owners and producers of animals, intensification of agriculture and improved livelihoods of the poorest of the poor (Devendra, 2004). However, these challenges are not without problems and include improved production systems, public health concerns, serious environmental hazards arising from for example, intensive peri-urban dairy production.

Associated with the projected requirements, questions have been raised about the contribution by components of the animal industries, the efficiency of individual animal production systems, and their capacity to meet the increased demand for animal products. Central to these questions are the opportunities and ways to significantly improve per animal performance and current productivity from animals in the future.

This presentation discusses the situation in Malaysia, potential opportunities and attendant challenges for increasing animal protein supplies, against the background of the prevailing animal production systems and trends in Asia. Specific reference is made to oil palm – based production systems in which cattle and goat production are attractive economic opportunities.

DEMAND-DRIVEN FACTORS

The strong demand-led process for projected foods of animal origin, and specifically total meat and milk human consumption levels in Asia in 2020 is awesome. This demand is far in excess of anticipated supplies (Degaldo *et al.*, 1999). This trend is consistent with the fact that consumers have been obtaining an increasingly greater share of calories and protein from animal food products in 1993 than before (FAO, 1997). Between 1982-1994, the annual growth rate for total meat consumption was generally high for South East and East Asia (5.6 to 5.8%) and especially high for China (8.6%). With meat, the shortfall in projected consumption levels in China and other South East Asian countries are about 50-115%. With milk, the supply deficits in China, India and South East Asia are approximately 100%, 89% and 433%, respectively. Overall, the rapid growth in the consumption of foods of animal origin is especially spectacular in East and South East Asia.

[†] A large portion of the information was taken from the Academy of Sciences Malaysia, Inaugural Lecture, presented at the University of Malaya on 3 October 2006

* Contact address: 130A Jalan Awan Jawa, 58200 Kuala Lumpur, Malaysia.
E-mail: cdev@pc.jaring.my

The strong demand-led process is directly influenced by the following factors:

- Population growth
- Urbanisation
- Income growth
- Efficiencies in natural resource management (NRM)
- Supplies being unable to meet the demand changing consumer preferences (meat to product cuts)
- WTO provisions on market access and export subsidies, and
- Animal diseases and food safety issues.

Increased human population growth together with increasing urbanisation, will significantly drive the demand for food of animal origin. The increases are awesome, and at projected human population growth rates of 0.7%, 1.6% and 1.4% per year up to year 2010. In China, India and Asia, the population increase by that time will be 33%, 18% and 12%, respectively.

The demand for and increased consumption of animal food is directly related to increased affluence and disposable income. At higher levels of income per capita consumption of meat levels off because of saturation (Delgado *et al.*, 1999). China and India fall out of this trend because of the very high consumption of pork in the former and religious preferences for meat in the latter (Figure 1).

Currently, the non-ruminant production systems continue to contribute to the major share of meat and egg production to meet projected human needs. By comparison, meat production from ruminants comes mainly from the slaughter of numbers rather than improved animals having good growth rates, optimum slaughter weights, and short duration to slaughter. Additionally, about 150,000 metric tonne (MT) annually of meat from male buffaloes produced in India, are exported to countries in South East Asia and the Middle East. Considerable opportunities exist for increasing productivity in the ruminant sector in

tandem with the need to increase animal protein supplies, food security and reduced poverty issues.

DEMAND-DRIVEN CONSEQUENCES

The projected needs for more food of animal origin in Asia have a number of demand-driven consequences, which also need to be addressed. These include *inter alia*:

- Stress on the use of natural resources
- Emphasis on increased productivity per animal
- Improved efficiency in feed resource use
- Intensification of animal production systems
- Increased concentration of animals in peri-urban areas
- Increased disease risks, pollution and human health issues; and
- Urbanisation associated with increased consumption of pork, mutton and poultry.

The demand growth has placed unprecedented pressure on the management of the natural resources (crops, animals, land and water) and also animal production systems. Among these, land use systems are especially important. In the past, emphasis on the productivity of cereals through the 'Green Revolution' came mainly from the irrigated arable areas. Many benefits and prosperity reached rice farmers, but the higher agricultural growth exacerbated poverty and food insecurity among the poor in rainfed areas. With the exception of non-ruminants (pig and poultry production) in mainly peri-urban areas, ruminant production was secondary and lagged behind.

ROLE AND CONTRIBUTION OF ANIMALS AND TRENDS

The animal populations in Asia are characterised by diversity and considerable variation in size. These are distributed widely across the preponderance of small farms, which are the reservoir of a large proportion of the main animal species (buffaloes, cattle, goats, sheep, chickens, pigs and ducks). These together form an important economic and ecological niche throughout Asia. Their functions and contribution are numerous. They are consistently and widely owned by small farmers for a variety of advantageous reasons (Devendra, 1983; Chantalakhana, 1990; Devendra and Chantalakhana, 2002):

- Diversification in the use of production resources and reduction of socio-economic risks
- Promotion of linkages between system components (land, crops and water)
- Generation of value-added products (e.g. meat, milk, eggs and skins)
- Income generation, investment, insurance and economic security

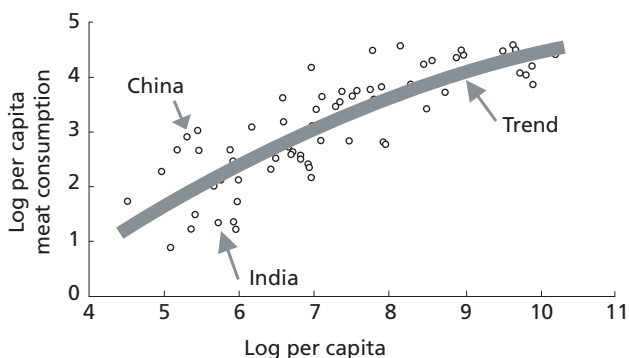


Figure 1. Increase in per capita meat consumption with increase in per capita income.

- Supply of draught power for crop cultivation, transportation and haulage operations
- Contribution to soil fertility through nutrient cycling (dung and urine)
- Contribution to sustainable agriculture and environmental protection
- Prestige, social and recreational values, and
- Development of stable farm households.

ANIMAL PRODUCTION SYSTEMS

Animal production involves both non-ruminants and ruminants and a variety of systems integrated with crops. Systems vary as a function of agro-ecological zone and the intensity of farming operations. Development of these systems has considerable potential, the benefits being associated with the complementary interactions of the subsystems, the products from which are additive.

Animal production trends in Asia are of two categories (Steinfeld, 1999):

- i) Modern, demand-driven, capital intensive, mainly industrial, peri-urban and private sector-led non-ruminant systems which produce poultry meat, eggs and pork. These are very efficient and have good market access. Increasing intensification and concentration of animals increases pollution and disease risks to humans. Some milk is also produced from dairy cattle and buffaloes.
- ii) Traditional, resource-driven and labour intensive ruminant sector, which produces a multitude of services to subsistence farms. These are characterised by low technology uptake, low productivity, insufficient market facilities and infrastructure and small economies of scale are common.

Types

Animal production involves both non-ruminants and ruminants and a variety of systems integrated with crops. The systems vary as a function of agro-ecological zone and intensity of farming operations. These and other aspects, including the genesis of crop-animal systems has recently been reviewed (Devendra, 2007a), and highlight the importance of animal in a crop-based systems.

The prevailing animal production systems in Asia fall into one of three categories and it is appropriate to discuss these briefly:

1. Landless
2. Crop-based, and
3. Rangeland-based.

1. *Landless systems*. These are of two categories, as follows:

i) Urban and peri-urban industrial landless systems

These landless systems are generally large, mainly industrial, very intensive and vertically integrated pig and poultry enterprises whose economic outputs are higher than those of the ruminant enterprises. The systems involve the use of largely imported production inputs at high cost – germplasm, feeds, supplements, medication and technologies which during times of economic crisis make these systems very vulnerable, compared to the ruminant sector. The systems are also very efficient with production cycles of four to five crops of broilers of eight weeks each, and an average efficiency of feed conversion of about 1.8. They are usually run by the private-sector and found concentrated in peri-urban areas close to processing facilities and the markets. Examples of such enterprise are common throughout South, South East, and East Asia. Individual enterprises are large with broiler units as large as 500, 000 birds, and with 2000 or more breeding sows in pig units. In China's largest 18 cities over half of the pork and poultry demand was produced in the urban area in Katmandu 11% of the animal food needs were met, and in Singapore 80% of the poultry products stemmed from urban farmers (UNDP, 1996).

ii) Rural landless production systems

Rural landless production systems refer mainly to ruminants, and are prevalent in the arid and semi-arid agro-ecological zones such as in North India. These involve zero grazing practices and extensive systems that are associated with resource-poor nomads, transhuman or agricultural labourers and seasonal migrations with small ruminants, cattle and camels (Devendra, 1999a; 1999b). They are very common in the arid and semi-arid regions notably Pakistan and India, and also in the Hindu-Kush Himalayan region in South Asia. The movements are annual cycles that are triggered by reduced feed and water supplies, and market opportunities. They are also a way of life for the poor. Two common problems are overgrazing and environmental degradation due to 'slash and burn' for agriculture.

2. *Crop-based systems*. In Asia it mainly encompass mixed farming or crop-animal systems. These systems form the backbone of Asian agriculture, and are especially important in terms of land area involved, extent of poverty, integrated natural resource management (NRM), food security and potential opportunities for increased food

production. Diversification and integration of the production resources are common.

i) Relevance of mixed farming

Mixed farming systems are synonymous with crop-animal systems; they are varied and integrated with cropping in various ways. Both ruminants and non-ruminants are involved and the choice of one or more species is dependent on overriding influence of preference, market dictates, potential to generate income, contribution to crop cultivation and livelihood. Much will depend on the extent of the functional contribution of animals.

In Asia, mixed farming provided 90% of the milk, 77% of the ruminant meat, 47% of pork and poultry meat, and 31% of the eggs. Past growth trends indicate (Steinfeld, 1998) that mixed farming systems grew half as fast (2.2% per year) compared to industrial systems (4.3% per year) and three times as fast as that of pastoral systems (0.7% per year). The data indicates that ruminant production in mixed farming systems will continue to be important in the future.

ii) Integration, integrated systems and their importance

Integration involves various components, namely crops, animals and land water. Integrated systems refer to approaches that link the components to economic, social and ecological perspectives. The process is holistic, interactive, multi-disciplinary and promotes efficiency in NRM. The integration of various crops and animals enable synergistic interactions, which have a greater total contribution than the sum of their individual effects (Edwards *et al.*, 1998). Thus for example, the integration of beef cattle with oil palm results in increased FFB and palm oil, and also beef. Additionally, both ecological and economic sustainability are addressed in a mutually reinforcing manner. Such integrated systems are especially well developed in East and South East Asia. An overview of their potential importance and relevance to small farms in Asia and description of the distinctive characteristics has been reported (Devendra, 1995; 1996). The characteristic features include *inter alia*:

- Diversified and integrated use of the production resources, mainly crops and animals
- Use of both ruminants (buffaloes, cattle, goats and sheep) and non-ruminants (chickens, ducks and pigs)

- Animals and crops play multi-purpose roles
- The process is holistic, interactive, multi-disciplinary and promotes NRM
- Crop-animal-soil interactions are varied and have socio-economic and ecological implications
- Low inputs use, indigenous and traditional systems, and
- Is associated with demonstrable sustainability and sustainable production systems.

iii) Categories

Two broad categories of mixed farming systems can be identified:

- (a) Systems combining animals and annual cropping in which there are two further sub-types:
- Systems involving non-ruminants, ponds and fish eg. vegetables-pig-ducks-fish systems in Vietnam, rice-maize-vegetables-sweet potatoes – pigs – dairy cattle (China)
 - Systems involving ruminants eg. Maize-groundnuts/soyabean – goats systems (Indonesia), Rice-finger millets – goats (Nepal).
- (b) Systems combining animals and perennial cropping in which there are again two subtypes:
- Systems involving ruminants eg. Coconuts – sheep integration (Philippines), oil palm – cattle integration (Malaysia)
 - Systems involving non-ruminants eg. oil palm – chickens integration (Malaysia).

With ruminant production systems, there are four categories: landless systems; extensive systems; systems combining arable cropping (tethering, communal and arable grazing systems, and cut-and-carry feeding); and systems integrated with tree cropping. These production systems are unlikely to change in the foreseeable future (Mahadevan and Devendra, 1986; Devendra, 1989), however, there will be increasing intensification and a shift especially from extensive to systems combining arable cropping, induced by population growth. The principal aim should therefore be improved feeding and nutrition, and maximum use of the available feed resources, notably crop residues and low quality roughages, and various leguminous forages as supplements.

3. *Rangeland-based systems*. These are found mainly in the semi-arid and arid regions of South Asia and China. Sparse vegetation, containing mainly native grasses and shrubs are characteristic of this area. These however are important sources of feeds in Pakistan, some 65% of the total land area, from altitudes of 0–>4000 m are rangelands, and it is estimated that 60% and 5% of the total feed requirements of small ruminants and large ruminants, respectively are met by the rangelands (Devendra *et al.*, 2000). These areas support low carrying capacities of 5-8 sheep/ha such as is found in the Baluchistan Province of Pakistan. Three major concerns about rangeland-based systems are the need for strategies to use of common property grazing lands, communal management of these lands, and drought feeding.

SITUATION IN MALAYSIA

Turning to the situation in Malaysia, Table 1 indicates the current and projected per capita consumption of individual foods of animal origin, and the corresponding levels of sufficiency for each species. The awesome scenario is that relative to the advances and major contributions made by the non-ruminant sector, the ruminant sector lags well behind. The level of ruminant production is generally low. While the non-ruminant sector has made outstanding progress and is self-sufficient in the meats, by comparison, the situation with ruminant is dismal. With beef, the levels of self-sufficiency are decreasing but are projected to marginally increase by 2010. With small ruminant meats, the situation is expected to remain static. There is justification therefore for urgent attention for developing strategies that can significantly increase the supplies of food of animal origin to match rising human requirements. Table 1 also shows that with all meats without exception, per capita consumption is rising and is projected to rise even further.

A recalculation of the data on dressed meat (Table 2), and conversion to per capita intake of animal proteins is

given in Table 2. The data reiterates that per capita intake are increasing, and compared to the intake in 2005, the projected consumption in 2010 of 97 g/day represents an increase of about 378%. Additionally, Table 2 also indicates that non-ruminants contributed to between 90.1–93.7% of the protein intake, with ruminants contributing only 6.3–9.9%. The increasing per capita intake of animal proteins is also indicative of some degree of energy availability going towards the substitution of lower cost carbohydrate food such as rice to meet the adult requirement of about 2100 calories per day.

Tables 1 and 2 point to the fact that there is an urgent priority need to increase ruminant animal numbers and also productivity. This is also justified by the trend towards decreasing animal numbers and relatively low annual population growth rates (Table 3). Among ruminants, positive growth rates were only recorded in cattle at 1.5%/yr and 2.7%/yr between 1998–2004 (DVS, 2004). Buffalo numbers had a negative growth rate as also sheep and pigs. The down trend has been apparent since the 1990s, and increased numbers in recent years has come from imports of live animals. The projections for improved self-sufficiency rates in year 2010 remains to be realized.

In 2004, the total cost of imports of livestock and livestock products into the country was about RM5 billions, of which animal feeds accounted for 44%, milk and milk products 30%, beef 11% and live animals 4%. Malaysia imported approximately 110 MT of beef, within which about 77% is buffalo beef from India and is increasing. The import of live cattle, goats and sheep for slaughter are increasing.

POTENTIAL OPPORTUNITIES

Among ruminants production systems, there are two major opportunities and development pathways that can be beneficially addressed, both of which merit urgent attention. These are as follows:

Table 1. Per capita consumption and percentage of self-sufficiency levels of livestock commodities (kg/yr) in Malaysia (1990–2010).

Commodity	1990	1995	2000	2005**	2010**
Poultry	18.9 (115.2)	29.6 (112.4)	27.3 (112.5)	27.3 (112.5)	36.8 (125.2)
Pork	10.1 (126.3)	10.1 (135.2)	6.9 (99.5)	9.3 (91.5)	9.2 (102.3)
Beef	3.2 (23.9)	4.2 (19.7)	4.8 (15.8)	6.7 (23.2)	8.5 (28.3)
Goat meat and mutton	0.4 (8.8)*	0.6 (5.9)	0.6 (5.9)	0.7 (8.9)	0.7 (10.2)

Source: Department of Veterinary Services, Malaysia (2003)

* Refer to self-sufficiency data (%)

** These are projections

Oil Palm-based Cattle Production

The potential for developing integrated oil palm-based cattle production in Malaysia is underestimated, and has huge potential. It embodies efficiency in NRM, sustainability, value addition, and total productivity returns. This production system involving ruminants therefore merits urgent attention and emphasis, as an important avenue to significantly contribute to increased animal protein supplies. Among the ruminant animals, cattle and goats are the priority animals because of the high demand for their meats. The sections below briefly discuss the interrelated components involved:

- (i) *The oil palm environment*. It provides the following natural advantages for animal production:
- An abundance of shade
 - A variety of useful feeds
 - An entry point for development of integrated NRM and production systems

- Value addition and total productivity returns
- Development of sustainable production systems, and
- A hedge for possible reduction in the price of crude palm oil.

- (ii) *Available feeds from the oil palm*. Two categories of feeds are involved. One is the undergrowth under oil palm, consisting of grasses, shrubs and ferns. Among the available feeds in Malaysia, those from the oil palm are potentially and by far the most important, and are currently under-utilised. This is associated with the very large land area of about four million hectares under oil palm in Malaysia. Table 4 presents the range of the feeds produced, and the magnitude of production. The principal feeds from oil palm are palm oil, oil palm trunks (OPT) oil palm fronds (OPF), and palm kernel cake (PKC). The other feed is palm oil mill affluent (POME). Grazing the undergrowth and supplementary

Table 2. Per capita animal protein consumption and trends (g/day, 1990 – 2010).

Type of meat	Year				
	1990	1995	2000	2005	2010
Poultry	38.8	60.8	56.0	56.0	75.6
Pork	13.8	13.8	9.5	12.7	12.6
Beef	3.4	4.0	4.6	7.1	8.2
Goat meat and mutton	0.4	0.6	0.6	0.7	0.7
Total intake	56.1	79.2	70.7	75.8	97.1
% share from non-ruminants	93.7	94.2	92.6	90.1	90.8
% share from ruminants	6.3	5.8	7.4	9.9	9.2
Population (x 10)*	20.7	20.7	23.3	26.2	28.4
Per capita income (MYR)*	6224	13,680	13,359	16,902	22,612

*Mad Nasir Shamsudin (2004–2005).

Table 3. Animal populations (10³) in Peninsular Malaysia (1998–2004).

Species	Year				Annual growth rate (%)
	1998	2000	2002	2004	
Buffaloes	96.2	87.9	79.4	83.5	Negative
Cattle	660.6	685.4	663.5	731.5	1.5
Goats	189.1	200.5	196.8	225.5	2.7
Sheep	153.7	134.2	118.7	109.5	Negative
Chickens	90.8	96.3	101.2	156.6	104
Ducks	3980.6	4640.4	6152.8	7478.7	126
Pigs	2364.6	1391.4	1486.7	1483.5	Negative

Source: Department of Veterinary Services, Malaysia (2004)

feeding with feeds such as PKC are economically feasible.

- (iii) *Research and development.* Of the research side, very useful progress has been made notably by the Malaysian Agricultural Research and Development Institute (MARDI) on various aspects of the feeds from the oil palm. Over the last three decades, some 124 projects have been conducted on availability, production, nutritive value, utilisation and performance by animals, processing and engineering aspects, and enhanced value. However, two main conclusions of these efforts are that the research efforts have been singularly disciplinary in approach, and secondly, there has been inadequate application of the research results at the plantation level.

Associated with above are a few reports of several tangible economics which are as follows:

(a) Yield of crop

One example of increased yield and economic benefit concerns the use of cattle and goats to graze the undergrowth of oil palm plantations. The work was done in an oil palm plantation where the estate allocated grazing land within the estate to the workers for grazing their animals, and also to help them earn supplementary income. For the first two years (1980 – 1981), only cattle were owned and used; in 1982 and 1983 however, goats were also introduced in addition to cattle, to supply meat and milk as well for home consumption. Over four years of the study, there was an increased production of 3.52 MT/ha/yr in the grazed

area. This yield, equivalent to approximately 0.7 MT/ha is considerable when it is translated into monetary value (Devendra, 1991).

A 30% yield increase in oil palm plantations have also been reported by Chen and Chee (1993) due to grazing. These authors have also reported 20–40% reduced weeding costs for cattle under oil palm, comparable to a savings of 16–35% using grazing sheep reported by Chee and Faiz (1991). Also in Malaysia, utilising buffaloes to transport oil palm fruit bunches from the field to collecting centres increased the farmers' income by as much as 30% (Liang and Rahman, 1985). More recently, Samsuddin (2001) has reported a mean increased yield of 0.49/ ha of FFB due to integration with cattle over six years of study.

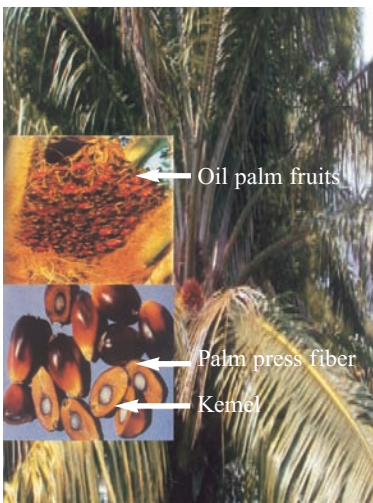
(b) Savings on weeding costs

With appropriate stocking rate, savings on weeding costs is a significant advantage on account of grazing. The control of weeds is thus achieved with concurrent savings in the use of weedicides. Ongah (2004) has reported from data from four estates that following integration, the mean weeding cost was 41.34/ha MYR which was 68.6% lower in comparison to areas that were not grazed.

(c) Use of many feeds from oil palm

One example of the use of oil palm by-products concerns the development of oil palm-based intensive and sustainable pro-

Table 4. Availability of feeds from the oil palm.

Oil palm fronds	By-product	Yield (MT/ha/yr)
	Edible:	
	1. Oil palm fronds	0.62
	2. Palm kernel cake	0.96
	3. Palm oil mill effluent	0.04
	4. Palm press fibre	0.23
	Non-edible:	
1. Bunch trash	10.74	
2. Palm nut shells	0.15	

duction systems *in situ*, is a comparison of a cut-and-carry feedlot system, a semi-feedlot system, and free grazing for beef cattle in Johore, Malaysia, where coffee was grown as an intercrop under coconuts. Stall-fed local x Jersey yearling males were fed for 178 days (Sukri and Dahlan, 1986) using rations consisting of coffee by-products (30%), palm kernel cake (37%), urea (2%) and mineral-vitamin premix (1%) and various native forage species (*Paspalum*, *Axonopus*, *Ottochloa*, *Ischaemum* and *Brachiaria*) for grazing. The animals under the feedlot system were confined and fed the feed ration *ad libitum*; the semi-feedlot treatment involved tethering and grazing on the native grasses for five hours daily before the animals received the same feed ration *ad libitum*; the free-grazing animals were tethered to graze the native grasses. Average daily gains of the animals in the feedlot, semi-feed lot and free-grazing systems were 0.48, 0.37 and 0.15 kg, respectively. The feedlot and semi-feedlot groups were extended for a further 116 days with average daily gains of 0.60 and 0.38 kg/animal respectively, demonstrating that the gross profit was higher for the feedlot animals than the semi-feedlot or grazing groups, emphasising that feedlot and semi-feedlot systems had great potential for increasing beef production in estate environments among smallholder farmers.

Despite the apparent benefits, there is inadequate attention to develop the alternative options in the estate environments, due to a combination of such factors as inadequate investments, lack application of technologies, resistance by the tree crop sector to integrate animals, and lack of policies that can enhance the development of the systems. Additionally, the system is also not viewed holistically to push development.

- (iv) *Value addition to oil palm cultivation*. In sum, the benefits of developing integrated systems in general and oil palm – ruminant systems in particular, hold much economic potential in Malaysia. The value additions to oil palm cultivation are:
- Increased yield of FFB and palm oil due to beneficial crop-animal-soil interactions
 - Increased total factor productivity and income (palm oil + meat)
 - Demonstrable sustainable production system, and
 - Returns to investments: 8.1–16.3 % for indigenous and imported cattle.

- (v) *Reasons for the poor adoption by the plantation sector*. Given the apparent economic benefits that are associated with integrating cattle with oil palm, the question can be asked why is this production system continuing to be neglected and underestimated? The reasons for this are associated *inter alia* with the following:

- Current R & D programmes are small and piecemeal
- Technology delivery and application are weak and not based on systems perspectives
- Failure to look at the oil palm environment in holistic and interdisciplinary terms
- Inadequate dissemination of information and transfer of technology on the significance and importance of integrated systems
- Resistance by the private sector plantation and service groups who view integration with animals as an additional burden and is uneconomic
- Reluctance to use additional capital outlays for beef production, and
- Absence of a coherent policy for stimulating large-scale oil palm-based beef production, backed with appropriate incentives.

In the last few years, the technologies developed have been extended to several other agencies such as the Federal Land Development Authority (FELDA), Rubber Industries Smallholder Development Authority (RISDA), Farmers Organisation Authority (FOA), State Economic Development Corporations, as well as the private sector. The technologies include processing of oil palm by-products and development of feed mills, applied nutrition and integration of oil palm with cattle. These activities are largely component technology-oriented and small-scale, and rates of adoption are uncertain. Until and unless these efforts are scaled up large-scale, addressed holistically along multi-disciplinary lines using systems perspectives, it is unlikely that there will be a major take off for the development oil-palm based beef production.

- (vi) *Urgent attendant considerations*. It is relevant in formulating the development strategies, to also consider the following:

- Plan for a reduced chosen number of exotic breeds for beef, goat and sheep production
- Define a breeding policy and well developed breeding plans that have the primary objective of large scale multi-locational production of animals of improved quality that fits specific production systems and the local environment
- Incorporate clear objectives of production, including consumer requirements that are needs-based, realistic and achievable within a time frame, and

- Ensure that the development plans are consistent with the real needs of farmers, the farming systems and can provide predictable responses.
- (vii) *The way forward.* In the light of the discussion hitherto, one way forward to promote development of oil palm-based ruminant production is as follows:
- Critical assessment of current R & D efforts involving the main players, objectives and relevance of programmes concerned with integrated systems
 - Address coherent policy options eg. incentives to promote wide development of integrated systems
 - Seek increased investments specifically for large-scale integrated systems, and
 - Provide strong leadership and institutional support for sustained development.
- (ix) *Opportunity and strategy.*
- Encourage urgent and permanent dialogue between participating agencies eg. MARDI, MPOB, DVS, FELDA, RISDA, private sector etc. and

- Define complementary approaches, time frame, a unified agenda for concerted R & D, and potential impact.

Goat Production

A second major opportunity concerns goat production. The production systems can be similar to oil-palm based production, or be on its own. Goats are favoured more than sheep for the following reasons:

- (i) Their feeding behaviour is more suited for the use of the natural grasses and browse under oil palm
- (ii) Generally higher fertility than sheep
- (iii) Biomass production
- (iv) Greater market demand and for goat meat
- (v) Higher price for goat meat presently, about 2–3 times more than mutton and also beef
- (vi) Greater availability of numbers
- (vii) Requires less land, capital outlays and has faster turnover
- (viii) Currently, the returns to investments are highest
- (ix) Presence of several ‘improver breeds’ within Asia, and
- (x) Presence of large regional and international markets.

Table 5. Estimated gross margin of profits for meat production using crossbred Katjang goats with varying levels of fertility (Devendra, 2007b).

Fertility level (% kids weaned/does mated)	80	100	120	140
I. The goat flock				
Flock size (breeding does)	10	10	10	10
Increase due to kids born	8	10	12	14
Less mortality ¹	7	8	10	12
Net increase in numbers less culls ²	17	18	20	22
Cost of goats ³ (\$ US)	1870	1980	2200	2420
Cost of cull goats ³ (\$ US)	110	220	220	220
Less cost of foundation does ³	1100	1100	1100	1100
Total gross revenue (\$ US)	880	1100	1320	1540
II. Cost of production				
(i) On cultivated forages, conc. with labour ⁴	68.2	74.1	82.5	90.5
(ii) On uncultivated forages with family labour ⁵	–	–	–	–
III. Gross margin of profit (\$ US)				
(i) Cultivated forages and conc.:				
Per flock	811.8	1035.1	1237.5	1449.5
Per breeding doe	81.2	103.5	123.8	144.9
Per month	67.7	86.2	103.1	120.8
(ii) Uncultivated forages:				
Per flock	825	855	885	915
Per breeding doe	82.5	85.5	88.5	91.5
Per month	68.7	71.3	73.8	76.3

¹15% among kids

²25% culling per annum

³\$110 US per goat weighing about 30 kg

⁴Cost of cultivated grass is 3.6 US\$ cents per kg. fresh weight

⁵No costs attached; both components are considered free.

An important biological advantage influencing productivity and income generation from goats concerns fertility and the productive lifespan of goats. The higher fertility, the number of kids born and good management to keep mortality low ultimately manifests itself in more animals for slaughter. With goats, fertility is at a peak around the fifth parturition, corresponding to about seven years of age.

It is most essential therefore that breeding does are kept in the flock for not less than seven years of age. The increased income is from more numbers born. The income generated can be even higher with the expansion of the flock and inclusion of additional does into the flock for breeding. Table 5 demonstrates the significance of rising levels of fertility on the generation of numbers, and the impact of this on increased economic benefits. Cursory calculations of the returns to investments in Table 5 give values in the range 21.7 – > 35.0%; the higher values being influenced by the increasing numbers born and therefore cumulative profits.

NEED FOR INCREASED RESEARCH INVESTMENTS

The objectives of increasing productivity from animals through the application and wide adoption of appropriate technologies in target agro-ecological zones, as well as the eradication of poverty, will require increased research investments. Past investments in agricultural research have had major payoffs and clearly justify their increased support (Alston *et al.*, 1998). These much needed investments, backed by systems perspectives and community-based research and development activities (Devendra, 2000) can enhance demonstrable impact on improved productivity in rainfed environments. The approaches together can significantly benefit the owners and producers of animals, projected needs of consumers, improve livelihoods of the poorest of the poor, stimulate agricultural growth and environmental sustainability.

CONCLUSION

Enhancing animal protein supplies to meet the projected increased human demand for animal proteins in the future is an awesome and challenging task in Malaysia. Promoting productivity growth and increasing the supplies of foods of animal origin requires concerted strategies that involve a high efficiency in NRM that can target specific production systems. Market forces will also dictate policies and priorities. Two distinct economic opportunities are the development of oil palm-based cattle and goat production. The value addition to oil palm cultivation due to the beneficial crop-animal-soil interactions are enormous and underestimated. Concerted inter-disciplinary efforts are necessary,

involving holistic systems, investments and a policy environment that can enhance productivity from animals in the future. In the final analysis, institutional will and capacity to address these issues will determine the success of our collective efforts.

REFERENCES

- Alston, JM, Pardey, PG & Rosebroom, G 1998, 'Financing agricultural research: international investment patterns and policy interventions'. *World Development*, vol. 26, pp. 1057–1071.
- Chantalakhana, C 1990, 'Small farm animal production and sustainable agriculture', in *Proceedings of the Asian-Australasian Animal Science Congress, 27 May 1990*, vol. 2, pp. 39–58.
- Chen, CP & Chee, YK 1993, 'Ecology or forages under rubber and oil palm', in *Advances in sustainable small ruminant – tree cropping integrated systems*, eds S Sivaraj, P Agamuthu, & TK Mukherjee, University of Malaya and International Development Research Centre, Kuala Lumpur, Malaysia, pp. 9–18.
- Chee, YK & Faiz, A 1991. 'Sheep grazing reduces chemical weed control in rubber', in *Forages for plantation crops, 27 June 1990*, Bali, Indonesia, eds Shelton HM & Stur WW, *Australian Centre for International Agricultural Research Proceedings, no 32, Canberra, Australia*, pp. 120–123.
- Delgado, C, Rosegrant, M, Steinfeld, H, Ehui, S & Courbois, C 1999, *Livestock to 2020. The next food revolution*. International Food Policy Research Institute, Washington DC, USA, pp. 72.
- Devendra, C 1983, 'Small farm systems combining crops and animals' in *Proceedings Fifth World Conference on Animal Production, 14 August 1983, Tokyo, Japan*, pp. 173–191.
- Devendra, C 1989, 'Ruminant production systems in the developing countries: resource utilization', in *Proceedings Feeding Strategies for Improved Productivity of Ruminant Livestock in Developing Countries*, International Atomic Energy Commission, 13 March 1989, Vienna, Austria, pp. 5–30.
- Devendra, C 1991, 'The potential for integration of small ruminants and tree cropping in South East Asia'. *World Animal Review*, (Food and Agriculture Organisation) no. 66, pp. 13–22.
- Devendra, C 1995, 'Mixed farming and intensification of animal production in Asia', in *Proceedings International Livestock Research Institute/Food and Agriculture Organisation Round Table on Livestock Development in Low-income Countries, 27 February 1995*, eds RT Wilson, S Ehui, & S Mack, International Livestock Research Institute, Addis Ababa, Ethiopia, pp. 133–144.
- Devendra, C 1996, 'Overview of integrated, animals-crops-fish production systems: achievements and future potential', in *Proceedings Symposium on Integrated Systems of Animal Production in the Asian Region, 13 October 1996*, eds H Hayakawa, M Sasaki, & K Kimura, Chiba, Japan, pp. 9–22.

- Devendra, C 1999a, 'Small ruminant production systems in semi-arid and arid environments of Asia', *Annals of Arid Zone*, vol. 37, no 3, pp. 215–232.
- Devendra, C 1999b, 'Goats: challenge for increased productivity and improved livelihoods', *Outlook on Agriculture*, vol. 29, no. 4, pp. 215–226.
- Devendra, C 2000, 'Animal production and rainfed agriculture in Asia: potential opportunities for productivity Enhancement', *Outlook on Agriculture*, vol. 29, no. 3, pp. 161–175.
- Devendra, C 2004, 'Meeting the increased demand for animal products in Asia-opportunities and challenges for research' in *Proceedings Responding to the Livestock Revolution: the role of globalisation and implications for poverty alleviation, 12 November 2002*, eds E Owen, T Smith, MA Steele, S Anderson, AJ Duncan, M Herrero, JD Leaver, CK Reynolds, JI Richards, & JC Ku-Vera, Yucatan, Mexico, British Society of Animal Science, Publication. No. 33, pp. 209–228.
- Devendra, C 2007a, 'Perspectives on animal production systems in Asia', *Livestock Science*, vol. 106, no.1, pp. 1–18.
- Devendra, C 2007b. 'Goats : biology, production and development in Asia'. Academy of Sciences Malaysia.
- Devendra, C & Chantalakhana, C 2002. 'Animals, poor people and food insecurity: opportunities for improved livelihoods through efficient natural resource management', *Outlook on Agriculture*, vol. 31, no 3, pp. 161–175.
- Devendra, C, Thomas, D, Jabbar, MA & Zerbini, E 2000, 'Improvement of livestock production in crop-animal systems in agro-ecological zones of South Asia'. International Livestock Research Institute, Nairobi, Kenya, 107 pp.
- Department of Veterinary Services 2003, 'Animal genetic resources in Malaysia'. Department of Veterinary Services, Ministry of Agriculture and Agro-based Industry, Kuala Lumpur Malaysia (Mimeograph).
- Department of Veterinary Services 2004, Livestock statistics. Department of Veterinary Services, Ministry of Agriculture and Agro-based Industry, Kuala Lumpur, Malaysia, 96 pp.
- Edwards, P, Pullin, RSV & Gartner, JA 1998, 'Research and education for the development of crop-livestock-fish farming systems in the tropics'. International Centre for Living Aquatic Resources Management Studies and Review, no. 16, 53 pp.
- FAO 1989, 'Sustainable agricultural production. Implications of international agricultural research'. Food and Agriculture Research Organisation Research and Technology. Paper No 4, FAO, Rome, Italy.
- FAO 1997, Food and Agriculture Organisation (FAO) statistics database. <http://faostat.fao.org/default.htm>. Accessed December 1999.
- Liang, JB & Rahman, S 1985, 'Dual-purpose (drought-meat) buffalo: the last resort to save the dying species in Malaysia', in *Proceedings, First World Buffalo Congress, Cairo, Egypt*, pp. 926–928.
- Ongah, H 2004, 'Estate experience II – the husbandry of systematic beef cattle integration with oil palm', in *Proceedings 2nd National Seminar on Livestock and Crop Integration with Oil Palm, 25 March 2003, Selangor*, eds MB Wahid, ZZ Zakaria, R Awalludin, and S Ismail, Malaysian Palm Oil Board (MPOB), Kuala Lumpur, Malaysia, pp. 32–36.
- Mad Nasir Shamsudin 2004–2005, 'Malaysia. Infrastructure issues: implications for the food and agriculture system', *Pacific Food System Outlook*, pp. 1–4.
- Mahadevan, P & Devendra, C 1986, 'Present and projected ruminant production systems of South East Asia and the South Pacific', in *Forages in South East Asia and the Pacific, Australian Centre for International Agricultural Research Proceedings, no. 12, Canberra, Australia*, pp. 1–6.
- Samsuddin, S 1991, 'System operated by estate contractors', in *Seminar on Economic Benefit from Integration of Cattle under Oil Palm, 26 February, 1991, Negeri Sembilan, Malaysia* (Mimeograph).
- Steinfeld, H 1998, 'Livestock production in the Asia and Pacific region: current status, issues and trends', *World Animal Review*, (Food and Agriculture Organisation) no. 90, pp. 14–21.
- Steinfeld, H 1999. 'The industrialisation of livestock production in the light of the Asian economic crisis', in *Proceedings of the Workshop on the Implications of the Asian Economic Crisis on the Livestock Industry*, Food and Agriculture Organisation (FAO), Bangkok, Thailand, pp. 27–40.
- Sukri, MI & Dahlan, I 1984, 'Feedlot and semi-feedlot systems for beef cattle fattening among smallholders', in *Proceedings, 8th Annual Conference, 13 March 1984, Genting Highlands, Pahang*, Malaysian Society of Animal Production, pp. 74–78.
- TAC (Technical Advisory Committee) 1992, *Review of CGIAR of Priorities and Strategies, Part 1*, TAC Secretariat, Food and Agriculture Organisation (FAO), Rome, Italy, 250 pp.
- UNDP (United Nations Development Programme) 1996, *Urban agriculture, food, jobs and sustainable cities*, Publication Series for Habitat II. United Nations Development Programme, New York, USA.

Malaysian Antarctica Research Programme

Malaysia's instigation into the issue of Antarctica has drawn the interest of the Antarctic Treaty Consultative Party (ATCP) members culminating in an invitation to attend a workshop on the Antarctic Treaty System at South Beardmore Camp on Antarctica in January 1985. Consequently, Academician Dr Omar Abdul Rahman, one of the delegates, proposed that a Malaysian scientific group on Antarctica be formed and the means found to enable them to use the research centres in Antarctica. However, the conditions at the time did not permit the establishment of the research entity.

This changed when a bilateral scientific cooperation between Malaysia and New Zealand was signed in 1996. Under the collaboration agreement, the New Zealand government offered then logistics support as well as scientific collaboration. The then Hon. Minister of Transport (Malaysian) Ling Leong Sik, headed an official visit to Scott Base in Antarctica, following which the Malaysian Cabinet endorsed the setting up of a Malaysian Antarctic research programme in the areas of climate change and biodiversity in November 1997.

The Academy of Sciences Malaysia (ASM) was given the mandate to set up a taskforce to oversee and coordinate the Malaysian Antarctic Research Programme (MARP). ASM is the focal point and serves as the secretariat to the programme.

MARP is funded under the 8th Malaysian Plan (2000-2005) with an allocation of RM10 million to initiate and set up Malaysian research in Antarctica. It aims to develop resilient and innovative researchers to cultivate world class scientific research capacity. The Malaysian Antarctica Research Centre located in Universiti Malaya was established on August 5th 2002 as a centre to coordinate the research activities of the members of the Programme.

Objectives of the Malaysian Antarctica Research Programme

One of the challenges of Vision 2020 is the establishment of a progressive society that is an innovative contributor to science and technology development of the future. The establishment of MARP is a big step towards the realisation of this goal. As such, the Programme aims to:

- Facilitate and coordinate Malaysian scientific efforts in the areas of global sciences such as climate change and biodiversity, one of the niche areas being the relationship between the tropics and the poles.
- Encourage and foster efforts to develop the capability and capacity of Malaysian scientists to compete at international level *via* international networking.
- Promote and maintain Malaysia's presence as a significant player in Antarctic research to pave the

way for Malaysia's entrance into the Antarctic Treaty System and to be admitted as an Antarctica Treaty Consultative Party.

To date, the Programme has successfully accomplished its mission to make Malaysia's scientific presence felt. Among others, the Programme has managed to secure Malaysia a position as an Associate Member of the Scientific Committee of Antarctic Research (SCAR) as well as setting up a network of international and local scientists for technology transfer activities and research in areas such as atmospheric science, life science, solar and terrestrial science and remote sensing. Apart from elevating Malaysian research, the Programme is also invaluable in human resource development necessary to power a knowledge-based economy.

Malaysia's Antarctica research focussed on several key areas such as atmospheric science, geology, upper atmosphere and solar terrestrial physics, biological science and remote sensing research. Each team in all fields have distinguished themselves not only nationally, but also has gained recognition internationally for their contribution in the field.

In atmospheric science research, the Malaysian team is among those in the forefront of polar numerical weather modelling and the head of this project has been entrusted to head a four-year action group on Modelling and Observation of Antarctic Katabatics (MOSAK) under SCAR.

The geology research projects had provided greater insight as to how the landscape of the Antarctica was formed millions of years ago. The findings contribute towards understanding geological processes with applications for mineral and fossil fuel excavation in other parts of the world.

The upper atmosphere and solar terrestrial physics researchers have been responsible for a number of new developments in the area, leading to greater understanding of understanding of the sun-earth relationship and how it impacts the technology the world is increasingly relying upon. The project has been selected for the international study of sun-earth connection under the banner of International Heliophysical Year IHY 2007.

The establishment of the Malaysian Antarctic Microalgae Collection is a noteworthy accomplishment of the biological science researchers. Apart from that, the researchers in this area are looking to solve problems from biomonitoring to improving industrial processes to be cleaner and with less impact on the environment.

The remote sensing research project has been invaluable in understanding how the environment responds to man-

made climactic stresses, a critical step towards alleviating the earth's environmental strain and improving global well being. The researchers are also working to increase the country's remote sensing capability and to forge the country's place as the first ASEAN country to be involved in remote sensing research in the Antarctica.

The contribution of Malaysian researchers in Antarctica has culminated in seven researchers accepted as project leaders for the International Polar Year IPY 2007-2008. The IPY has a long and illustrious history in promoting international cooperation for the advancement of science.

This acknowledgment is significant as Malaysia is still a novice in Antarctic research.

Strategy for the Future

MARP is also looking into the feasibility of establishing an 'Antarctica Research Institute' under the auspices of the Academy of Sciences Malaysia. This Institute will be the hub of Malaysia's polar research and is viewed for development to be a centre of excellence. The Antarctica Research Institute will provide a focus point for polar research in the region.

Enquiries:

Academy of Sciences Malaysia
902-4, Jalan Tun Ismail
50480 Kuala Lumpur
MALAYSIA
Tel: (603) 2694 9898
Fax: (603) 2694 5858
E-mail: nasa@akademisains.gov.my

Malaysian Antarctic Research Centre
B303, IPS Building,
University of Malaya,
50603 Kuala Lumpur
MALAYSIA
Tel: (603) 7960 8950 / 79676947 / 7967 4638
Fax: (603) 7960 5935
E-mail: talhady@gmail.com
URL: <http://www.akademisains.gov.my/antarctica/>

Recipient of Mahathir Science Award 2005

Prof J. S. Mackenzie



Prof John Sheppard Mackenzie

Professor John Sheppard Mackenzie is the first recipient of the ASM Scientific Excellence Award for 2005 which was given for his outstanding contribution and breakthroughs in the field of tropical medicine.

One of the major areas of his contribution was in solving the problems of the tropics in his studies related to the Japanese Encephalitis virus (JEV). He has been involved in the investigation of the phylogeny, virus movement into Indonesia, Papua New Guinea and the Torres Strait Islands, the kind of mosquitoes involved in transmission, risk analysis about establishment in new areas, and elucidating the ecology of the virus in Papua New Guinea and the Torres Strait.

Prof Mackenzie was closely involved in the discovery and investigation of the Hendra virus, which is related to the Nipah virus. These viruses cause considerable morbidity, mortality and economic distress, and continue to trouble many countries.

He first graduated with a B.Sc (Hons) degree from the University of Edinburgh in 1965, and obtained his Ph.D from the Australian National University in 1969. He is also the Fellow of the Australian Society for Microbiology Inc., Australasian College of Tropical Medicine, and Member of the Australian Institute of Company Directors.

At present, he is the Premier's Fellow and Professor of Tropical Infectious Diseases at the Division of Health Sciences, Curtin University of Technology, Australia, a post that he took up in May 2004. He also holds several other positions, including Adjunct Professor of International Health, Curtin University; Honorary Professor, University of Queensland (2004–2007); Honorary Senior Principal Research Fellow, Queensland Institute of Medical Research (2001 to date); Technical Consultant, World Health Organization (WHO), (2004–2006); and Member, Board of Directors, PANBIO (2004 to date). Over the years, He has also served a number of institutions; these include: Professor of Microbiology, University of Queensland (1995–2004); Technical Consultant WHO (2003–2004); Interim Chief Executive Officer, Australian Biosecurity Cooperative Research Centre (2003); Head, Department of Microbiology and Parasitology, University of Queensland (1995–2000); Senior Lecturer, Associate Professor and Professor at the Department of Microbiology, University of Western Australia (1973–1994); Head, Genetics Department, Animal Virus Research Institute, Pirbright, United Kingdom (1970–1972); and Fellow, Public Health Research Institute of the City of New York (1969–1970).

Since migrating to the Asia Pacific region 30 years ago, Prof Mackenzie has embraced the region and its challenges. His work became increasingly focused on viruses of this region leading to his contributions to JEV along with other emerging tropical infectious diseases. Through continued and careful investigations, he has contributed to solving the problems of the tropics in his studies related to JEV and has investigated the phylogeny, virus movement into Indonesia, Papua New Guinea and the Torres Straits Island; the kind of mosquitoes involved in transmission, risk analysis about establishment in new areas, and elucidating the ecology of the virus in Papua New Guinea and the Torres Strait. Subsequently, Prof Mackenzie was closely involved in the discovery and investigation of the Hendra virus, which is closely related to the Nipah virus. These viruses caused considerable morbidity, mortality and economic distress, and continue to trouble some of the countries. Through Prof Mackenzie's efforts, we now know the link between Hendra virus and flying foxes, as well as the reservoir host.

Earlier, Prof Mackenzie contributed much to influenza research. Through his works at his laboratory, he discovered the H15 component of avian influenza, and demonstrated the role of migratory waders in carrying the virus between continents. This work remains vitally relevant as the world faces an influenza pandemic which is likely to start in, and poses most threat to, the tropical parts of Asia.

Throughout his career, Prof Mackenzie has taken continuous steps to bring about change through his research using a four-fold approach. He starts by undertaking

excellent science research, followed by making sure that the findings of the science are well-known by publishing and speaking in international fora. He ensures training is available to junior scientists as well as facilitating training for scientists; and finally he does everything possible to translate science into policy and putting it to practice.

Prof Mackenzie's contributions both in terms of value and impact are well reflected through his recent involvement in two major events affecting the Asian region, namely the SARS outbreak and the Tsunami. He led the first major team that went into China to study SARS and has subsequently revisited to advice on investigating the source and transmission of the SARS virus, as well as laboratory safety surrounding the handling of the coronavirus virus that was shown to be the cause of SARS. During the tragic Indian Ocean Tsunami, Prof Mackenzie was one of the first experts called to help in setting up laboratory capacity by coordinating the various offers of assistance and providing practical advice. Prof Mackenzie shuttled between Jakarta and Banda Aceh in Indonesia, to bring together Indonesian and international efforts to establish laboratory capacity.

Recognition of his expertise by the world can be gauged from his involvement in the WHO. Prof Mackenzie sits in the Steering Committee for the Global Outbreak Alert and Response Network (GOARN) (2000 to the present). He is also a member of the Scientific Advisory Group for Global Health Security, (2001 to the present). Other involvements with the WHO include, (1982 to the present), Consultant in Virus Diseases; Director, WHO Collaborating Centre for the Collection and Dissemination of Data on Virus Diseases of Southeast Asia and the Western Pacific (1984–1998); Member, Technical Consultation on Nipah Virus, Kuala Lumpur (2000); Team Leader, Expert Technical Mission to China to investigate the possible cases of severe respiratory diseases from Guangdong (2003); Convenor, SARS International Research Advisory Committee (2003 to the present); and Member, Tsunami Relief Team, Indonesia (2005).

Prof Mackenzie's contribution to his field of expertise is evidenced by his publications. He has authored or co-authored more than 250 publications on emerging diseases, in particular emerging tropical infectious diseases. He has also served in many international editorial boards, including Ecohealth (2003 to date); *FEMS Microbiological Reviews* (1996–2003); *Emerging Infectious Diseases* (1998 to date); *Microbiology Australia* (1995–2004); *Research in Virology* (1996–1999); *Virus Genes* (1995 to date); *World Journal of Microbiology and Biotechnology* (1993–1997); *Journal of Clinical Virology* (1992 to date); and *Virus Information Exchange Newsletter* (1984–92); and *Ecology of Disease* (1982–1986).

Prof Mackenzie has also shown his commitment to ensure appropriate fora are available for regional scientists. As the Foundation Editor for the Virus Information Exchange

Newsletter, published for laboratories in South East Asia and the Western Pacific by the WHO Collaborating Centre for Collection and Dissemination of Data on Virus Disease, he provides the means through the Newsletter for the laboratories in the region to share information about viruses and virus disease and the activities and diagnostic results in each laboratory.

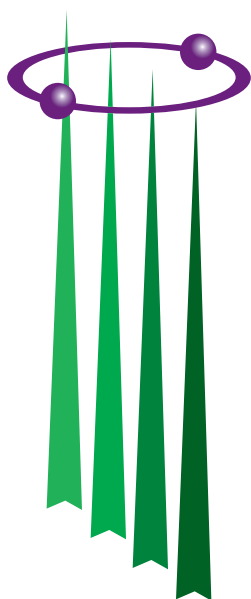
His eminence in emerging tropical diseases research has been recognized by his election as a member of numerous national and international scientific/expert committees, including at present the Expert Committee on Lyssaviruses, Commonwealth Department of Health and Aged Care; Australian National Certification Committee for the Eradication of Poliovirus; Australian Army Malaria Institute Advisory Board; National Arbovirus and Malaria Advisory Committee; National Consultative Group for the Biological Weapons Convention; Executive Board of Asian Pacific Society for Medical Virology; Executive Board of Federation of Asian Pacific Microbiological Society; Executive Board of International Union of Microbiological Societies; Advisory Board of Cordlife Pte. Ltd.; Advisory Board, Centre for Emerging Infectious Disease, Chinese University of Hong Kong; and Associate of Consortium of Conservation Medicine, New York.

Over the years, Prof Mackenzie has received numerous awards and accolades, among others, Officer in the Order of Australia (2002); Queen's Birthday Honours List (1999); Co-recipient, James H. Nakano Citation of the National Centre for Infectious Diseases of the Centres for Disease Control and Prevention (2000); Excellence in Virology Award, Asian-Pacific Society for Medical Virology (1999); nomination for a share in the Charles C. Shepard Science Award for the most outstanding peer-reviewed research paper published by CDC/ATSDR scientists; Distinguished Service Award (1999); the Australian Society for Microbiology, Inc. (1996); and Co-recipient, the *Medical Journal of Australia*/Wyeth Research Award for the best original research paper published in the *Medical Journal of Australia* in 1996.

For his scientific contributions and his scientific generosity in sharing his knowledge, his untiring efforts to ensure that knowledge is used and is relevant, and for his excellent community service records, the Academy of Sciences Malaysia found Prof Mackenzie a worthy recipient of the Academy of Sciences Malaysia Scientific Excellence Award/Mahathir Science Award.

Corresponding address:

Premier's Fellow and Professor of Tropical Infectious Diseases
Australian Biosecurity Cooperative Research Centre for Emerging Infectious Disease
Curtin University of Technology, Australia
(e-mail: mackenzie@curtain.ed.au)



MAHATHIR SCIENCE AWARD 2008

Invitation for Nominations

The Academy of Sciences Malaysia (ASM) is a body set up with a mission that encompasses pursuit, encouragement and enhancement of excellence in the fields of science, engineering and technology for the development of the nation and the benefit of mankind. The Academy has instituted the Mahathir Science Award (Formerly Known as ASM Award For Scientific Excellence in Honour of Tun Dr Mahathir Mohamad) in recognition of scientists/institutions who have contributed to cutting-edge tropical research that have had an impact on society.

This Award is Malaysia's most prestigious Science Award for tropical research launched in honour of Tun Dr Mahathir Mohamad who promoted and pursued with great spirit and determination his convictions in science and scientific research in advancing the progress of mankind and nations. Tun Dr Mahathir was the major force and the man who put into place much of the enabling mechanisms for a scientific milieu in our country.

This Award will be given to researchers who have made internationally recognised breakthroughs in pioneering tropical research in the fields of Tropical Medicine, Tropical Agriculture, Tropical Architecture and Engineering, and Tropical Natural Resources.

One Award will be conferred in 2008 covering any of the above four fields. The Award carries a cash prize of RM100 000, a gold medal and a certificate.

NOMINATION CRITERIA

- Awards will be given to researchers who have made internationally recognised breakthroughs in pioneering tropical research that have brought greater positive impacts on the well-being of society.
- Nominations can be made by individuals or institutions.
- A recipient could be an individual or an institution.

Nomination forms may be downloaded from the Academy's website:
www.akademisains.gov.my

Closing date: 31st May 2008

For more information please contact:

Academy of Sciences Malaysia
902-4, Jalan Tun Ismail, 50480 Kuala Lumpur
Tel : 603-2694 9898; Fax : 603-2694 5858
E-mail: hazami@akademisains.gov.my
admin@akademisains.gov.my

Workshop on Integrated Tree Crops – Ruminant Systems: Assessment of Status and Opportunities in Malaysia

4 – 5 September 2007

Venue: Palace of the Golden Horses, Seri Kembangan, Selangor

Objectives:

- Assess the current status of integrated systems in Malaysia, with reference to policies, current incentives, practice, extent and importance;
- Enumerate problems and constraints as well as impediments for the development of the system;
- Identify opportunities, including inter-agency cooperation, for improving and promoting the development process;
- Identify policy options to assist the nation's development agenda; and
- Produce an Advisory Report to the Government of Malaysia.

Fee:

A non-refundable Registration Fee of Ringgit Malaysia One Hundred only (RM100) is payable to Academy of Sciences Malaysia on registration.

Enquires:

Academy of Sciences Malaysia

902-4, Jalan Tun Ismail

504080 Kuala Lumpur

Tel: 03-2694 9898; Fax: 03-2694 5858

E-mail: admin@akademisains.gov.my

Second International Conference on Science and Mathematics Education 2007

13 – 16 November 2007

Venue: SEAMEO RECSAM, Penang, Malaysia

Theme:

Redefining Learning Culture for Sustainability

Objectives:

- To provide a forum to review issues, exchange of ideas and share experiences especially on the learning culture in science and mathematics instruction at all levels;
- Review and recognize the integration of ICT to sustain a learning culture in the teaching of science and mathematics;
- Review and enhance continuous professional development as a means to sustain the learning culture in science and mathematics education;
- Encourage the sharing of knowledge, skills and experiences of experts working on new strategies to sustain the learning culture for effective reforms in teaching and assessment;
- Strengthen professional networking among science and mathematics educationist both locally and globally; and
- Maintain professional contacts to enhance cooperation among a consortium of international organizations and educational institutions to facilitate greater dissemination and exchange of expertise at an international level.

Enquiries:

Tel : (6) 04-658 3266

Fax : (6) 04-657 2541

E-mail: cosmed@recsam.edu.my; cosmed07@yahoo.com.my

Nanotech Malaysia 2007 and Asia Nano Forum Summit 2007

29 November – 1 December 2007

Venue: Kuala Lumpur Convention Centre

Theme:

“Nanotechnology: A New Dimension of Living”

Nanotech Malaysia 2007

Objectives:

- To organize the Nanotech Symposium and Nano Forum in order to introduce nanotechnology, disseminate and provide current information on its development;
- To initiate the establishment of Malaysian nanotechnology society;
- To establish research-business relationship on nanotechnology among local researchers, corporate and commercial sectors;
- To foster relationship among Asian countries in nanotechnology;
- To educate and promote awareness in nanotechnology to the public; and
- To host the Asia Nano Summit 2007.

Asia Nano Forum Summit 2007

Objectives:

- Foster nanotechnology in the region by creating mechanisms to share information, human and physical resources and expertise;
- Initiate, promote and manage co-operative scientific and technology research projects within the member economies;
- Support regional economic and environmental development through joint projects addressing major regional issues, with an emphasis on support of developing and emerging economies; and
- Enhance public awareness and education of nanotechnology and associated social, environmental, health and economic issues.

Programme:

1. Nanotechnology Security and Defence Forum

Venue: Kuala Lumpur Convention Centre

Admission: By invitation

Enquiries:

Dr Mohamad Asri Abd Ghani

Tel.: 03-8732 4400 / 4453 / 4402

E-mail: sre1161@hotmail.com; maag.kst@mod.gov.my

2. R&D Nanotechnology Symposium

Venue: Kuala Lumpur Convention Centre

Fees: RM1200 / RM700 (for students)

Enquiries:

Dr Azmi Haji Idris

Tel : 03-5544 6861 / 04-401 7102

E-mail: azmi_idris@sirim.my

3. Nanotechnology Business and R&D Matching Luncheon

Venue: Kuala Lumpur Convention Centre

Price of table: RM3000, RM5000, RM7000 and RM10 000

(10 participants per table)

(Registration before 30 September 2007)

Enquiries:

Dr Zamri Ishak

Tel : 03-8943 7927

E-mail: zamri@mardi.my

4. Nanotechnology Exhibition

Venue: Kuala Lumpur Convention Centre

Admission: Free

Registration fees for exhibition:

RM5000 per Booth (3 m × 3 m)

(Registration before 30 September 2007)

Enquiries:

Prof Ibrahim Abdullah

Tel: 03-8921 5441

E-mail: dia@ukm.my

Enquiries for all Programme:

Academy of Sciences Malaysia

Tel: 03-2694 9898 Fax: 03-2694 5858

<http://www.akademisains.gov.my>;

<http://www.nano.gov.my>

E-mail: sharizad@akademisains.gov.my;

azhar@akademisains.gov.my

RNAi and Human Diseases (The 7th Dr Ranjeet Bhagwan Singh Technical Workshop)

11–14 December 2007

Venue: Department of Molecular Medicine, Faculty of Medicine
University of Malaya, Kuala Lumpur

Consultants:

Prof Kandiah Jeyaseelan
(*Professor of Biochemistry and Molecular Biology*) and
Dr A. Armugam (*Senior Research Fellow, Department of Biochemistry*),
Yong Loo Lin School of Medicine, National University of Singapore

Objectives:

- To learn the principles underlying RNA interference (RNAi);
- To learn about the part played by miRNAs and siRNAs in human diseases;
- To acquire hands on experience in isolating small RNAs and to detect specific miRNAs in blood and tissues; and
- To gain hands on experience on specific inhibition of gene expression using RNAi.

Enquires:

Assoc. Prof. Dr Mary Anne Tan Jin Ai
Department of Molecular Medicine
Faculty of Medicine
University of Malaya
Tel: 03-7967 4903; Fax: 03-7967 6600
E-mail: jamatan@hotmail.com

Ms Seetha Ramasamy
Academy of Sciences Malaysia
902-4, Jalan Tun Ismail
50480 Kuala Lumpur
Tel: 03-2694 9898; Fax: 03-2694 5858
E-mail: seetha@akademisains.gov.my

Malaysian Science and Technology Convention 2007

29 – 30 November 2007

Venue: Putra World Trade Centre, Kuala Lumpur

Theme:

“Malaysian Science and Technology: Strategizing and Investing in the future”

Objectives:

- To review the achievements, challenges and potential of science, technology and innovation in the country; and
- To recommend strategies on the way forward to the government.

Malaysian Science and Technology Convention (MASTEC) aims to bring together policy makers, academics, members of the scientific community; key people from Institutes of higher learning and research institutions; leaders in trade and finance; middle and upper management from the public and private sector, representatives of the science, engineering and technology (SET) professional bodies as well as all relevant stakeholders in the SET scenario of the nation for discussion and formulating strategies along with targeted action plans on MASTEC’s designated theme or issue of national importance that is being focussed upon.

Tentative Programme:

29 November 2007

Luminary Lecture

Overview of Report: Rising Above the Gathering Storm

Speaker from the National Academies of Science, USA

Plenary Session 1

The Role of Science, Technology and Innovation in the New Economy

Panel Discussion

Plenary Session 2

Preparing Human Capital for the New Economy

Panel Discussion

30 November 2007

Plenary Session 3

Strengthening Science Education for a Knowledge Economy

Panel Discussion

Plenary Session 4

Enhancing Indigenous K-based Industries in an Advanced Economy

Panel Discussion

Plenary Session 5

Planning, Investing and Funding for a Knowledge Economy

Panel Discussion

Enquiries:

Ms Nitia K. Samuel
Academy of Sciences Malaysia

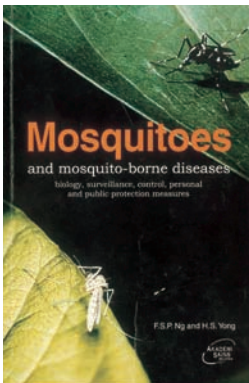
902-4, Jalan Tun Ismail
50480 Kuala Lumpur

MALAYSIA

Tel: 603 2694 9898

Fax: 603 2694 5858

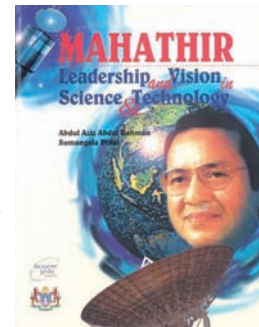
E-mail: nitia@akademisains.gov.my



Mosquitoes and Mosquito-borne Diseases: Biology, Surveillance, Control, Personal and Public Protection Measures.

F.S.P. Ng and H.S. Yong (Editors)
(2000)

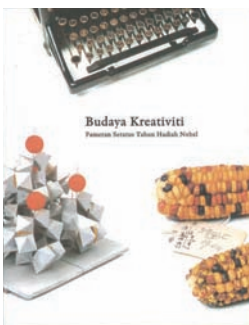
ISBN 983-9445-05-7
Price: RM60.00 / USD20.00



Mahathir: Leadership and Vision in Science and Technology

Abdul Aziz Abdul Rahman and Sumangala Pillai
(1996)

ISBN 983-9319-09-4
Price: RM100.00 / USD30.00



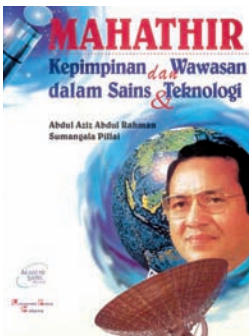
Budaya Kreativiti: Pameran Seratus Tahun Hadiah Nobel.

Ulf Larsson (Editor)
(2004)

ISBN 983-9445-09-X
Price: RM100.00 / USD30.00

CD Kompilasi estidotmy

Edisi 1 – 12, 2002/03
Price: RM13.00 / USD4.00



Mahathir: Kepimpinan dan Wawasan dalam Sains dan Teknologi

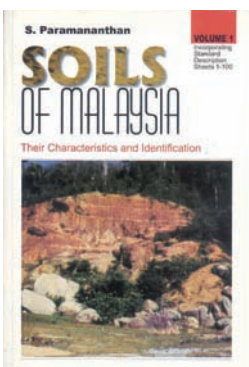
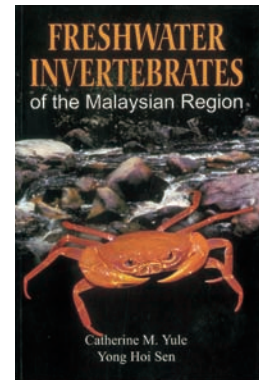
Abdul Aziz Abdul Rahman dan Sumangala Pillai
(1996)

ISBN 983-9319-09-4
Price: RM100.00 / USD30.00

Freshwater Invertebrates of the Malaysian Region

Catherine M. Yule and Yong Hoi Sen
(2004)

ISBN 983-41936-0-2
Price: RM180.00 / USD52.00



Soils of Malaysia: Their Characteristics and Identification (Vol. 1)

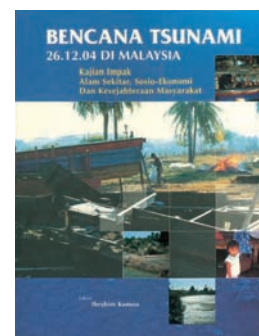
S. Paramanathan
(2000)

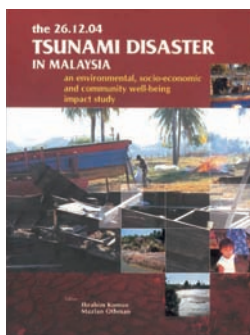
ISBN 983-9445-06-5
Price: RM100.00 / USD30.00

Bencana Tsunami 26.12.04 di Malaysia: Kajian Impak Alam Sekitar, Sosio-Ekonomi dan Kesejahteraan Masyarakat

Ibrahim Komoo (Editor)
(2005)

ISBN 983-9444-62-X
Price: RM100.00 / USD30.00





**The 26.12.04 Tsunami Disaster in Malaysia:
An Environmental, Socio-Economic and
Community Well-being Impact Study**

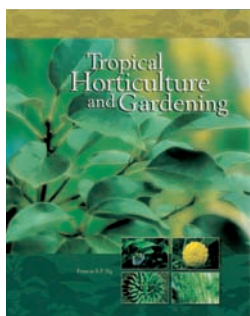
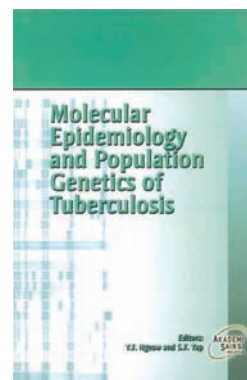
Ibrahim Komoo and Mazlan Othman (Editors)
(2006)

ISBN 983-9444-62-X
Price: RM100.00 / USD30.00

**Molecular Epidemiology and Population
Genetics of Tuberculosis**

Y.F. Ngeow and S.F. Yap (Editors)
(2006)

ISBN 983-9445-14-6
Price: RM40.00 / USD12.00



Tropical Horticulture and Gardening

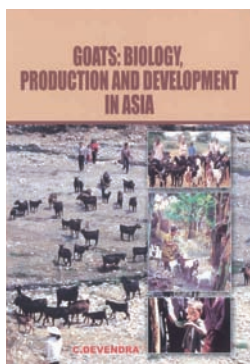
Francis S.P. Ng
(2006)

ISBN 983-9445-15-4
Price: RM260.00 / USD75.00

**Kecemerlangan Sains Dalam Tamadun Islam:
Sains Islam Mendahului Zaman Scientific
Excellence in Islamic Civilization:
Islamic Science Ahead of its Time**

Fuat Sezgin
(2006)

ISBN 983-9445-14-6
Price: RM40.00 / USD12.00



**Goats: Biology, Production and
Development in Asia**

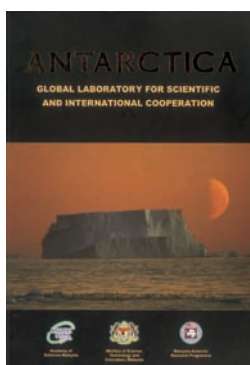
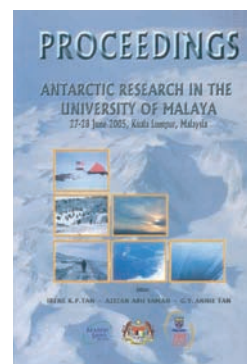
C. Devendra
(2007)

ISBN 978-983-9445-18-3
Price: RM180.00 / USD52.00

**Proceedings: Seminar on Antarctic Research,
27–28 June 2005, University of Malaya,
Kuala Lumpur, Malaysia**

Irene K.P. Tan et al. (Editors)
(2006)

ISBN 978-983-9445-17-6
Price: RM40.00 / USD12.00



**Antarctica: Global Laboratory for Scientific
and International Cooperation**

Aileen Tan Shau-Hwai et al. (Editors)
(2005)

ISBN 983-9445-13-8
Price: RM40.00 / USD12.00

For on-line purchasing,
please access:
<http://www.akademisains.gov.my>

About the Journal

Mission statement

To serve as the forum for the dissemination of significant research, S&T and R&D policy analyses, and research perspectives.

Scope

The ASM Science Journal publishes advancements in the broad fields of medical, engineering, earth, mathematical, physical, chemical and agricultural sciences as well as ICT. Scientific articles published will be on the basis of originality, importance and significant contribution to science, scientific research and the public.

Scientific articles published will be on the basis of originality, importance and significant contribution to science, scientific research and the public. Scientists who subscribe to the fields listed above will be the source of papers to the journal. All articles will be reviewed by at least two experts in that particular field. The journal will be published twice in a year.

The following categories of articles will be considered for publication:

Research Articles

Each issue of the journal will contain no more than 10 research articles. These are papers reporting the results of original research in the broad fields of medical, engineering, earth, mathematical, physical, chemical and life sciences as well as ICT. The articles should be limited to 6000 words in length, with not more than 100 cited references.

Short Communications

These are articles that report significant new data within narrow well-defined limits or important findings that warrant publication before broader studies are completed. These articles should be limited to 2000 words and not more than 40 cited references. Five (5) Short Communications will be accepted for publication in each issue of the journal.

Research Perspectives

These are commissioned papers that analyse recent research in a particular field, giving views on achievements, research potential, strategic direction etc. A Research Perspective should not exceed 2000 words in length with not more than 40 cited references. Each writer will be paid an honorarium of RM1000.

Reviews/Commentaries

Each issue of the journal will also feature five commissioned Reviews/Commentaries presenting overviews on aspects such as Scientific Publications and Citation Ranking, Education in Science and Technology, Human Resources for Science and Technology, R&D in Science and Technology, Innovation and International Comparisons or Competitiveness of Science and Technology etc. Reviews/Commentaries will encompass analytical views on funding, developments, issues and concerns in relation to these fields and not exceed 5000 words in length and 40 cited references. Writers of Reviews/Commentaries will be paid an honorarium of RM1500 per review/commentary.

Science Forum

Individuals who make the news with breakthrough research or those involved in outstanding scientific endeavours or those conferred with internationally recognised awards will be featured in this section. Policy promulgations, funding, science education developments, patents from research, commercial products from research, and significant scientific events will be disseminated through this section of the journal. The following will be the categories of news:

- Newsmakers
- Significant Science Events
- Patents from Research
- Commercial Products from Research
- Scientific Conferences/Workshops/Symposia
- Technology Upgrades
- Book Reviews.

Instructions to Authors

The ASM Science Journal will follow the Harvard author-date style of referencing' examples of which are given below.

In the text, reference to a publication is by the author's name and date of publication and page number if a quote is included, e.g. (Yusoff 2006, p. 89) or Yusoff (2006, p. 89) "conclude....." as the case may be. They should be cited in full if less than two names (e.g. Siva & Yusoff 2005) and if more than two authors, the work should be cited with first author followed by *et al.* (e.g. Siva *et al.* 1999).

All works referred to or cited must be listed at the end of the text, providing full details and arranged alphabetically. Where more than one work by the same author is cited, they are arranged by date, starting with the earliest. Works by the same author published in the same year are ordered with the use of letters a, b, c, (e.g. Scutt, 2003a; 2003b) after the publication date to distinguish them in the citations in the text.

General Rules

Authors' names:

- Use only the initials of the authors' given names.
- No full stops and no spaces are used between initials.

Titles of works:

- Use minimal capitalisation for the titles of books, book chapters and journal articles.
- In the titles of journals, magazines and newspapers, capital letters should be used as they appear normally.
- Use italics for the titles of books, journals and newspapers.
- Enclose titles of book chapters and journal articles in single quotation marks.

Page numbering

- Books: page numbers are not usually needed in the reference list. If they are, include them as the final item of the citation, separated from the preceding one by a comma and followed by a full stop.
- Journal articles: page numbers appear as the final item in the citation, separated from the preceding one by a comma and followed by a full stop.

- Use the abbreviations p. for a single page, and pp. for a page range, e.g. pp. 11-12.

Whole citation

- The different details, or elements, of each citation are separated by commas.
- The whole citation finishes with a full stop.

Specific Rules

Definite rules for several categories of publications are provided below:

Journal

Kumar, P & Garde, RJ 1989, 'Potentials of water hyacinth for sewage treatment', *Research Journal of Water Pollution Control Federation*, vol. 30 no. 10, pp. 291-294.

Monograph

Hyem, T & Kvale, O (eds) 1977, *Physical, chemical and biological changes in food caused by thermal processing*, 2nd edn, Applied Science Publishers, London, UK.

Chapter in a monograph

Biale, JB 1975, 'Synthetic and degradative processes in fruit ripening', eds NF Hard & DK Salunkhe, in *Postharvest biology and handling of fruits and vegetables*, AVI, Westport, CT, pp. 5-18.

Conference proceedings

Common, M 2001, 'The role of economics in natural heritage decision making', in *Heritage economics: challenges for heritage conservation and sustainable development in the 21st century: Proceedings of the International Society for Ecological Economics Conference, Canberra, 4th July 2000*, Australian Heritage Commission, Canberra.

Report

McColloch, LP, Cook, HT & Wright, WR 1968, *Market diseases of tomatoes, peppers and egg-plants*, Agriculture Handbook no. 28, United States Department of Agriculture, Washington, DC.

Thesis

Cairns, RB 1965, *Infrared spectroscopic studies of solid oxygen*, PhD thesis, University of California, Berkeley, CA.

Footnotes, spelling and measurement units

If footnotes are used, they should be numbered in the text, indicated by superscript numbers and kept as brief as possible. The journal follows the spelling and hyphenation of standard British English. SI units of measurement are to be used at all times.

Submission of Articles

General. Manuscripts should be submitted (electronically) in MS Word format. If submitted as hard copy, two copies of the manuscript are required, double-spaced throughout on one side only of A4 (21.0 × 29.5 cm) paper and conform to the style and format of the *ASM Science Journal*. Intending contributors will be given, on request, a copy of the journal specifications for submission of papers.

Title. The title should be concise and descriptive and preferably not exceed fifteen words. Unless absolutely necessary, scientific names and formulae should be excluded in the title.

Address. The author's name, academic or professional affiliation, e-mail address, and full address should be included on the first page. All correspondence will be only with the corresponding author (should be indicated), including any on editorial decisions.

Abstract. The abstract should precede the article and in approximately 150-200 words outline briefly the objectives and main conclusions of the paper.

Introduction. The introduction should describe briefly the area of study and may give an outline of previous studies with supporting references and indicate clearly the objectives of the paper.

Materials and Methods. The materials used, the procedures followed with special reference to experimental design and analysis of data should be included.

Results. Data of significant interest should be included.

Figures. If submitted as a hard copy, line drawings (including graphs) should be in black on white paper. Alternatively sharp photoprints may be provided. The lettering should be clear. Halftone illustrations may be included. They should be submitted as clear black and white prints on glossy paper. The figures should be individually identified lightly in pencil on the back. All legends should be brief and typed on a separate sheet.

Tables. These should have short descriptive titles, be self explanatory and typed on separate sheets. They should be as concise as possible and not larger than a Journal page. Values in tables should include as few digits as possible. In most cases, more than two digits after the decimal point are unnecessary. Units of measurements should be SI units. Unnecessary abbreviations should be avoided. Information given in tables should not be repeated in graphs and vice versa.

Discussion. The contribution of the work to the overall knowledge of the subject could be shown. Relevant conclusions should be drawn, and the potential for further work indicated where appropriate.

Acknowledgements. Appropriate acknowledgements may be included.

Reprints. Twenty copies of reprints will be given free to all the authors. Authors who require more reprints may obtain them at cost provided the Editorial Committee is informed at the time of submission of the manuscript.

Correspondence

All enquiries regarding the ASM Science Journal, submission of articles, including subscriptions to it should be addressed to:

The Editor-in-Chief
ASM Science Journal
 Academy of Sciences Malaysia
 902-4, Jalan Tun Ismail
 50480 Kuala Lumpur, Malaysia.
 Tel: 603-2694 9898; Fax: 603-2694 5858
 E-mail: sciencejournal@akademisains.gov.my

RESEARCH PERSPECTIVE

Enhancing Animal Protein Supplies in Malaysia: Opportunities and Challenges C. Devendra	63
---	----

ASM SCIENTIFIC ACTIVITIES

Malaysian Antarctica Research Programme	75
---	----

SCIENTIST IN PROFILE

Recipient of Mahathir Science Award 2005 Prof J. S. Mackenzie	77
--	----

ANNOUNCEMENTS

Mahathir Science Award 2008	79
Workshop on Integrated Tree Crops – Ruminant Systems: Assessment of Status and Opportunities in Malaysia	80
Second International Conference on Science and Mathematics Education 2007	80
Nanotech Malaysia 2007 and Asia Nano Forum Summit 2007	81
RNAi and Human Diseases	82
Malaysian Science and Technology Convention 2007	83
ASM Publications	84

Contents

ASM Sc. J.
Volume 1(1), 2007

RESEARCH ARTICLES

- Prevention of Ethanol-induced Gastric Mucosal Injury by *Ocimum basilicum* Seed Extract in Rats** 1
A. A. Mahmood, K. Sidik and H. M. Fouad
- New Reaction Kinetic Model Derived from Molecular Dynamics Simulation Data on Non-linearity of Rate Coefficients and Their Relation to Activity Coefficients** 7
C. G. Jesudason
- Simulation Study of Carrier-to-Interference Power Ratio Enhancement in Orthogonal Frequency Division Multiplexing System** 19
S. Y. Sharifah, F. Norsheila and Muladi
- Optical Tomography: Real Time Image Reconstruction for Various Flow Regimes in Gravity Flow Conveyor** 27
R. Abdul Rahim, J. F. Pang, K. S. Chan, L. C. Leong and M. H. Fazalul Rahiman
- Purification of Metallurgical Grade Silicon by Acid Leaching** 37
V. A. Lashgari and H. Yoozbashizadeh
- Fourth Order Centred Total Variation Diminishing Scheme for Hyperbolic Conservation Laws** 43
Y. H. Zahran
- Stability of Marangoni Convection in Superposed Fluid and Porous Layers** 57
N. M. Arifin, N. F. M. Mokhtar, R. Nazar and I. Pop

Continued on the inside of the back cover.

ISSN 1823-6782

